Immunological, Epidemiological, and Economic Modeling of HIV, Influenza, and Fungal Meningitis

Nargesalsadat Dorratoltaj

Dissertation submitted to the Faculty of the

Virginia Polytechnic Institute and State University

in partial fulfillment of the requirements for the degree of

Doctor of Philosophy

in

Biomedical and Veterinary Sciences

Dissertation Committee:

Kaja Abbas, Chair

Josep Bassaganya-Riera

Stephen Eubank

Hazhir Rahmandad

Margaret O'Dell

Andreas Handel

Blacksburg, Virginia

Immunological, Epidemiological, and Economic Modeling of HIV, Influenza, and Fungal Meningitis

Nargesalsadat Dorratoltaj

Abstract

This dissertation focuses on immunological, epidemiological, and economic modeling of HIV, influenza, and fungal meningitis, and includes three research studies. In the first study on HIV, the study objective is to analyze the dynamics of HIV-1, CD4+ T cells and macrophages during the acute, clinically latent and late phases of HIV infection in order to predict their dynamics from acute infection to clinical latency and finally to AIDS in treatment naive HIV-infected individuals. The findings of the study show that the peak in viral load during acute HIV infection is due to virus production by infected CD4+ T cells, while during the clinically latent and late phases of infection infected macrophages dominate the overall viral production. This leads to the conclusion that macrophage-induced virus production is the significant driver of HIV progression from asymptomatic phase to AIDS in HIV-infected individuals. In the second study on influenza, the study objective is to estimate the direct and indirect epidemiological and economic impact of vaccine interventions during an influenza pandemic in Chicago, and assist in vaccine intervention priorities. Population is distributed among high-risk and non-high risk within 0-19, 20-64 and 65+ years subpopulations. The findings show that based on risk of death and return on investment, high-risk groups of the three age group subpopulations can be prioritized for vaccination, and the vaccine interventions are cost-saving for all age and risk groups. In the third study on fungal meningitis, the study objective is to evaluate the effectiveness and cost of the fungal meningitis outbreak response in New River Valley of Virginia during 2012-2013, from the local public health department and clinical perspectives. We estimate the epidemiological effec-

tiveness of this outbreak response to be 153 DALYs averted among the patients, and the costs incurred by the local health department and clinical facilities to be $30,413 and $39,580 respectively. Moving forward, multi-scale analysis of infectious diseases connecting the different scales of evolutionary, immunological, epidemiological, and economic dynamics has good potential to derive meaningful inferences for decision making in clinical and public health practice, and improve health outcomes.

Keywords: Infectious Disease Modeling, HIV, Influenza, Fungal Meningitis, Immunology, Epidemiology, Economics

Dedication

To my dear Maman and Baba,

Fahimeh Navabi and Hamid Doratoltaj

Acknowledgments

The works presented in this dissertation owe much to people I have had privileged to work throughout my journey at Virginia Tech. First, I would like to thank my adviser, Kaja Abbas. To say he has only been my adviser is definitely an understatement. I express my most sincere and gratitude to him who trusted me and provided me with this opportunity to learn and work on the projects of my interest. Not only he taught me public health and how to do a good science, but also he taught me how to think about the benefits of my research for populations before being a scientist. I am extremely grateful to my committee members, Stephen Eubank, Margaret O'Dell, Josep Bassaganya Riera, and Hazhir Rahmandad who were patient with me, always understood the challenges I was facing, and had the brightest ideas about how to improve my work.

The interdisciplinary nature of my work gave me the opportunity to interact with scholars from different disciplines. I am thankful for Stanca Ciupe at the Math Department of Virginia Tech for her mentorship, encouragement, and guidance on how to stay in a right path. I am thankful for the opportunity that I had to get in contact with Jessica Conway at Penn State University for the research ideas that she had and I am still following her suggestions to address the significance of HIV treatment interruption. I would like to thank Bryan Lewis, Achla Marathe, and Samarth Swarup for their true mentorship and supervision in my study on Influenza vaccine and also on setting my career goals. I thank Kate Corvese and Laurie Forlano at the Virginia Department of Health for data on the fungal meningitis attack rate in Virginia. I would like

to thank Paige Bordwine and Lex Gibson for their supervision and patience during my study on fungal meningitis. I would like to thank Thomas Kerkering at Virginia Tech Carilion School of Medicine who gave the opportunity to be the student observer at the infectious disease division of Carilion Clinic Crystal Springs Imaging Services.

I am thankful for all the faculty and staff at the biomdeical and veterinary sciences program, population health sciences department, and network dynamics and simulation science laboratory at biocomplexity institute of Virginia Tech. I would like to thank my officemates and more importantly friends at the population health sciences department, Patricia Baltazar, Ivette Valenzuela, and Monica Motley, whose lives and strength are keeping me encouraged. I am also thankful for my second family in Blacksburg, Gloria Kang, James Schlitt, Daniel Chen, and Alex Telionis who do not stop surprise me with their unconditional friendship and kindness. I would also like to express my gratitude to Milad Moh, who has been by my side through all these years and his endless support and patience make all I do possible. I would like to thank my friends, Yasaman Ashki, Sara Shashaani, Aida Farough, and Behnaz Ghahestani for their love and support.

And most importantly I would like to thank my parents, sister, and brother, I owe them everything I have in my life, for their continuous support and sacrifice for every decision I made and for never telling me I had limits on what I could do. I would never have made it without their encouragement and support. And finally I would like to thank you for your interest in my work. Enjoy!

Nargesalsadat Dorratoltaj

June, 2016

Blacksburg, VA

Contents

List of Figures

List of Tables

Chapter 1

Introduction

According to the Global Burden of Disease study in 2013, 11.37% of the global burden of diseases are caused by infectious diseases (1). It includes individual, societal, and economic levels of impact, that come from the total loss of health due to the injury and/or death. Although different biomedical and socio-behavioral interventions such as vaccination, treatment, and social distancing have been developed to control the epidemics of infectious diseases, implication of these interventions is limited by time, personnel, and budget. Thereby, it is crucial to allocate available resources optimally for effective public health policy and practice. Model-based analysis at different scales of evolutionary, immunological, epidemiological, and economic dynamics can quantify the impact of interventions and help decision makers to use the limited resources effectively and optimally.

1.1 Evolutionary dynamics of infectious diseases

Evolutionary dynamics of infectious diseases focus on the adaptation of the pathogen to survive within-host and in the environment (2). It includes the emergence of different strains that can be more or less

pathogenic. Understanding the evolutionary dynamics of infectious diseases enhances scientists to discover characteristics of the disease within-host for immunological models and treatment designs. At the population level, understanding the evolutionary dynamics of infectious diseases assist us to predict the infectious disease pattern or trace back the origin of the pathogen to prevent re-emerging infectious disease outbreaks. The evolutionary dynamics of influenza and dengue virus have been studied extensively by Nelson (3; 4; 5) and Koelle (6; 7) respectively.

1.2 Immunological dynamics of infectious diseases

Dynamics of the immune system and infectious diseases can be studied through systems biology of host-pathogen interactions at different levels of molecules, cells, organisms, or the entire species. At the cell level, pathogen replicates itself in target cells and the immune system responds to the replication of the pathogen. Mathematical models have been used to represent the host-pathogen interactions, and predict the immune system responses (8; 9; 10). These types of models can be developed and connected at different scales, and provide a better understanding of the host-pathogen interaction dynamics.

1.3 Epidemiological dynamics of infectious diseases

Infectious diseases spread among populations due to the direct or indirect contacts between individuals. Based on the density of the population, type of contacts, infectiousness of the pathogen, rate of migration between different populations, and individuals' characteristics, outbreaks vary in size and length. Mathematical models are useful to estimate the impact of infectious disease epidemics (11). The theory of "mass-action principle" based on the rate of contact between infected and susceptible individuals, built the foundation of infectious disease transmission and the framework of compartmental models (12), in which

population divides into mutually exclusive groups based on their status: Susceptible (S), Infected (I), Recovered (R). SIR model is one of the common forms of compartmental models that study the flow of individuals between different states through differential equations, that shows how disease transmits from infected to susceptible individuals, and with what rate people get recovered. Although compartmental models can provide a good estimation on disease spread among-populations, it has limitations in taking into account heterogeneity in individuals' contact patterns.

Network models are the extended form of compartmental models by adding the heterogeneity of socio-behavioral dynamics. In networks, nodes act as the individuals with specific characteristics and number of contacts over time (13). Edges show how nodes are connected with each other. Dynamic networks represent the duration of contacts, infectiousness of the node, and different types of contacts which play an important role in infectious disease transmission. Adding more heterogeneity and computational complexity, dynamic agent based models are introduced. Agent based models has the capability of computing spatial, temporal, and social behavior of individuals in a complex system (14).

1.4 Economic dynamics of infectious diseases

Outbreak of infectious diseases and pandemics inflict damage and cost to the society that include the direct cost of treating and controlling the illness, and indirect cost of productivity loss (15). Epidemiological models can be extended to add the economic impact of infectious disease outbreaks (16). Since public health resources are limited, it is essential to measure the cost of epidemics, and examine the benefits and effectiveness of interventions. Depending on the question to be answered, different measures of evaluation are being used. Two widely used methods of economic evaluation are: cost effectiveness analysis and cost-benefit analysis. Cost effectiveness analysis (CEA) compares the costs and effectiveness, in which effectiveness is measured in terms of quality-adjusted life year (QALY) gained or disability-adjusted life

year (DALY) averted due to implementation of the intervention (see (17; 18)). Incremental cost-effectiveness ratio (ICER), the ratio of change in cost due to change in effectiveness of intervention, is measured in the cost effectiveness analysis. On the other hand, cost-benefit analysis compares the cost and benefits of an intervention by reporting the net benefit or return on investment (ROI), which implies dollars saved/gained per $1 investment in the intervention.

Depending on the questions to be answered and the acceptable measure from the policy and practice perspective, cost-effectiveness or cost-benefit analysis can be used to evaluate the economic and epidemiological impact of different interventions, Thereby estimating an optimal prioritization of limited public health resources.

1.5 Dissertation focus

The focus of this dissertation is to enhance the understanding of the infectious disease impact at the individual and population scales to improve decision making in clinical and public health practice through mathematical modeling. Figure 1.1 illustrates the dissertation outline and objectives of the research studies. In chapter 2, the study objective is to analyze the viral and immune system dynamics of HIV-1, CD4+ T cells and macrophages during the acute, clinically latent and late phases of HIV infection to estimate the progression dynamics from acute infection, clinical latency to AIDS stage in treatment naive HIV-infected individuals. In chapter 3, the study objective is to estimate the direct and indirect epidemiological and economic impact of vaccine interventions during an influenza pandemic in Chicago, and assist in vaccine intervention priorities. In chapter 4, the study objective is to evaluate the effectiveness and cost of the fungal meningitis outbreak response in New River Valley of Virginia during 2012-2013, from the local public health department and clinical perspectives. In chapter 5, I present the significance of understanding and connecting infectious disease dynamics at evolutionary, immunological, epidemiological, and economic scales, and

propose multi-scale modeling framework to analyse infectious disease dynamics.

1.6 Ethics approval

The Institutional Review Board (IRB) at Virginia Tech has given ethics approval of the research studies in this dissertation.

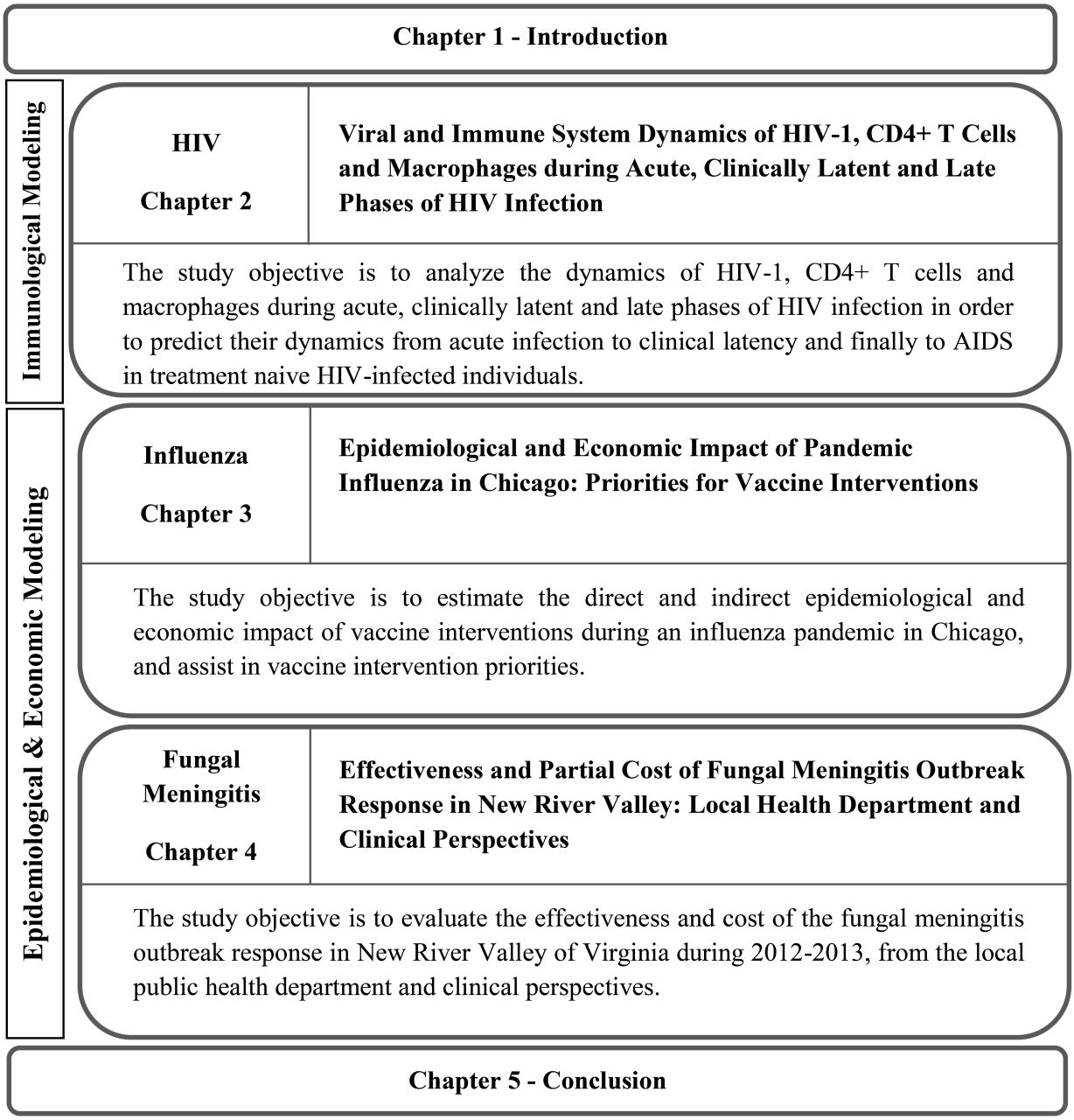

Figure 1.1: **Immunological, epidemiological, and economic modeling of HIV, influenza, and fungal meningitis.** The figure illustrates the focus and outline of the research studies in this dissertation.

Chapter 2

Viral and Immune System Dynamics of HIV-1, CD4+ T Cells and Macrophages during the Acute, Clinically Latent and Late Phases of HIV Infection

This study is based on the following paper:
Dorratoltaj N, Ciupe S, Eubank S, Borrow P, Pellegrino P, Williams I, Abbas K, Viral and Immune System Dynamics of HIV-1, CD4+ T Cells and Macrophages during the Acute, Clinically Latent and Late Phases of HIV Infection (in preparation)

2.1 Abstract

The study objective is to analyze the dynamics of HIV-1, CD4+ T cells and macrophages during the acute, clinically latent and late phases of HIV infection in order to predict their dynamics from acute infection to clinical latency and finally to AIDS in treatment naive HIV-infected individuals. While the viral-host dynamics of HIV-1 and CD4+ T cells are well studied, our understanding of the dynamics of macrophages in HIV progression to AIDS is limited. This study incorporates the macrophage dynamics and studies their contribution to both the viral reservoir and viral production during all stages of HIV infection. We develop a deterministic mathematical model of virus-host dynamics that incorporates the HIV-1, CD4+ T cell and macrophage populations. We calibrate the model against longitudinal clinical data of HIV viral load and CD4+ T cell count from a cohort of 39 treatment naive HIV-infected individuals, collected at the Mortimer Market Centre in London, UK. Based on model calibration to rapidly-progressing patient cohort, we infer that the mean HIV progression timeline from time of infection to AIDS stage is 5.75 years. The model predicts that the peak in viral load during acute HIV infection is due to virus production by infected CD4+ T cells, while during the clinically latent and late phases of infection infected macrophages dominate the overall viral production. This leads to the conclusion that macrophage-induced virus production is the significant driver of HIV progression from asymptomatic phase to AIDS in HIV-infected individuals.

Keywords: Viral immune dynamics, HIV-1, CD4+ T cells, macrophages, mathematical model, system dynamics model

2.2 Introduction

In this study, we analyze viral and immune system dynamics of HIV-1 infection. Hereafter, HIV refers to HIV-1 and the HIV-2 dynamics is not included. CD4+ T cells are the major target population in the blood and lymph nodes of HIV-infected individuals (19; 20; 21). However, other immune cells that express the CD4 entry receptor and chemokine coreceptor CCR5 and CXCR4 on their surfaces can also serve as target cells for HIV. Among them, macrophages are one of the main target cells for HIV (22; 23; 24; 25; 26; 27). Macrophages along with CD4+ T cells contribute to HIV replication in HIV-infected individuals during the acute, clinically latent, and late phases of HIV progression from acute infection, clinical latency to AIDS stage.

2.2.1 Acute phase of HIV infection: Acute infection

The acute phase of HIV infection lasts for around 12 weeks from initial infection, with onset of acute retroviral syndrome 2 to 4 weeks after initial infection. Symptoms include fever, chills, rash, night sweats, muscle aches, sore throat, fatigue, swollen lymph nodes and mouth ulcers. In newly infected HIV individuals, HIV initially replicates primarily in infected CD4+ T cells at the mucosal infection site (28; 29). Dendritic cells and macrophages secrete chemokines that signal the migration of T lymphocytes to the site of infection, which amplifies infection by increasing the number of target cells, and also promote CD4+ T cell infection by transferring virions they have captured or are producing to CD4+ T cells. (30). Following virus replication at the transmission site and amplification in draining lymph nodes, infection undergoes systemic spread and a high level of HIV is observed in the plasma (31; 32). Although HIV primarily replicates in CD4+ T cells, with activated CD4+ T cells in gut associated lymphoid tissues constituting a major substrate for infection, other cell types, including monocytes and macrophages, are also infected during the acute phase of infection. Importantly macrophages are migratory and can traffic into tissues, carrying virus. There are

also specialized subsets of long-lived macrophages that reside in organs such as brain and lung, which can also become infected (33). Thus, macrophages play an important role in spreading the virus to different organs, and can constitute long-lived sites of HIV infection within tissues.

2.2.2 Clinically latent phase of HIV infection: Clinical latency

The clinically latent phase of HIV infection lasts for an average of around 9 years, and HIV-infected individuals are primarily asymptomatic during this phase, despite the fact that moderate-high levels of viral replication continue over time (34; 35). While most HIV-infected CD4+ T cells are eliminated due to virus cytopathicity and lysis by CD8 T cells and NK cells as part of the host immune response, a fraction of them become latently infected and do not produce virus (36). HIV also establishes a latent infection in macrophages (37). Latently infected macrophages have a long lifespan and act as HIV reservoirs that are invisible to cytotoxic T lymphocytes (38; 39). Thus, they pose a major challenge in eliminating HIV from infected individuals (22), and contribute to the progression toward the late phase of symptomatic AIDS. Macrophages also contribute to HIV pathogenesis by promoting inflammation, which has a variety of detrimental effects and promotes disease progression.

2.2.3 Late phase of HIV infection: AIDS stage

The circulating CD4+ T cell count undergoes a gradual decline during the clinically latent phase of infection; but in the later stages of infection there is an increase in viral replication and more rapid decline in CD4+ T cell numbers. Continual decline in the number of CD4+ T cells lead to an impaired immune response and acquired immune deficiency syndrome (AIDS). When the CD4+ T cell counts declines to 200 cells/mm^3, the HIV-infected individual is defined as having AIDS (40; 41). The late phase of HIV infection lasts for around 2 years, and infected individuals experience symptoms of fatigue, diarrhea, nausea, vomiting,

fever, chills, night sweats and wasting syndrome, and are vulnerable to opportunistic infections. During the AIDS phase, CD4+ T cells are highly depleted, while actively infected macrophages are increasing. Studies in SIV-infected macaques have shown that monocyte turnover and death of tissue macrophages are good predictors of disease progression in the later stages of infection, suggesting an important role for cells of the monocyte/macrophage lineage in pathogenesis at this time (42; 43; 44).

2.2.4 Mathematical models of macrophage dynamics during HIV infection

Mathematical models have been developed to study HIV viral immune dynamics, considering the impact of macrophages on HIV progression to AIDS (45; 46). But, there are a lack of mathematical models to analyze the dynamics of HIV infected macrophages during all three phases of HIV infection. We address this gap by developing a new mathematical model that includes the long term dynamics of macrophages in HIV progression to AIDS from acute to clinically latent to late phases and finally to AIDS. The deterministic mathematical model formulates the viral and immune system dynamics of HIV, CD4+ T cells and macrophages to simulate the progression dynamics from acute infection, clinical latency to AIDS stage in treatment naive HIV-infected individuals.

2.2.5 Clinical significance

HIV within macrophages in different tissues constitutes an important reservoir for virus persistence during the course of HIV infection, thereby making HIV elimination challenging. Understanding and analysing macrophage dynamics during the phases of acute infection, clinical latency and progression to the AIDS stage in HIV-infected individuals will assist in design of improved and macrophage targeted therapeutic regimens.

2.2.6 Study objective

The study objective is to analyze the dynamics of HIV, CD4+ T cells and macrophages during acute, clinically latent and late phases of HIV infection to estimate the HIV progression dynamics from acute infection to clinical latency and finally to AIDS stage in treatment naive HIV-infected individuals.

2.2.7 Ethical approval

The Institutional Review Board at Virginia Tech gave ethical approval for this study. We used clinical data of CD4+ cell count and viral load of 39 patients, which were collected with informed consent, from a prior study (47).

2.3 Methods

We develop a mathematical model, using ordinary differential equations, to formulate the viral-immune dynamics of HIV, CD4+ T cells and macrophages. We calibrate the model and estimate infection parameters using longitudinal data of viral-immune dynamics from a cohort of 39 treatment naive HIV-infected individuals, collected at Mortimer Market Centre in London, UK (47).

2.3.1 Conceptual model

Figure 2.1 illustrates the viral and immune system dynamics of HIV, CD4+ T cells and macrophages. CD4+ T cells mature from thymus or are generated in the periphery as a consequence of proliferation of existing CD4+ T cells, and die at a constant rate. Macrophages residing in tissues (including both monocyte-derived tissue macrophages and self-renewing tissue-resident macrophage populations), die at a constant rate. HIV virions can infect CD4+ T cells and macrophages, and they are cleared at a constant rate. A fraction of the infected cells become latently infected (do not produce HIV virions), and the remaining fraction become actively infected (can produce HIV virions) (48; 49; 50). CD4+ T cells and macrophages that are latently infected become the long term reservoir for HIV replication. The latently infected CD4+ T cells and latently infected macrophages become actively infected at different constant rates. Death rates of uninfected and latently infected CD4+ T cells are equal, while death rates of actively infected CD4+ T cells are significantly higher. Actively infected CD4+ T cells release HIV virions during their lifespan and subsequently undergo lytic death. Macrophages include long-lived cell populations that may live for the life time of the HIV-infected individual. Death rates of uninfected and latently infected macrophages are equal (51), while death rate of actively infected macrophages can be higher. Actively infected macrophages release HIV virions at a constant rate.

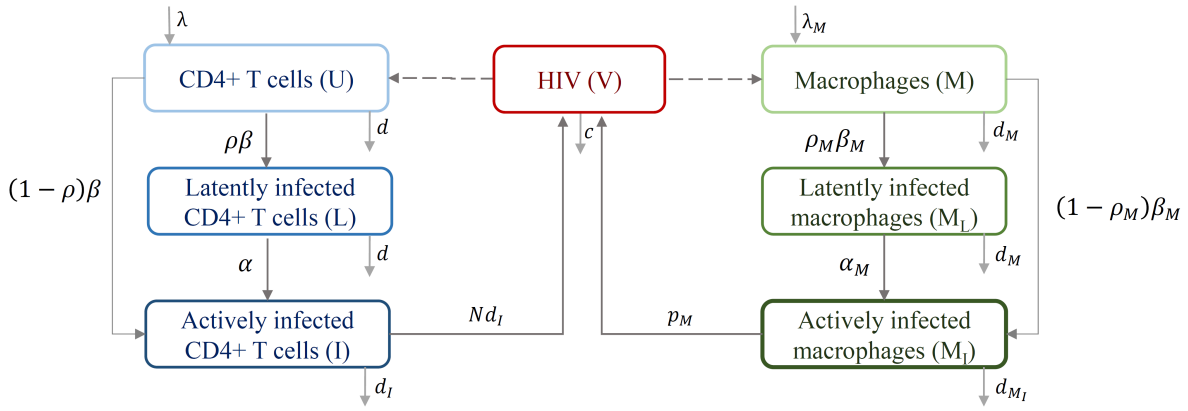

Figure 2.1: **Conceptual model of HIV viral immune dynamics.** The figure illustrates the viral and immune system dynamics of HIV, CD4+ T cells and macrophages. While HIV virions can infect CD4+ T cells and macrophages, HIV is cleared at a constant rate. A fraction of the infected cells become latently infected (do not produce new virions), and the remaining fraction become actively infected (can produce new virions).

2.3.2 Model parameters

Table 2.1 illustrates the parameters for mathematical modeling of the viral and immune system dynamics of CD4+ T cells, macrophages and HIV during the acute, clinically latent, and late phases of HIV progression from acute infection, clinical latency to AIDS stage.

Uninfected CD4+ T cells reproduce at rate λ=10 cells per mm^3 per day (52). Macrophages production rate is assumed to be λ_M=0.15 per mm^3 per day (53). Since establishment of latent infection in infected CD4+ T cells is rare, we assumed that the CD4+ T cells fraction that results in latent infection is $\rho = 1.5 \times 10^{-6}$ (54; 48; 36). Latently infected CD4+ T cells get activated at rate α=0.01 per day (36). Latently infected macrophages get activated at rate $\rho_M = 8 \times 10^{-3}$ per day (50). In average N=1200 virions are produced by an infected CD4+ T cell during its lifespan (53). Death rate of uninected and latently infected CD4+ T cells are assumed to be similar $d_M = 5{\times}10^{-3}$ per day (53; 51). Death rate of actively infected CD4+ T cells increases significantly compared to uninfected or latently infected CD4+ T cells and is assumed to be d_I=0.39 per day (55). Other parameters are estimated through the model calibration process.

Table 2.1: **Model parameters and state variables for viral and immune system dynamics of CD4+ T cells, macrophages and HIV.** The table illustrates the state variables and parameters used in within-host modeling of the viral and immune system dynamics of CD4+ T cells, macrophages and HIV during the acute, clinically latent, and late phases of HIV progression from acute infection, clinical latency to AIDS stage. The initial values of the viral load, and the values and ranges of parameters are primarily from prior studies. The values of two state variable, two CD4+ T cell related parameter, five macrophage related parameters, and one HIV related parameter are estimated by fitting the model to the longitudinal clinical data of CD4+ T cells count and viral load of HIV-infected individuals.

Variable	**Description**	**Initial Value**	**Unit**	**Reference**
U	Uninfected CD4+ T cells	(500, 1260.72)	cells.mm^{-3}	fitted
L	Latently infected CD4+ T cells	0	cells.mm^{-3}	-
I	Actively infected CD4+ T cells	0	cells.mm^{-3}	(53)
M	Uninfected macrophages	(231.3, 530.6)	cells.mm^{-3}	fitted
M_L	Latently infected macrophages	0	cells.mm^{-3}	-
M_I	Actively infected macrophages	0	cells.mm^{-3}	(53)
V	HIV virions	10^{-3}	virions.mm^{-3}	(53)

Parameter	**Description**	**Value**	**Unit**	**Range**	**Reference**
λ	CD4+ T cell production rate	10	mm^{-3}day^{-1}	$(7, 20)$	(52; 45)
λ_M	Macrophage production rate	0.15	mm^{-3}day^{-1}	$(0.1, 0.3)$	(53)
β	CD4+ T cell infection rate	4.60×10^{-5}	mm^{3}day^{-1}	$(2.40 \times 10^{-5}, 9.85 \times 10^{-5})$	fitted
β_M	Macrophage infection rate	4.32×10^{-8}	mm^{3}day^{-1}	$(4.22 \times 10^{-8}, 4.33 \times 10^{-8})$	fitted
ρ	CD4+ T cells latent infection fraction	1.5×10^{-6}		$(1.5 \times 10^{-9}, 1.5 \times 10^{-1})$	(48)
ρ_M	Macrophages latent infection fraction	0.7		$(10^{-4}, 1)$	fitted
α	Activation rate of latently infected CD4+ T cells	0.01	day^{-1}	$(10^{-4}, 10^{-2})$	(36)
α_M	Activation rate of latently infected macrophages	8×10^{-3}	day^{-1}	$(10^{-4}, 10^{-2})$	(50)
$a \times M_{max}$	Growth rate of macrophages	1.781	mm^{-3}day^{-1}	(1, 2.138)	fitted
N	HIV production by CD4+ T cell burst	1200	virions	(1000, 1200)	(53; 56; 57)
p_M	HIV production rate by macrophages	312.4	virions.day^{-1}	(183.5, 500)	fitted
c	HIV clearance rate	2324.46	day^{-1}	(23, 50.95)	fitted
d	Death rate of uninfected CD4+ T cells; Death rate of latently infected CD4+ T cells	0.012	day^{-1}	$(0.008, 0.02)$	fitted
d_M	Death rate of uninfected macrophages; Death rate of latently infected macrophages	5×10^{-3}	day^{-1}	$(10^{-4}, 10^{-2})$	(53; 51)
d_I	Death rate of actively infected CD4+ T cells	0.39	day^{-1}	$(0.15, 0.5)$	(57; 55; 45)
d_{M_I}	Death rate of actively infected macrophages	5.39×10^{-3}	day^{-1}	$(5 \times 10^{-3}, 6 \times 10^{-3})$	fitted

2.3.3 Mathematical model

The mathematical model defines the viral and immune system dynamics of HIV, CD4+ T cells and macrophages, as formulated in the ordinary differential equations (see equation set 2.1), and illustrated in Figure 2.1. The model parameters and state variables, and their values and ranges are described in Table 2.1.

$$
\begin{aligned}
\frac{dU}{dt} &= \lambda - \beta UV - dU \\
\frac{dL}{dt} &= \rho\beta UV - dL - \alpha L \\
\frac{dI}{dt} &= (1-\rho)\beta UV - d_I I + \alpha L \\
\frac{dM}{dt} &= \lambda_M - \beta_M MV - d_M M + M\gamma(M) \\
\frac{dM_L}{dt} &= \rho_M \beta_M MV - d_M M_L - \alpha_M M_L \\
\frac{dM_I}{dt} &= (1-\rho_M)\beta_M MV - d_{M_I} M_I + \alpha_M M_L \\
\frac{dV}{dt} &= N d_I I + p_M M_I - cV
\end{aligned}
\tag{2.1}
$$

The equations illustrate the system dynamics between HIV virions (V), CD4+ T cells and macrophages. CD4+ T cells are in uninfected (U), latently infected (L) and actively infected (I) states; similarly, macrophages are in uninfected (M), latently infected (M_L) and actively infected (M_I) states. CD4+ T cells and macrophages are infected by HIV virions at the rate of β and β_M respectively. A fraction (ρ and ρ_M) of the infected cells become latently infected and do not produce new HIV virions, while the remaining fraction ($1-\rho$ and $1-\rho_M$) become actively infected and produce new HIV virions. Latently infected CD4+ T cells and macrophages become actively infected at rates α and α_M respectively. HIV virions are produced by actively infected CD4+ T cells and macrophages at rates Nd_I and p_M respectively.

Decline in macrophages causes an increase in their production through differentiation from monocytes or production from tissue resident precursors to reach the homeostatic level (58) with the rate $\gamma(M)$, as de-

scribed in Equation 4.2. M_{max} is the maximum carrying capacity for macrophages, and a is the macrophage growth coefficient. Macrophage production is density dependant and slows down when the cell density reaches its homeostatic level (27).

$$\gamma(M) = a\frac{M_{max}}{M + M_L + M_I} \tag{2.2}$$

2.3.4 Data source of treatment naive HIV-infected individuals

We use longitudinal data of viral load and CD4+ T cell counts for 39 treatment naive HIV-infected individuals, which were collected at the Mortimer Market Centre for Sexual Health and HIV Research (London, UK) and reported as part of prior studies (47). The subjects were recruited after presentation with symptomatic acute HIV infection. All HIV-infected individuals were offered anti-retroviral therapy following diagnosis, but the subjects included in this study declined treatment during the acute and early phases of HIV infection. They were mostly male Caucasians and many remained untreated until disease progression to AIDS stage. Viral load and CD4+ T cell counts of the study subjects were measured longitudinally at serial time-points following infection. Number of data points for each treatment naive HIV-infected individual is illustrated in table 2.2.

2.3.5 Model calibration

Model calibration involves input parameter estimation that resultes in optimal fit of the immune and viral system dynamics from the model simulations to the clinical data of the treatment naive HIV-infected individuals. Table 2.1 includes the values for the model parameters and state variables, some of which are obtained from prior studies, and others are estimated by fitting the model to data. We fit the viral load and CD4+ T cell count from the model simulations to the clinical longitudinal data of viral load and CD4+ T cell count for each of the 39 treatment naive HIV-infected individuals.

Model calibration to each HIV-infected individual: Unknown parameters are estimated for each HIV-infected individual by calibrating the viral load and all (uninfected, latently infected, and actively infected) CD4+ T cell count generated by the HIV viral system dynamics model (formulated by Equation set 2.1) to the longitudinal clinical data of HIV viral load and CD4+ T cell count for the corresponding individual, thereby enabling the analysis in each HIV-infected individual.

Model calibration to patient cohort: The mean estimates amongst the HIV-infected individuals in the cohort allow for the analysis of expected cohort dynamics.

2.3.6 Parameter estimation

We adapt the weighted absolute percentage error (WAPE) method (59) in the model calibration and estimating unknown parameters process. We minimize the sum of weighted absolute percentage error between the observed and estimated values of CD4+ T cell count, and weighted absolute percentage error between the (base 10) logarithms of the observed and estimated values of viral load. The model calibration and parameter estimation process is repeated for each individual patient.

Equation 2.3 illustrates the objective function and weighted absolute percentage error (WAPE) measure for the model calibration and parameter estimation process. n denotes the number of clinical observation time points for each treatment naive HIV-infected individual. $A_C(t)$ and $A_V(t)$ are the observed/actual values of the CD4+ T cell count and viral load respectively for the treatment naive HIV-infected individuals. $P_C(t)$ and $P_V(t)$ are the estimated/predicted values of CD4+ T cell count and viral load respectively from the HIV viral immune system dynamics model. Equation 2.4 illustrates the mean absolute percentage error to estimate the mean percentage error of fitted model to each data point for every treatment naive HIV-infected individual in the cohort.

$$WAPE = \left(\sum_{t=1}^{n} \frac{|A_C(t) - P_C(t)|}{A_C(t)} \right) + \left(\sum_{t=1}^{n} \frac{|log(A_V(t)) - log(P_V(t))|}{log(A_V(t))} \right) \tag{2.3}$$

$$MAPE = \left(\frac{\sum_{t=1}^{n} \frac{|A_C(t) - P_C(t)|}{A_C(t)}}{n} \right) + \left(\frac{\sum_{t=1}^{n} \frac{|log(A_V(t)) - log(P_V(t))|}{log(A_V(t))}}{n} \right) \tag{2.4}$$

2.3.7 Simulation timeline

We focus our simulation timeline on the predicted time to the late phase AIDS stage for each of the 39 treatment naive HIV-infected individuals in our patient cohort. HIV progression to AIDS is reached when the CD4+ T cell count declines to 200 cells/mm^3. Upon reaching a CD4+ T cell count of 200 cells/mm^3, the simulation time is extended for 2 more years to account for the AIDS stage.

2.3.8 Sensitivity analysis, and model verification and validation

Model verification involves the process of determining that the implementation of the mathematical model is a good representation of the conceptual model (60). Model validation involves the process of determining that the results of the mathematical model are a good representation of the real world dynamics. Sensitivity analysis is the process of determining the impact of uncertainty in the model parameters on the model simulations. We conduct sensitivity analysis, and verify and validate the HIV viral immune system dynamics model.

2.3.9 Model software

We implement the HIV viral immune system dynamics model, execute the model simulations, and analyze the simulation results using R computer programming language (61).

Table 2.2: **Number of data points, mean absolute percentage error (MAPE) for both CD4+ T cell counts and viral load, estimated time to AIDS, and estimated parameters for each treatment naive HIV-infected individual in the cohort.** Number of available data points, the estimated parameters and absolute percentage error is illustrated for each patient.

Patient	Data points	Error % (CD4)	Error % (viral load)	Years to AIDS	β	aM_{max}	β_M	d_{M_I}	c	d	p_M	ρ_M
1	28	46.77	46.29	15.11	4.01E-05	1.002	4.22E-08	0.005	26.49	0.010	471.78	0.351
2	15	19.79	64.29	3.55	6.12E-05	1.468	4.33E-08	0.006	23.00	0.019	309.83	0.700
3	13	30.08	48.96	4.95	4.34E-05	1.925	4.33E-08	0.005075	23.00	0.011	285.76	0.426
4	17	23.21	49.33	8.81	7.26E-05	1.929	4.33E-08	0.005045	31.52	0.015	238.31	0.498
5	16	31.02	44.64	5.67	4.06E-05	2.059	4.33E-08	0.006	23.00	0.010	286.74	0.472
6	15	44.98	49.24	3.72	4.02E-05	2.012	4.33E-08	0.005	23.00	0.010	350.00	0.0001
7	16	23.96	68.89	4.52	4.37E-05	2.069	4.33E-08	0.005	23.00	0.017	311.40	0.808
8	16	26.00	45.88	4.75	4.02E-05	1.989	4.33E-08	0.005	23.00	0.010	302.35	0.302
9	14	24.80	44.02	14.35	3.77E-05	1.997	4.33E-08	0.005	28.70	0.008	294.35	0.771
10	17	36.44	48.21	5.77	4.17E-05	1.979	4.33E-08	0.006	23.00	0.011	290.39	0.363
11	12	70.47	60.53	7.35	4.67E-05	1.479	4.33E-08	0.006	23.00	0.010	305.09	0.417
12	24	20.60	62.23	11.97	2.76E-05	1.000	4.33E-08	0.005	23.00	0.010	500.00	1.000
13	17	39.75	37.10	5.91	4.37E-05	1.947	4.33E-08	0.006	23.29	0.010	284.29	0.837
14	19	45.71	46.57	2.22	6.25E-05	2.105	4.33E-08	0.005669	23.00	0.014	277.38	0.865
15	15	41.60	46.83	7.36	3.63E-05	2.000	4.22E-08	0.006	23.00	0.010	300.00	0.500
16	20	52.11	50.64	14.17	4.26E-05	1.000	4.33E-08	0.005	23.00	0.010	350.00	0.700
17	14	33.08	54.69	3.97	6.03E-05	1.943	4.33E-08	0.005	25.42	0.014	269.26	0.578
18	9	10.86	47.81	3.92	4.24E-05	1.995	4.33E-08	0.005207	23.53	0.010	341.68	0.824
19	23	47.95	35.72	4.65	4.65E-05	1.991	4.33E-08	0.006	23.00	0.015	299.32	0.801
20	13	32.02	59.75	8.49	3.88E-05	1.816	4.33E-08	0.005	23.00	0.011	258.04	0.700
21	14	22.62	48.33	5.68	2.86E-05	2.138	4.33E-08	0.005	23.00	0.010	350.00	0.595
22	14	45.10	45.95	5.49	4.33E-05	1.991	4.33E-08	0.005	25.05	0.009	302.79	0.700
23	17	44.91	29.19	4.81	4.00E-05	2.000	4.33E-08	0.005	23.00	0.010	300.00	0.568
24	17	55.09	26.98	2.99	7.94E-05	1.453	4.33E-08	0.006	23.35	0.019	183.54	0.539
25	15	48.75	50.46	9.54	4.23E-05	1.299	4.33E-08	0.006	23.00	0.010	350.00	0.700
26	7	47.63	44.66	4.61	4.27E-05	1.998	4.33E-08	0.005011	23.02	0.011	293.09	0.600
27	13	37.39	39.90	3.30	5.10E-05	1.965	4.33E-08	0.006	23.00	0.012	316.34	0.642
28	4	21.24	85.50	8.17	2.40E-05	2.000	4.33E-08	0.005	23.00	0.010	350.00	0.706
29	10	39.36	75.55	2.80	5.22E-05	1.991	4.33E-08	0.005	23.00	0.017	351.25	0.370
30	5	65.20	75.12	4.81	4.00E-05	2.000	4.33E-08	0.005	23.00	0.010	300.00	0.542
31	6	37.48	54.04	4.81	4.00E-05	2.000	4.33E-08	0.005	23.00	0.010	300.00	0.250
32	9	34.69	61.70	1.79	9.85E-05	2.022	4.33E-08	0.006	28.64	0.020	232.37	0.498
33	9	31.21	41.22	4.67	4.08E-05	1.999	4.33E-08	0.005	23.00	0.011	301.22	0.685
34	16	55.07	55.27	4.12	4.50E-05	1.990	4.33E-08	0.005	23.00	0.012	299.94	0.332
35	23	24.03	48.31	4.22	4.55E-05	1.973	4.33E-08	0.005161	23.00	0.012	297.64	0.120
36	8	79.22	61.93	5.72	5.34E-05	1.050	4.33E-08	0.005034	23.00	0.010	350.00	0.700
37	9	28.66	42.64	>30	6.47E-05	1.849	4.33E-08	0.006	50.95	0.008	277.54	0.311
38	11	34.20	48.89	>30	2.63E-05	1.003	4.33E-08	0.006	23.00	0.010	350.00	0.700
39	10	40.31	78.87	>30	2.92E-05	1.018	4.33E-08	0.006	23.01	0.010	350.00	0.367
Mean	**14**	**38.29**	**51.95**	**6.08**	**4.6E-05**	**1.781**	**4.32E-08**	**0.00539**	**24.46**	**0.012**	**312.35**	**0.698**

2.4 Results

2.4.1 Model calibration

While many parameters of HIV viral immune dynamics are obtained from prior studies, we estimated the remaining parameters by calibrating the model for an optimal fit between the clinical data and the model simulation for CD4+ T cell count and viral load, as illustrated in table 2.1. Model calibration and parameter estimation were conducted for each patient separately. The values of estimated parameters for each patient and mean absolute percentage error (see equation 2.4) from each data point are illustrated in table 2.2. The simulation results show reaching the AIDS stage with simulated CD4+ T cell count declining below 200 cells/mm^3 for 36 patients, while 3 patients reached an equilibrium state with a CD4+ T cell count above 200 cells/mm^3.

2.4.2 Parameter estimation

Table 2.1 includes the values for the estimated parameters. The mean estimated value for CD4+ T cell infection rate (β) is 4.60×10^{-5} mm^{3}day^{-1} (range: 2.4×10^{-5}, 9.85×10^{-5}). The mean estimated value for macrophage infection rate (β_M) is 4.32×10^{-8} mm^{3}day^{-1} (range: 4.22×10^{-8}, 4.33×10^{-8}). The mean estimated value for macrophages latent infection fraction (ρ_M) is 0.7 (range: 10^{-4}, 1). The mean estimated value for growth rate of macrophages ($a \times M_{max}$) is 1.781 mm^{-3}day^{-1} (range: 1, 2.138). The mean estimated value for death rate of infected macrophages (d_{M_I}) is 5.039×10^{-3} day^{-1} (range: 5×10^{-3}, 6×10^{-3}). The mean estimated value for HIV clearance rate (c) is 34.46 day^{-1} (range: 23, 50.95). The mean estimated value for death rate of uninfected or latently infected CD4+ T cells (d) is 0.012 day^{-1} (range: 0.008, 0.02). The mean estimated value for HIV production rate by macrophages (p_M) is 312.4 virions.day^{-1} (range: 183.5, 500).

2.4.3 Viral and immune system dynamics of HIV, CD4+ T cells and macrophages

We simulated the viral and immune system dynamics of HIV, CD4+ T cells and macrophages, as illustrated in Figure 2.2. The simulation is based on the known model parameter values, and mean values of estimated model parameters for the 39 treatment naive HIV-infected individuals in the patient cohort. The simulation results show a rapid decline in CD4+ T cell count and rapid increase in the HIV viral load during the acute phase of HIV infection. CD4+ T cell count recovers to a higher level but lower than the initial value before HIV infection, while HIV viral load stabilizes to a relatively lower level at the end of the acute phase in comparison to the earlier part of the acute phase. During the clinically latent and late phases of HIV infection, CD4+ T cell count declines and HIV viral load increases. We assumed that HIV progression to the AIDS stage is reached when CD4+ T cell count declines to 200 cells/mm^3. The results show macrophage numbers remain relatively stable during the three phases of HIV infection, while viral production from macrophages primarily drives the decline in CD4+ T cell count and increase in viral load during the clinically latent and late phases of HIV infection. During the transition from acute to clinically latent phase of HIV infection, CD4+ T cells had recovered to around 400 cells/mm^3, and then declined continually during the clinically latent and late phases of HIV infection. Due to the described dynamics in the model, the mean length of time for progression to the AIDS stage, when CD4+ T cell count has declined to 200 cells/mm^3, is estimated to be 5.75 years.

2.4.4 HIV and CD4+ T cell dynamics in each HIV-infected individual

The HIV viral immune system dynamics model was calibrated to the longitudinal clinical data of HIV viral load and CD4+ T cell count, and unknown parameters were estimated for each of the 39 treatment naive HIV-infected individuals in the patient cohort. Figure 2.3 illustrates the dynamics of HIV viral load and CD4+ T cell dynamics during the acute, clinically latent and late phases of HIV infection in the 36 patients

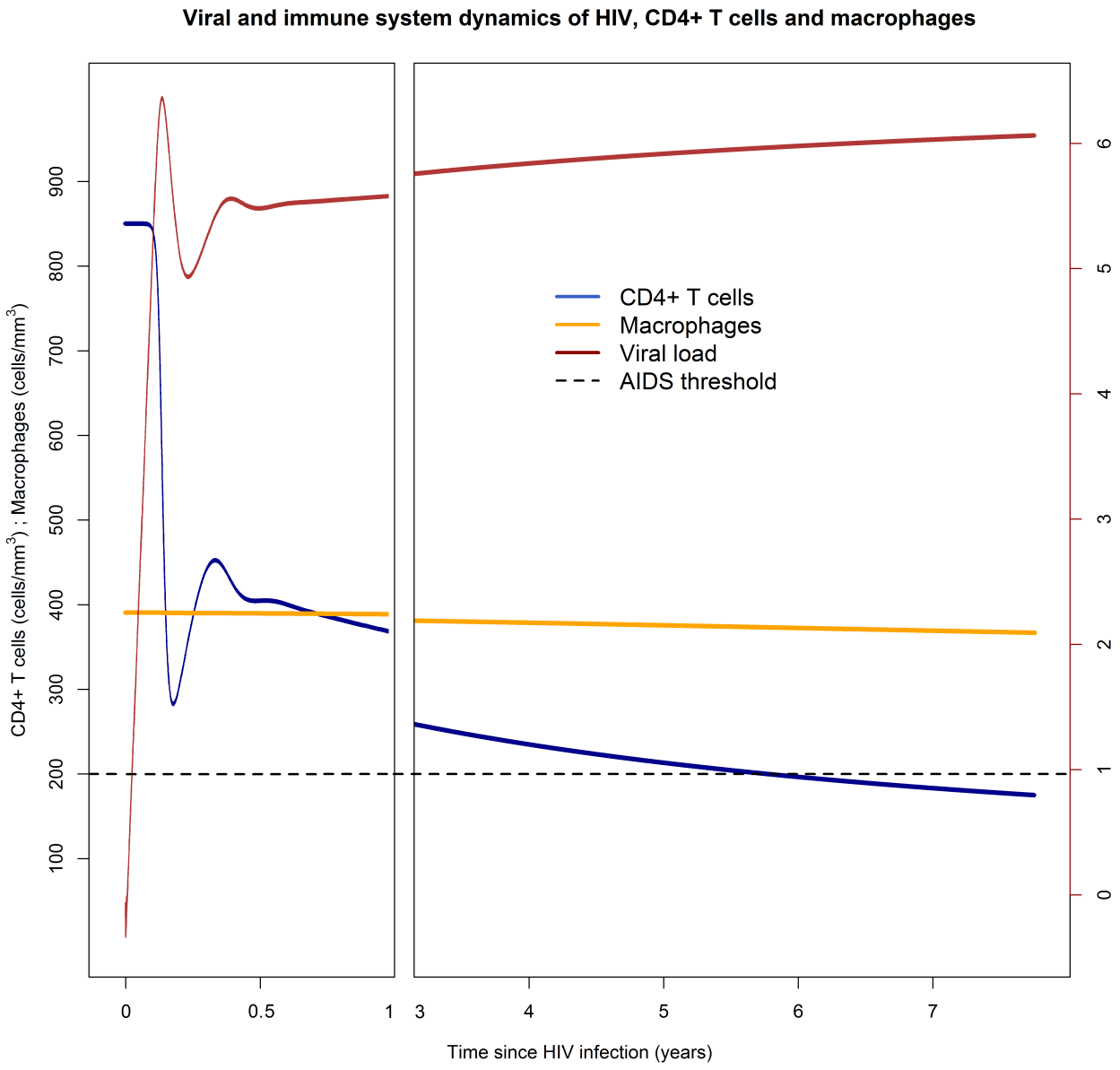

Figure 2.2: **Viral and immune system dynamics of HIV, CD4+ T cells and macrophages.** The figure illustrates the dynamics of CD4+ T cells (y-axis on the left), macrophages (y-axis on the left), and HIV viral load (y-axis on the right in base-10 log scale) since time of HIV infection (x-axis). The x-axis is broken to show the HIV dynamics during the acute phase.

who reached the AIDS stage, as per the simulation results. CD4+ T cell count declined to below 200 cells/mm^3 during the AIDS stage in these 36 patients. Figure 2.4 illustrates the dynamics of HIV viral load and CD4+ T cell dynamics during the acute and clinically latent phases of HIV infection in the 3 patients who did not reach the AIDS stage, as per the simulation results. CD4+ T cell count reached an equilibrium above 200 cells/mm^3 in these 3 patients.

(a)

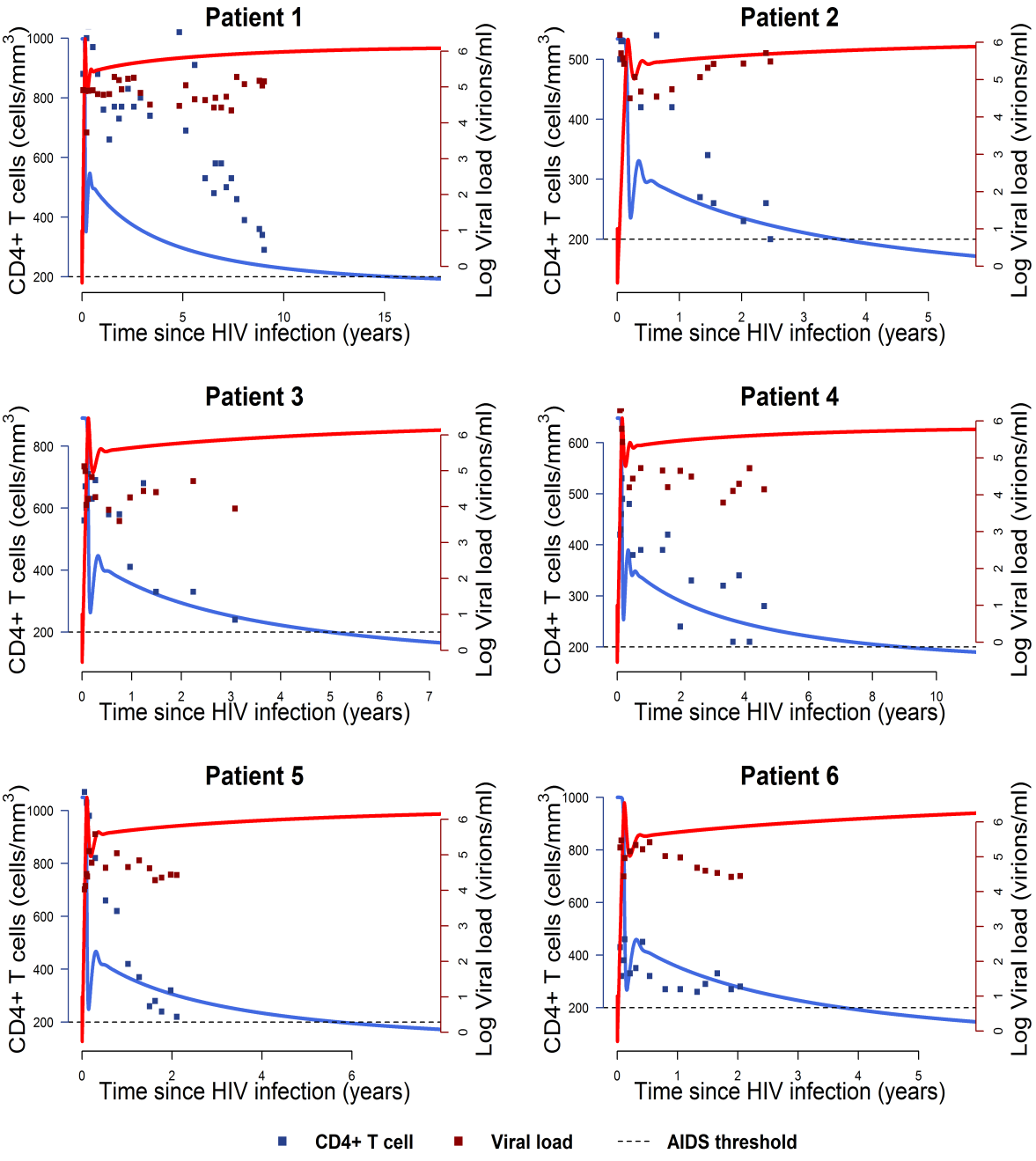

Figure 2.3: **HIV and CD4+ T cell dynamics in each HIV-infected individual who reached AIDS stage.** The HIV viral immune system dynamics model was calibrated to the longitudinal clinical data of CD4+ T cell count (blue points) and HIV viral load (red points), and unknown parameters were estimated for each treatment naive HIV-infected individual in the patient cohort who reached the AIDS stage. CD4+ T cell count (blue line) and HIV viral load (red line) are based on the simulation results from the HIV viral immune system dynamics model. CD4+ T cell count declined to 200 cells/mm^3 among 36 patients, who reached the late phase of AIDS stage. **(a)** Dynamics of CD4+ T cell and HIV viral load for HIV-infected individuals 1 to 6 in the patient cohort.

(b)

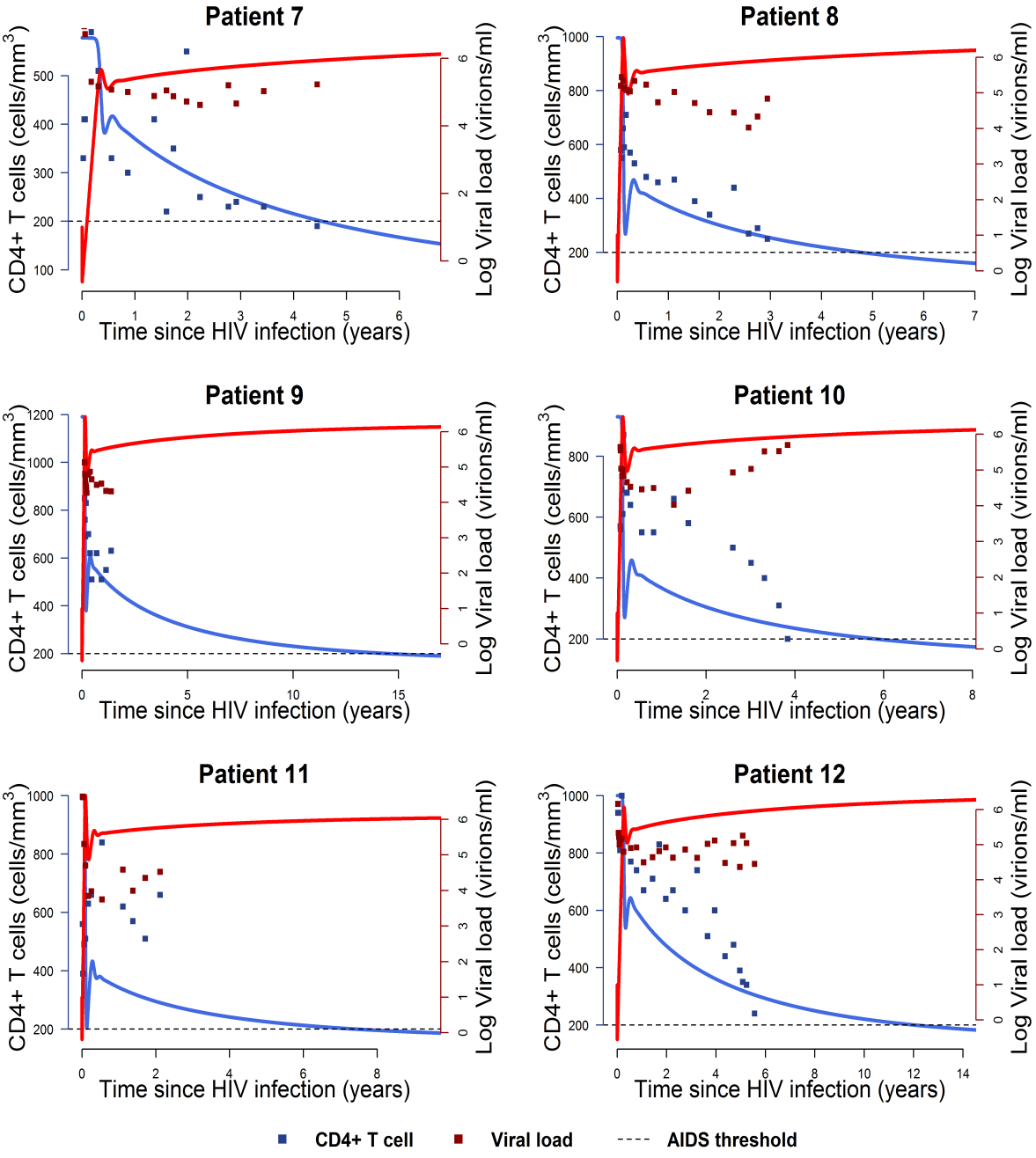

Figure 2.3: **(b)** Dynamics of CD4+ T cell and HIV viral load for HIV-infected individuals 7 to 12 in the patient cohort.

(c)

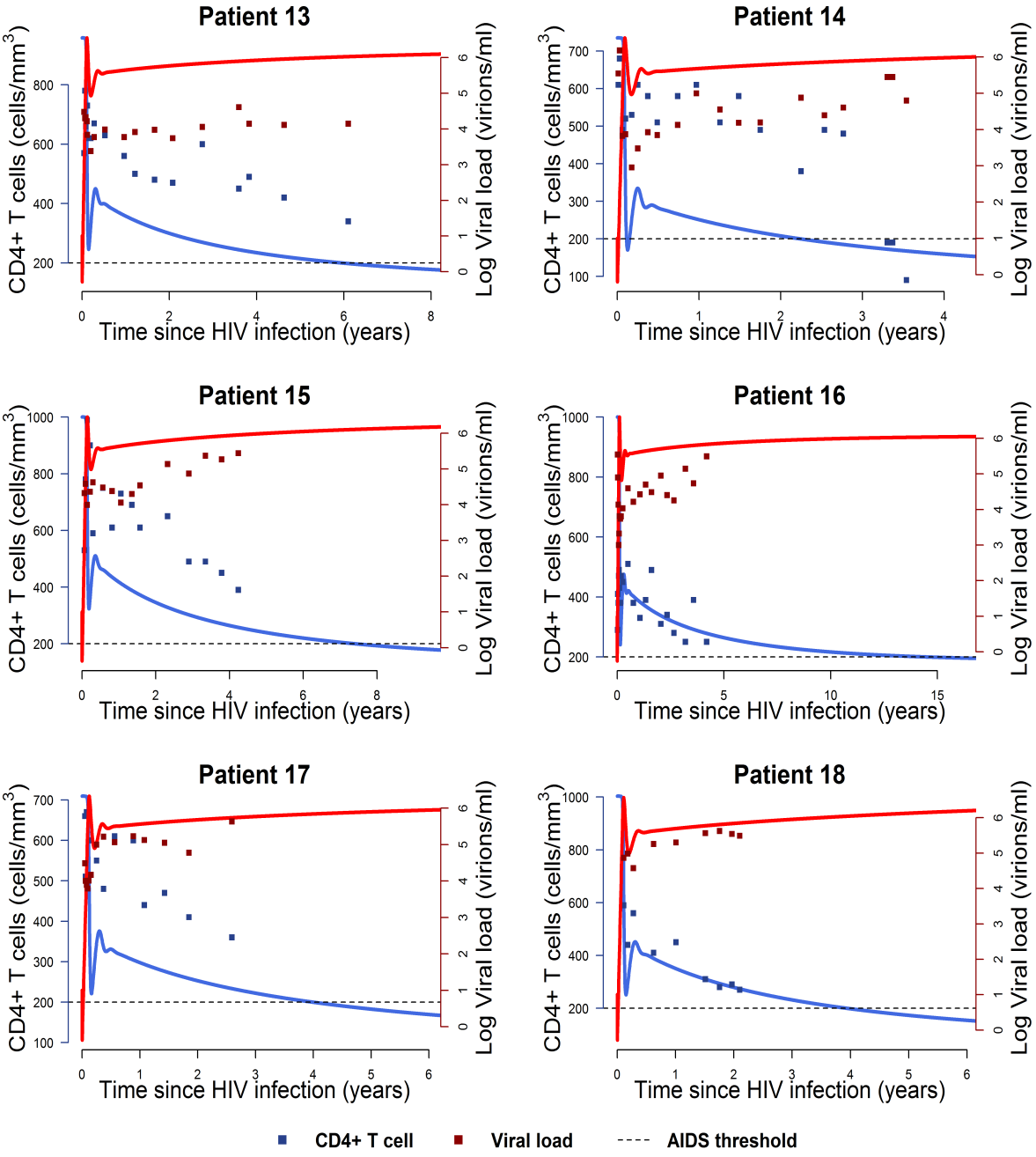

Figure 2.3: **(c)** Dynamics of CD4+ T cell and HIV viral load for HIV-infected individuals 13 to 18 in the patient cohort.

(d)

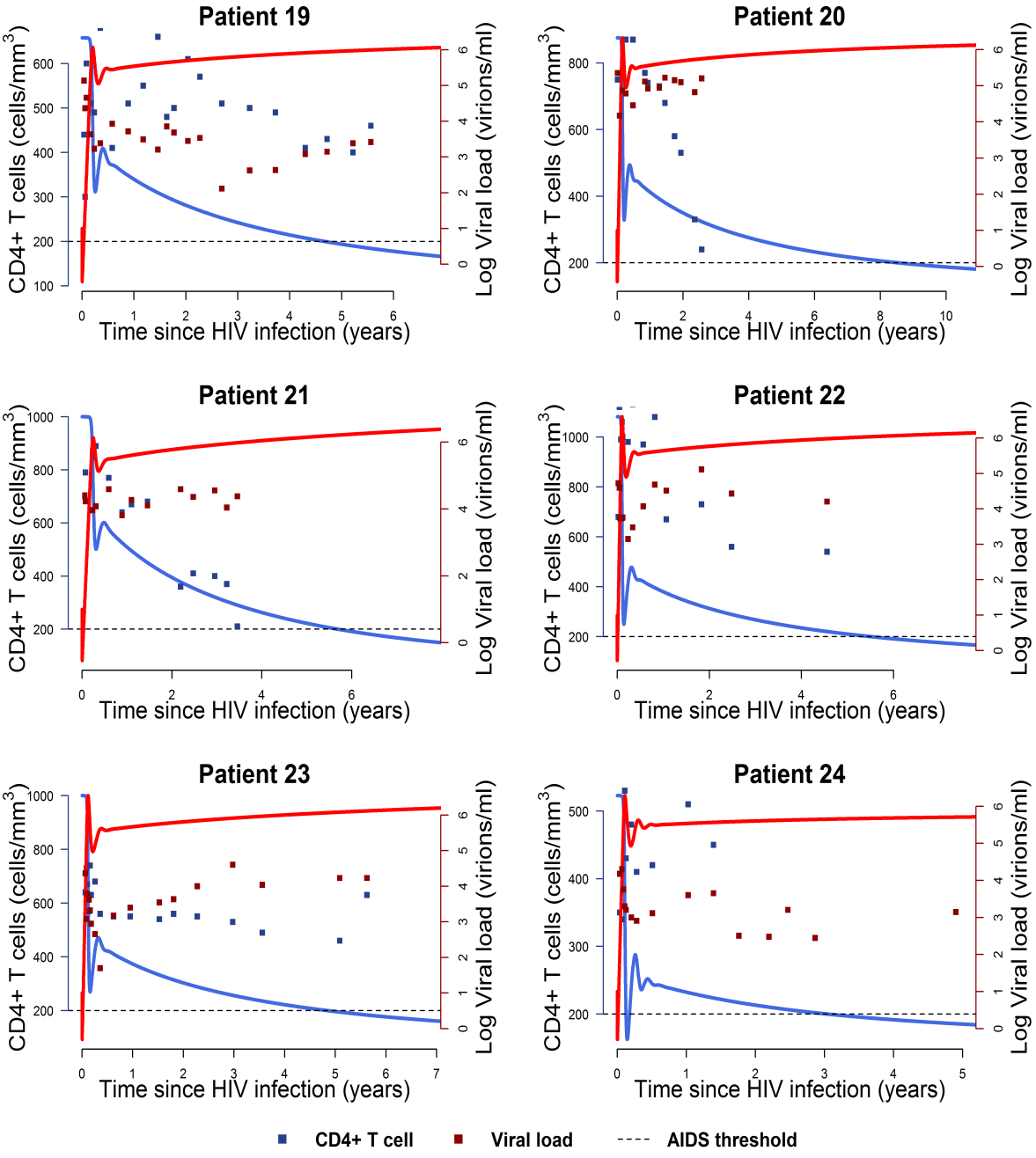

Figure 2.3: **(d)** Dynamics of CD4+ T cell and HIV viral load for HIV-infected individuals 19 to 24 in the patient cohort.

(e)

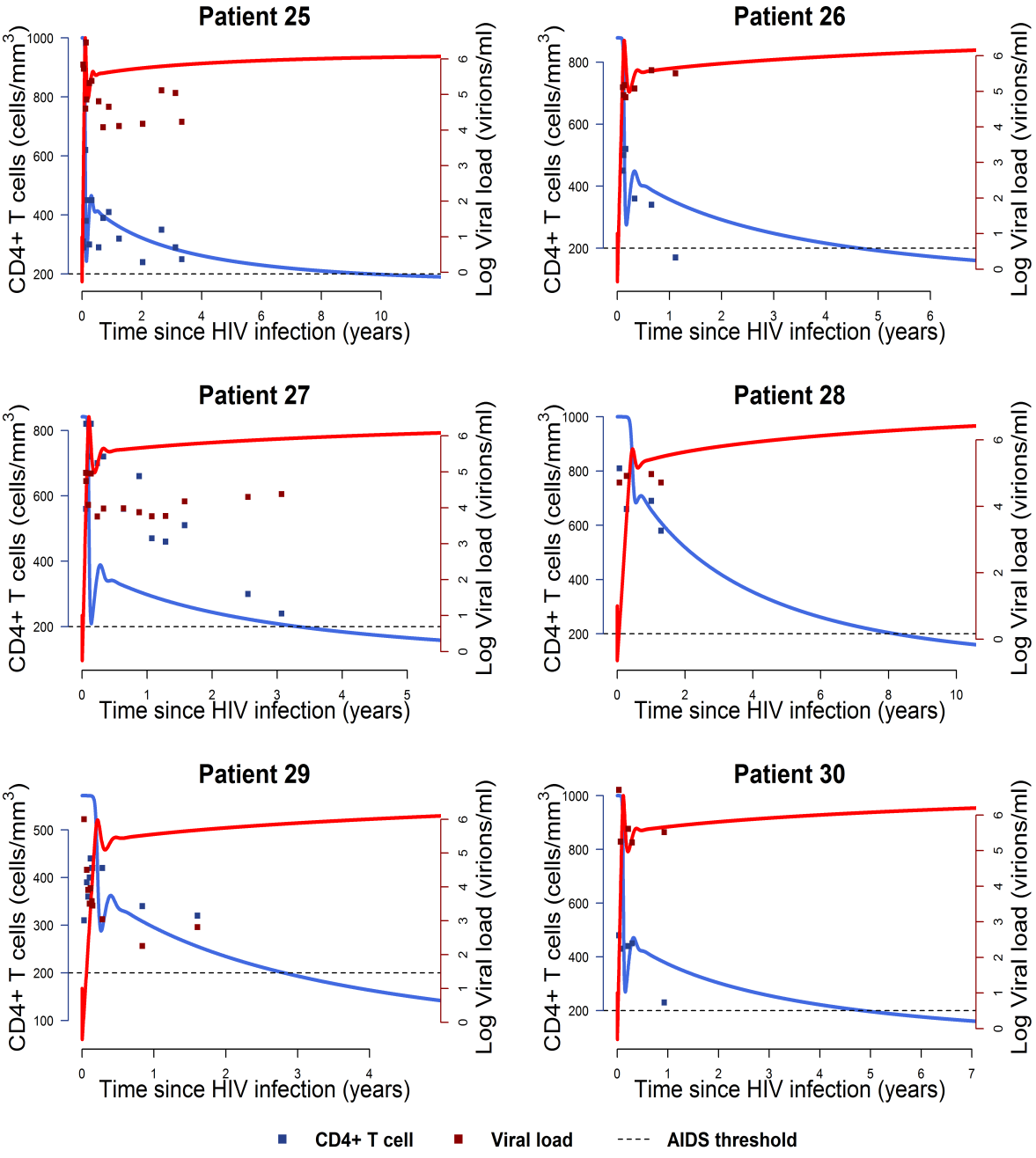

Figure 2.3: **(e)** Dynamics of CD4+ T cell and HIV viral load for HIV-infected individuals 25 to 30 in the patient cohort.

(f)

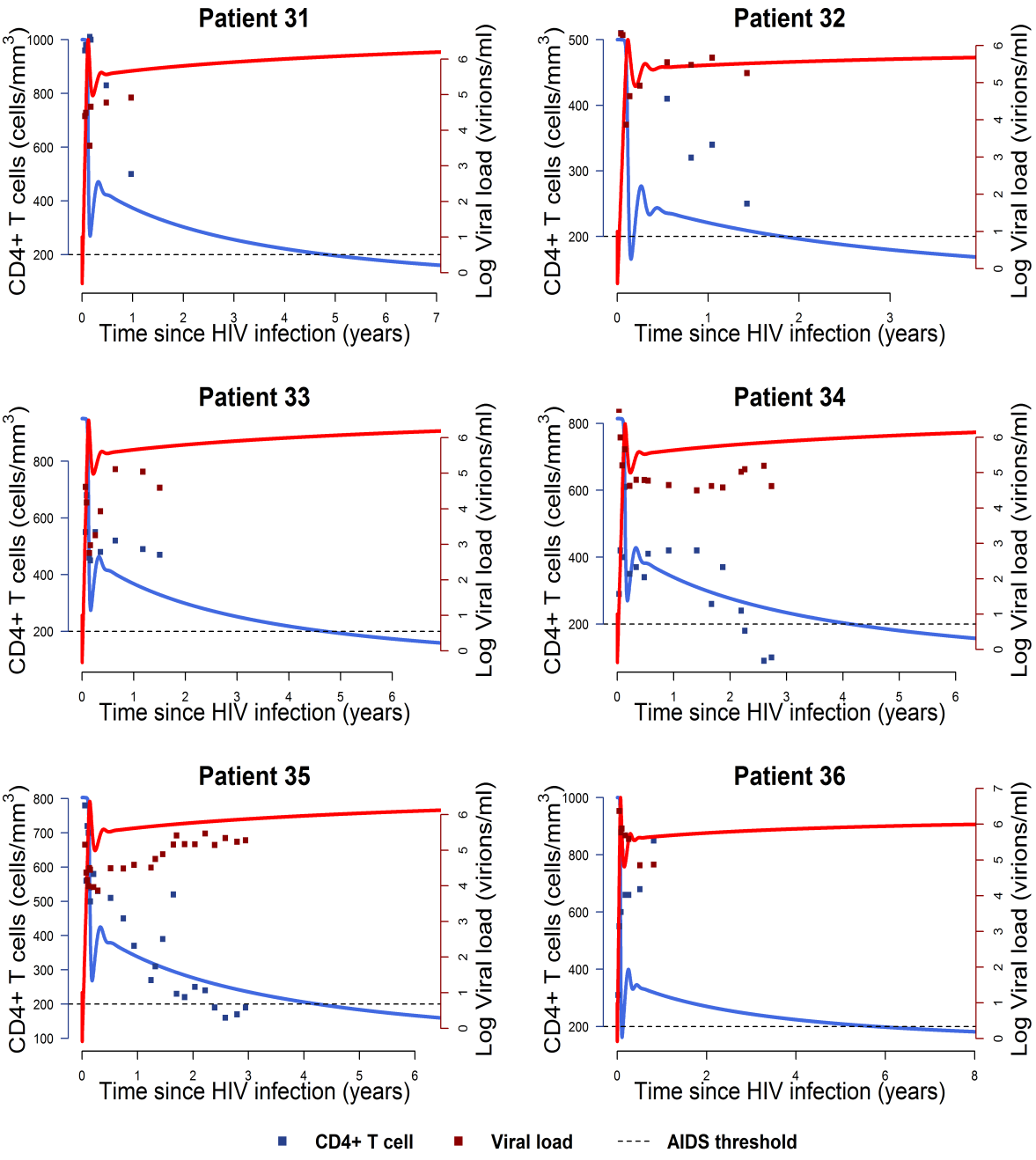

Figure 2.3: **(f)** Dynamics of CD4+ T cell and HIV viral load for HIV-infected individuals 31 to 36 in the patient cohort.

2.4.5 CD4+ T cell dynamics in HIV-infected individuals

Figure 2.5 illustrates the simulated dynamics of uninfected (Figure 2.5a), latently infected (Figure 2.5b), actively infected (Figure 2.5c), and all (Figure 2.5d) CD4+ T cells in the 39 treatment naive HIV-infected individuals during the acute, clinically latent and late phases of HIV infection. The simulation results show that uninfected CD4+ T cells decline at a higher rate during the acute phase, while they decline at a lower rate during the clinically latent phase of HIV infection. A low proportion of CD4+ T cells become latently infected. Therefore their impact on reproduction of HIV is not significant. The actively infected CD4+ T cells increase rapidly during the first part of the acute phase and decline to a lower level by the end of acute phase, and similar levels are maintained during the clinically latent and late phases of HIV infection. As seen in the simulation, the total CD4+ T cells decline at a high rate during the acute phase and recover to a level lower than before HIV infection, then decline at a relatively low rate during the clinically latent phase.

2.4.6 Macrophage dynamics in HIV-infected individuals

Figure 2.6 illustrates the dynamics of uninfected (Figure 2.6a), latently infected (Figure 2.6b), actively infected (Figure 2.6c), and all (Figure 2.6d) macrophages in the 39 treatment naive HIV-infected individuals of the patient cohort during the acute, clinically latent and late phases of HIV infection. While the uninfected macrophages decline at a low rate throughout infection, latently infected and actively infected macrophages increase at similar rates during the clinically latent and late phases of HIV infection. As seen in the simulation, the total macrophages decline at a low rate throughout the infection. However due to the activation of latently infected macrophages, rate of decline in total macrophages increases during later phases of HIV infection.

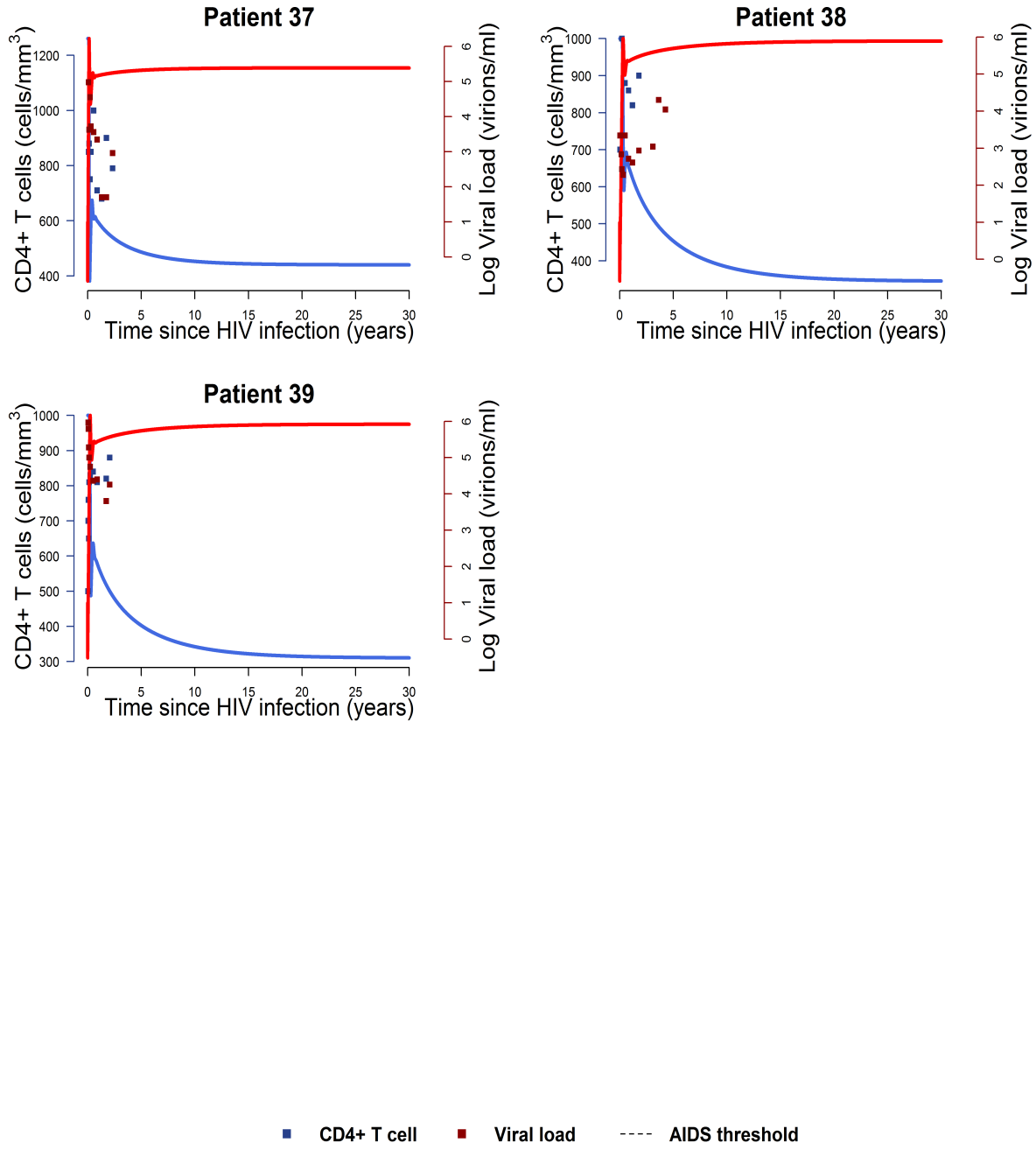

Figure 2.4: **HIV and CD4+ T cell dynamics in each HIV-infected individual who did not reach AIDS stage.** The HIV viral immune system dynamics model was calibrated to the longitudinal clinical data of CD4+ T cell count (blue points) and HIV viral load (red points) and unknown parameters estimated for each treatment naive HIV-infected individual in the patient cohort who did not reach the AIDS stage. CD4+ T cell count (blue line) and HIV viral load (red line) are based on the simulation results from the HIV viral immune system dynamics model. CD4+ T cell count reached an equilibrium above 200 cells/mm^3 among 3 patients, who did not reach the late phase of AIDS stage.

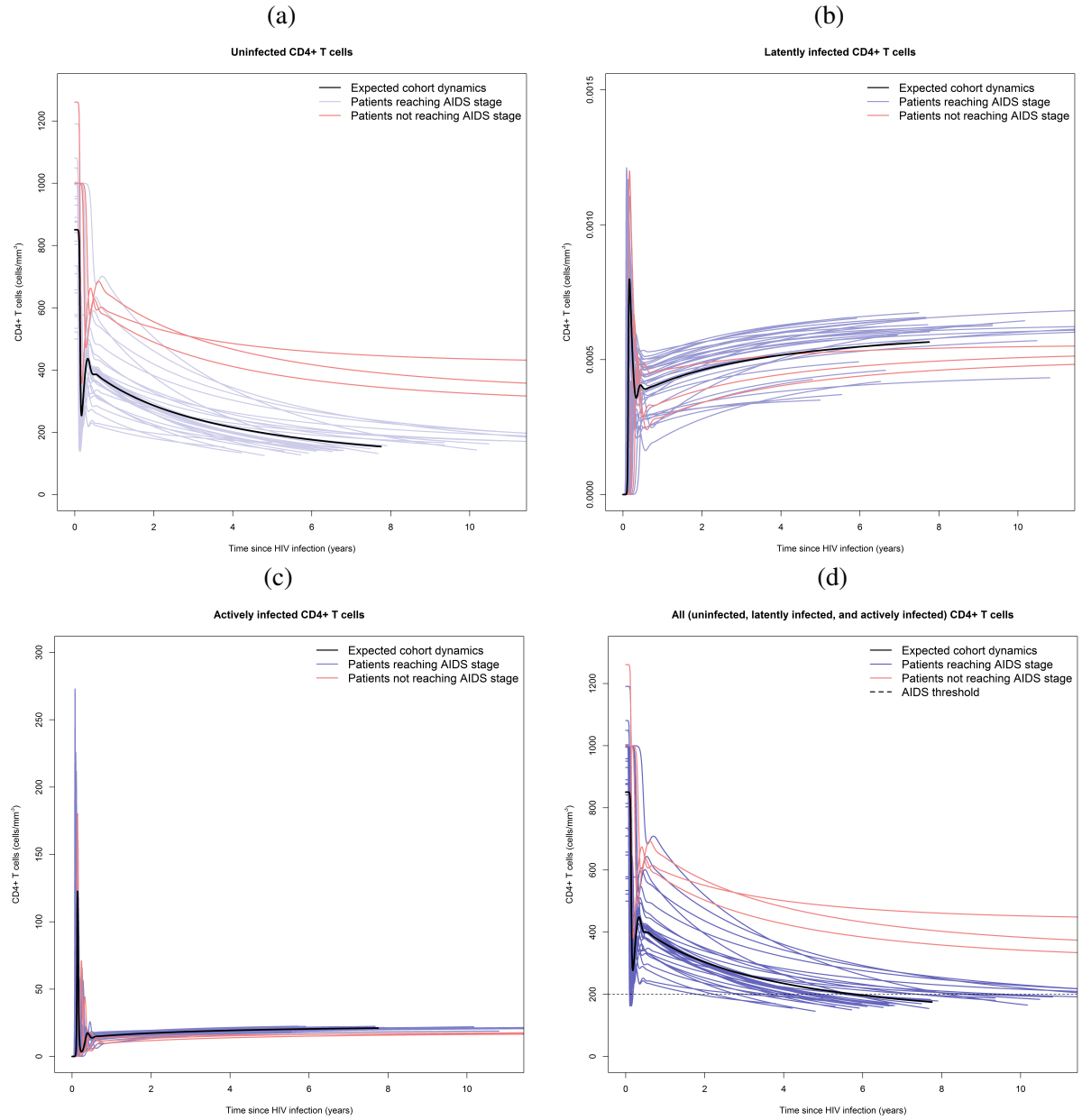

Figure 2.5: **CD4+ T cell dynamics in HIV-infected individuals.** The figure illustrates the dynamics of CD4+ T cells (uninfected, latently infected, actively infected, and combined) for each treatment naive HIV-infected individual in the 39 patient cohort. 36 patients (blue lines) reached the AIDS stage, and 3 patients (red lines) did not reach the AIDS stage. These results are based on model calibration to each HIV-infected individual, and expected cohort dynamics based on model calibration to patient cohort is also included (black line). **(a)** Dynamics of uninfected CD4+ T cells for each treatment naive HIV-infected individual in the 39 patient cohort. **(b)** Dynamics of latently infected CD4+ T cells for each treatment naive HIV-infected individual in the 39 patient cohort. **(c)** Dynamics of actively infected CD4+ T cells for each treatment naive HIV-infected individual in the 39 patient cohort. **(d)** Dynamics of all (uninfected, latently infected, and actively infected) CD4+ T cells for each treatment naive HIV-infected individual in the 39 patient cohort.

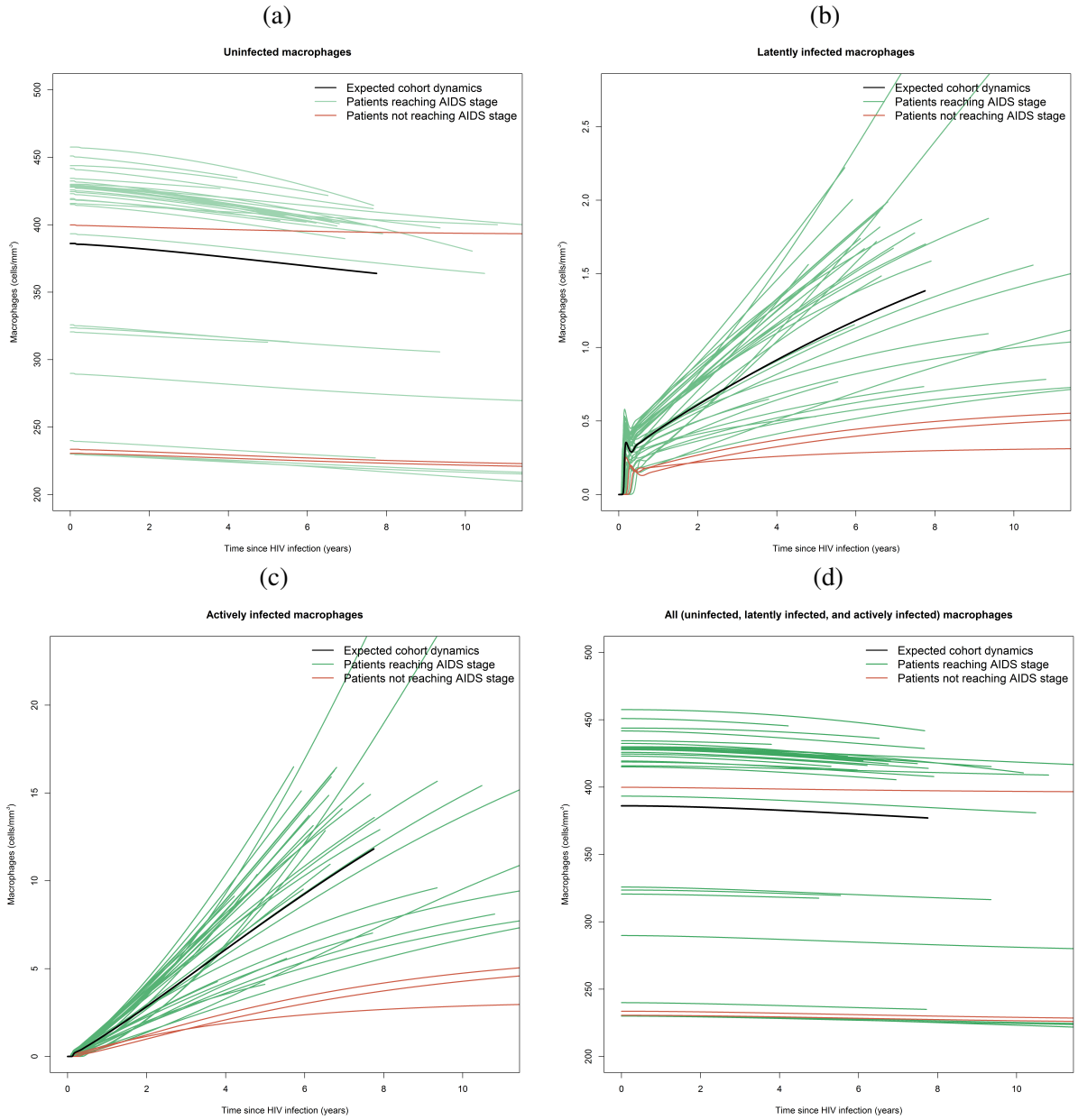

Figure 2.6: **Macrophage dynamics in HIV-infected individuals.** The figure illustrates the dynamics of macrophages (uninfected, latently infected, actively infected, and combined) for each treatment naive HIV-infected individual in the 39 patient cohort. 36 patients (green lines) reached the AIDS stage, and 3 patients (red lines) did not reach the AIDS stage. These results are based on model calibration to each HIV-infected individual, and expected cohort dynamics based on model calibration to patient cohort is also included (black line). **(a)** Dynamics of uninfected macrophages for each treatment naive HIV-infected individual in the 39 patient cohort. **(b)** Dynamics of latently infected macrophages for each treatment naive HIV-infected individual in the 39 patient cohort. **(c)** Dynamics of actively infected macrophages for each treatment naive HIV-infected individual in the 39 patient cohort. **(d)** Dynamics of all (uninfected, latently infected, and actively infected) macrophages for each treatment naive HIV-infected individual in the 39 patient cohort.

2.4.7 Dynamics of virus production from CD4+ T cells and macrophages

Figure 2.7 illustrates the simulated dynamics of virus production from CD4+ T cells and macrophages during the acute, clinically latent and late phases of HIV infection. As seen in the simulation, HIV virions are released by both actively infected CD4+ T cells and actively infected macrophages. The initial peak in viral load during the acute phase of HIV infection is primarily due to virus production from CD4+ T cells, which stabilizes to a lower rate during the clinically latent and late phases of HIV infection. While virus production from macrophages is relatively low during the acute phase of HIV infection compared to virus production from CD4+ T cells, virus production from macrophages steadily increases during the clinically latent and late phases to become relatively high compared to virus production from CD4+ T cells. Virus production from macrophages is the significant driver for HIV progression from the clinical latency to the late phase of AIDS in HIV-infected individuals.

2.4.8 HIV progression timeline to AIDS stage

Based on model calibration to patient cohort, we infer that the mean HIV progression timeline from time of infection to AIDS stage is 5.75 years (see Figure 2.2). Based on model calibration to each HIV-infected individual, we infer that 3 patients did not reach the AIDS stage, while 36 patients reached the AIDS stage during the simulation timeline which was 30 years. For the 3 patients who did not reach the AIDS stage, their CD4+ T cell counts reached a long term equilibrium above 200 cells/mm^3 (see Figure 2.4). For the 36 patients who reached the AIDS stage, Figure 2.8 illustrates the estimated time from initial infection taken for progression to AIDS. There is variation in the predicted timing of progression to AIDS stage among these 36 patients. The median value was 4.81 years and mean value was 6.1 years, with patient 32 reaching AIDS stage within 1.79 years and patient 1 reaching AIDS stage in around 15.11 years.

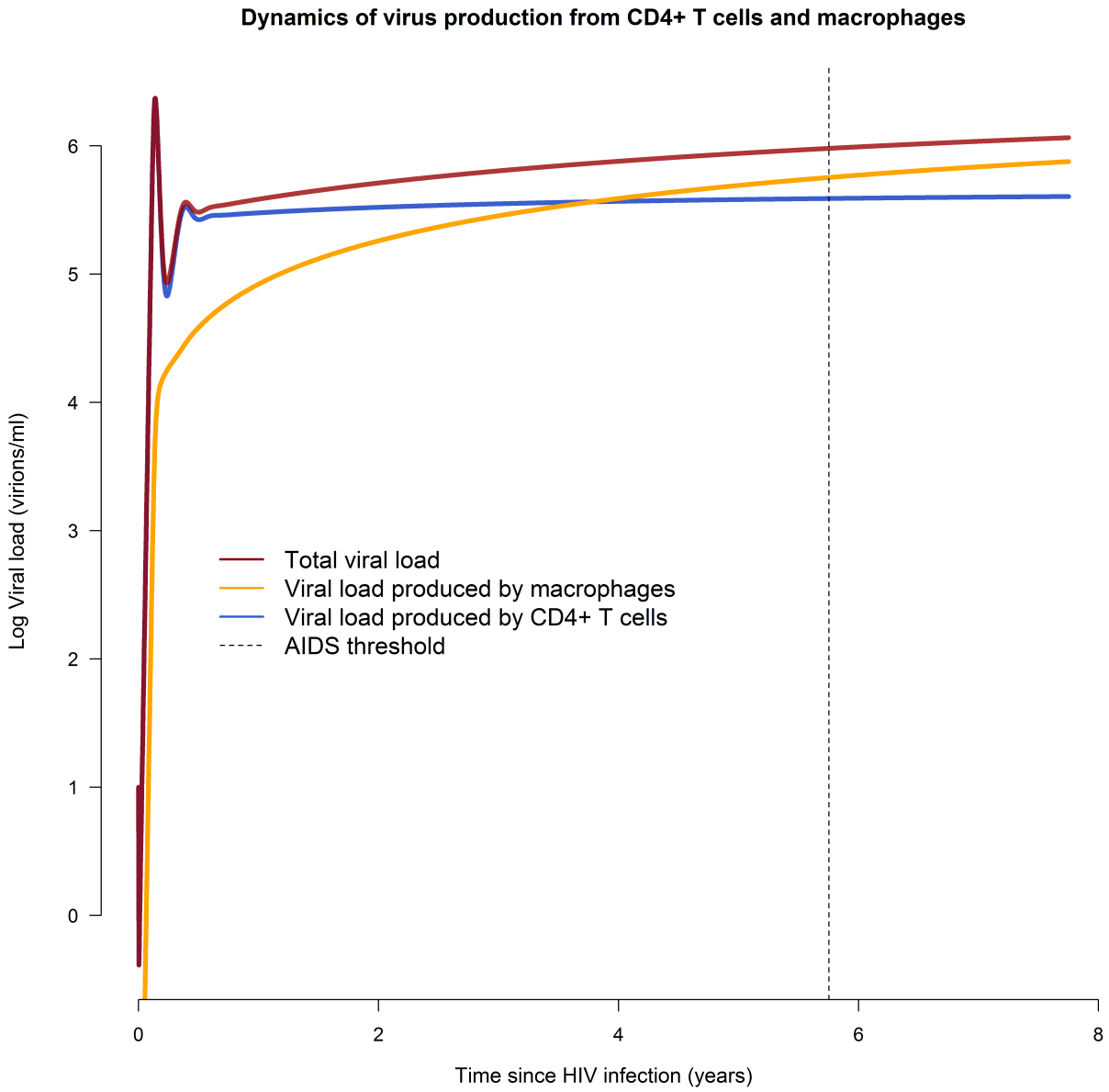

Figure 2.7: **Dynamics of virus production from CD4+ T cells and macrophages.** The figure illustrates the dynamics of viral load production from CD4+ T cells and macrophages during the acute, clinically latent and late phases of HIV infection.

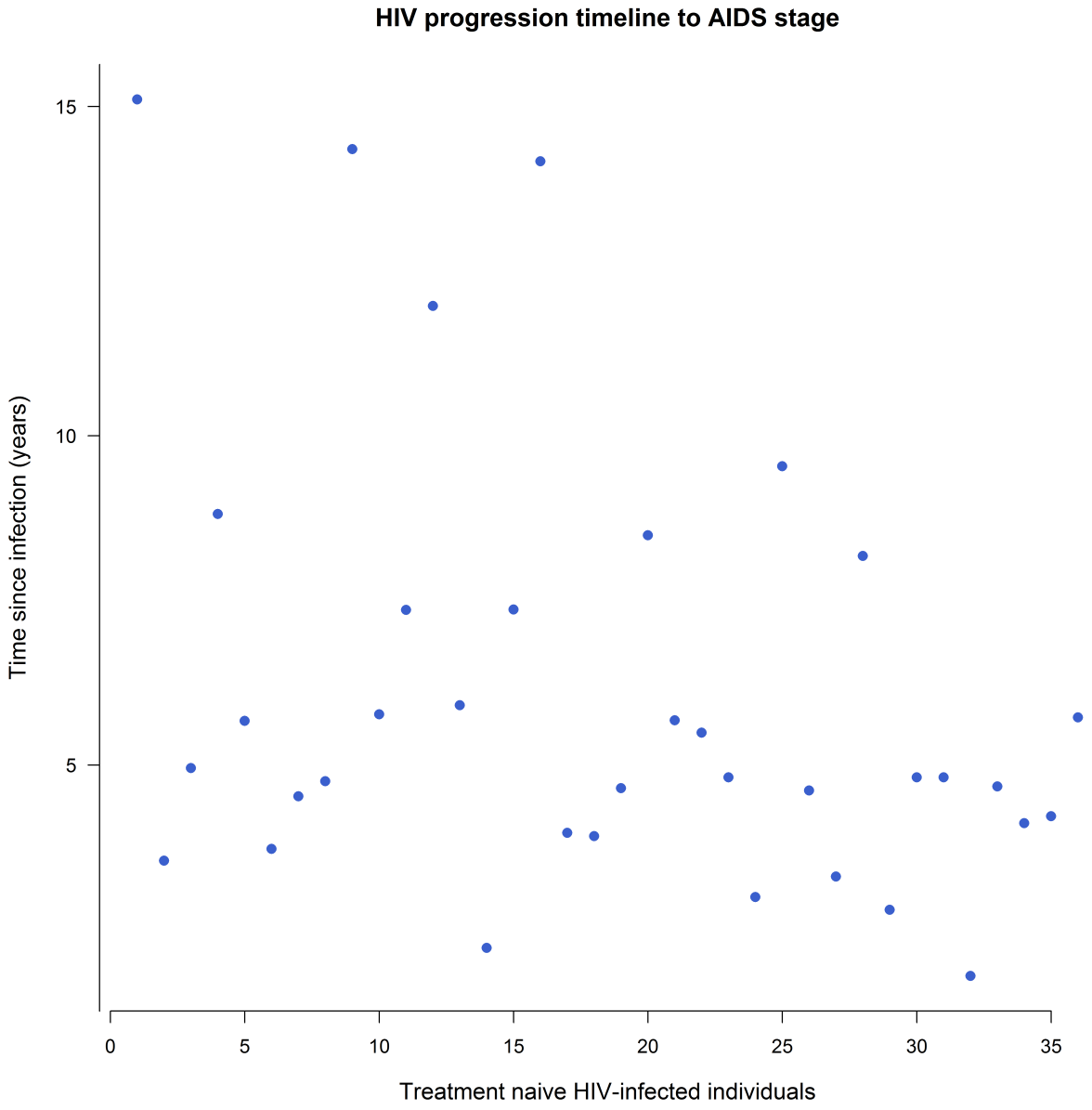

Figure 2.8: **HIV progression timeline to AIDS stage.** The figure illustrates the estimated HIV progression time from HIV infection to AIDS stage for the 36 treatment naive HIV-infected individuals in the patient cohort who reached the AIDS stage.

2.4.9 Sensitivity Analysis

We conducted univariate sensitivity analysis over the ranges of 16 parameters of the HIV viral immune system dynamics model to determine the reliability and robustness of the simulation inferences to uncertainty in parameter values. Table 2.1 includes the model parameters and their corresponding ranges used in the sensitivity analysis. Figure 2.9 illustrates the sensitivity of the 16 parameters on the HIV viral immune system dynamics, correlations with CD4+ T cell count and HIV viral load, and HIV progression timeline to AIDS stage.

CD4+ T cell production rate (λ): As shown in Figure 2.9a, we infer a positive correlation between CD4+ T cell production rate and CD4+ T cell count, HIV viral load and HIV progression timeline to AIDS stage, though the variations are minimal.

Macrophage production rate (λ_M): As shown in Figure 2.9b, we infer a negative correlation between macrophage production rate and CD4+ T cell count, positive correlation with HIV viral load, and negative correlation with HIV progression timeline to AIDS stage, though the variations are minimal.

CD4+ T cell infection rate (β): As shown in Figure 2.9c, we infer a significant negative correlation between CD4+ T cell infection rate and CD4+ T cell count, positive correlation with HIV viral load, and significant negative correlation with HIV progression timeline to AIDS stage.

Macrophage infection rate (β_M): As shown in Figure 2.9d, we infer a significant negative correlation between macrophage infection rate and CD4+ T cell count, positive correlation with HIV viral load, and significant negative correlation with HIV progression timeline to AIDS stage.

CD4+ T cells latent infection fraction (ρ): As shown in Figure 2.9e, we infer a significant positive correlation between CD4+ T cells latent infection fraction and CD4+ T cell count, insignificant negative correlation with HIV viral load, and significant positive correlation with HIV progression timeline to AIDS stage.

Macrophages latent infection fraction (ρ_M): As shown in Figure 2.9f, we infer a positive correlation between the macrophages latent infection fraction and CD4+ T cell count, negative correlation with HIV viral load, and positive correlation with HIV progression timeline to AIDS stage, though the variations are minimal.

Activation rate of latently infected CD4+ T cells (α): As shown in Figure 2.9g, we infer null effect between the activation rate of latently infected CD4+ T cells and CD4+ T cell count, HIV viral load, and HIV progression timeline to AIDS stage.

Activation rate of latently infected macrophages (α_M): As shown in Figure 2.9h, we infer a negative correlation between the activation rate of latently infected macrophages and CD4+ T cell count, positive correlation with HIV viral load, and negative correlation with HIV progression timeline to AIDS stage.

Growth rate of macrophages ($a \times M_{max}$): As shown in Figure 2.9i, we infer a negative correlation between the growth rate of macrophages and CD4+ T cell count, positive correlation with HIV viral load, and negative correlation with HIV progression timeline to AIDS stage.

HIV production by infected CD4+ T cells (N): As shown in Figure 2.9j, we infer a negative correlation between the HIV production by infected CD4+ T cells and CD4+ T cell count, positive correlation with HIV viral load, and negative correlation with HIV progression timeline to AIDS stage, though the variations are minimal.

HIV production rate by macrophages (p_M): As shown in Figure 2.9k, we infer a negative correlation between the HIV production rate by macrophages and CD4+ T cell count, positive correlation with HIV viral load, and negative correlation with HIV progression timeline to AIDS stage.

HIV clearance rate (c): As shown in Figure 2.9l, we infer a significant positive correlation between the HIV clearance rate and CD4+ T cell count, significant negative correlation with HIV viral load, and significant

positive correlation with HIV progression timeline to AIDS stage.

Death rate of uninfected CD4+ T cells; Death rate of latently infected CD4+ T cells (d): Death rate of uninfected CD4+ T cells (d) and death rate of latently infected CD4+ T cells (d) are assumed to be equal. As shown in Figure 2.9m, we infer a positive correlation between this parameter and CD4+ T cell count, positive correlation with HIV viral load, and positive correlation with HIV progression timeline to AIDS stage.

Death rate of uninfected macrophages; Death rate of latently infected macrophages (d_M): Death rate of uninfected macrophages (d_M) and death rate of latently infected macrophages (d_M) are assumed to be equal. As shown in Figure 2.9n, we infer a significant positive correlation between this parameter and CD4+ T cell count, significant negative correlation with HIV viral load, and significant positive correlation with HIV progression timeline to AIDS stage.

Death rate of actively infected CD4+ T cells (d_I): As shown in Figure 2.9o, we infer a negative correlation between the death rate of actively infected CD4+ T cells and CD4+ T cell count, nearly null effect with HIV viral load, and negative correlation with HIV progression timeline to AIDS stage, though the variations are minimal.

Death rate of actively infected macrophages (d_{M_I}): As shown in Figure 2.9p, we infer a significant positive correlation between the death rate of actively infected macrophages and CD4+ T cell count, significant negative correlation with HIV viral load, and significant positive correlation with HIV progression timeline to AIDS stage.

2.4.10 Model verification and validation

We verified our HIV viral immune system dynamics model by analyzing the dynamics of CD4+ T cells in the absence of HIV infection. The model simulated a stable healthy CD4+ T cell count through the

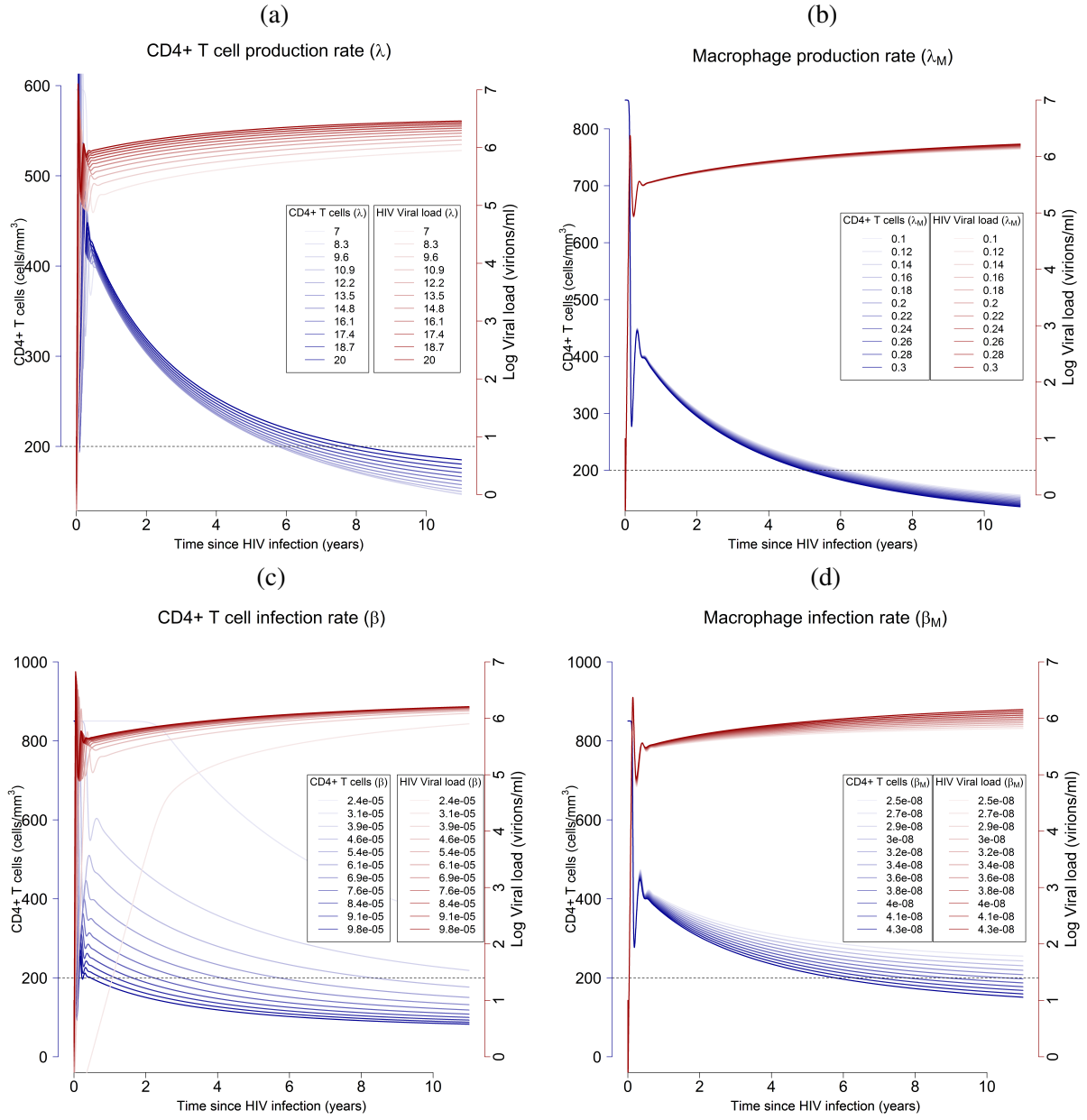

Figure 2.9: **Sensitivity analysis of model parameters:** Univariate sensitivity analysis is conducted to analyze the uncertainty in parameter values on the HIV viral immune system dynamics of CD4+ T cells and viral load, and progression timeline to AIDS stage (CD4+ T cell count depleted to 200 cells/mm^3). **(a)** CD4+ T cell production rate (λ). **(b)** Macrophage production rate (λ_M). **(c)** CD4+ T cell infection rate (β). **(d)** Macrophage infection rate (β_M).

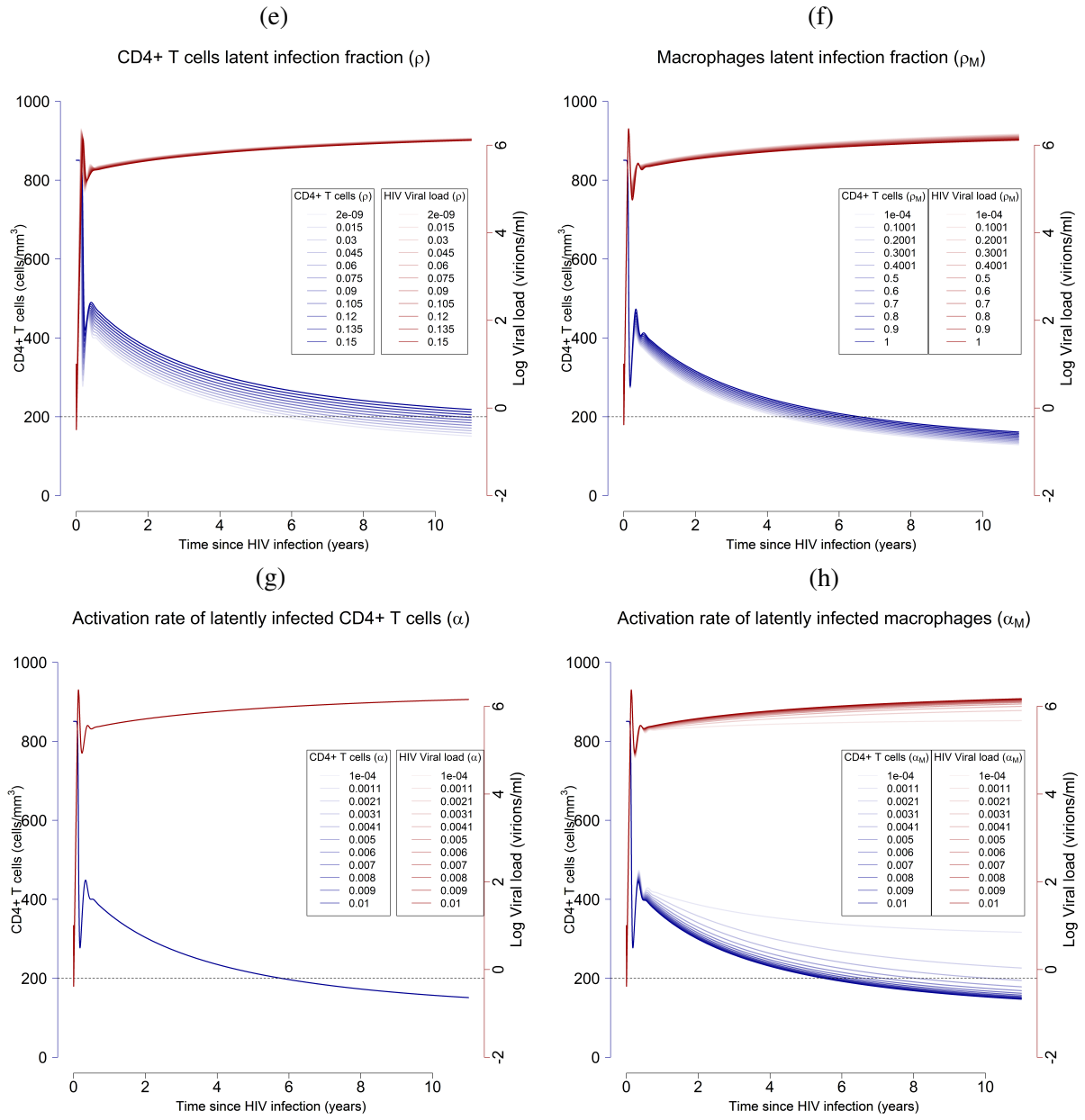

Figure 2.9: **(e)** CD4+ T cells latent infection fraction (ρ). **(f)** Macrophages latent infection fraction (ρ_M). **(g)** Activation rate of latently infected CD4+ T cells (α). **(h)** Activation rate of latently infected macrophages (α_M).

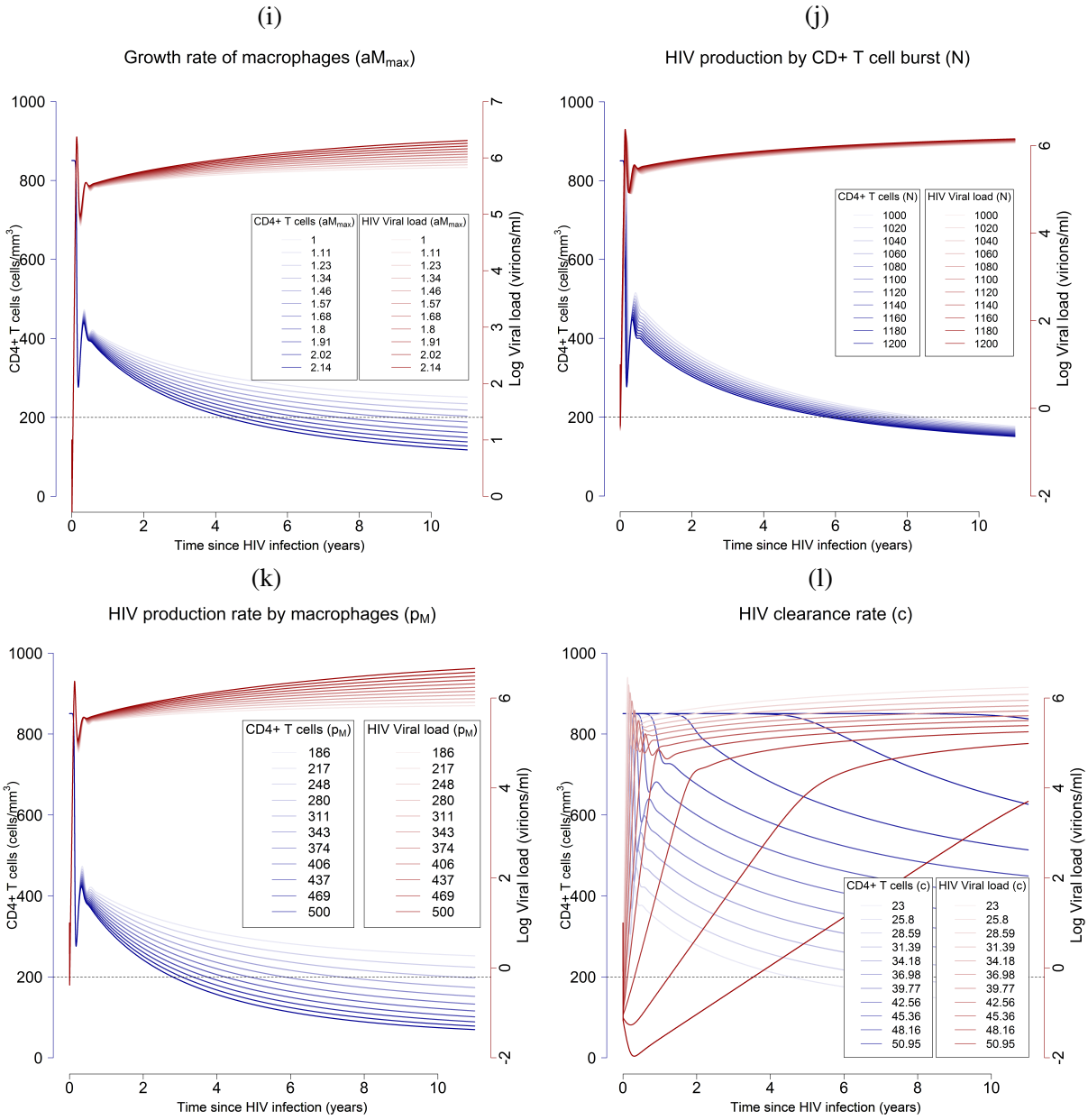

Figure 2.9: **(i)** Growth rate of macrophages ($a \times M_{max}$). **(j)** HIV production by CD4+ T cell burst (N). **(k)** HIV production rate by macrophages (p_M). **(l)** HIV clearance rate (c).

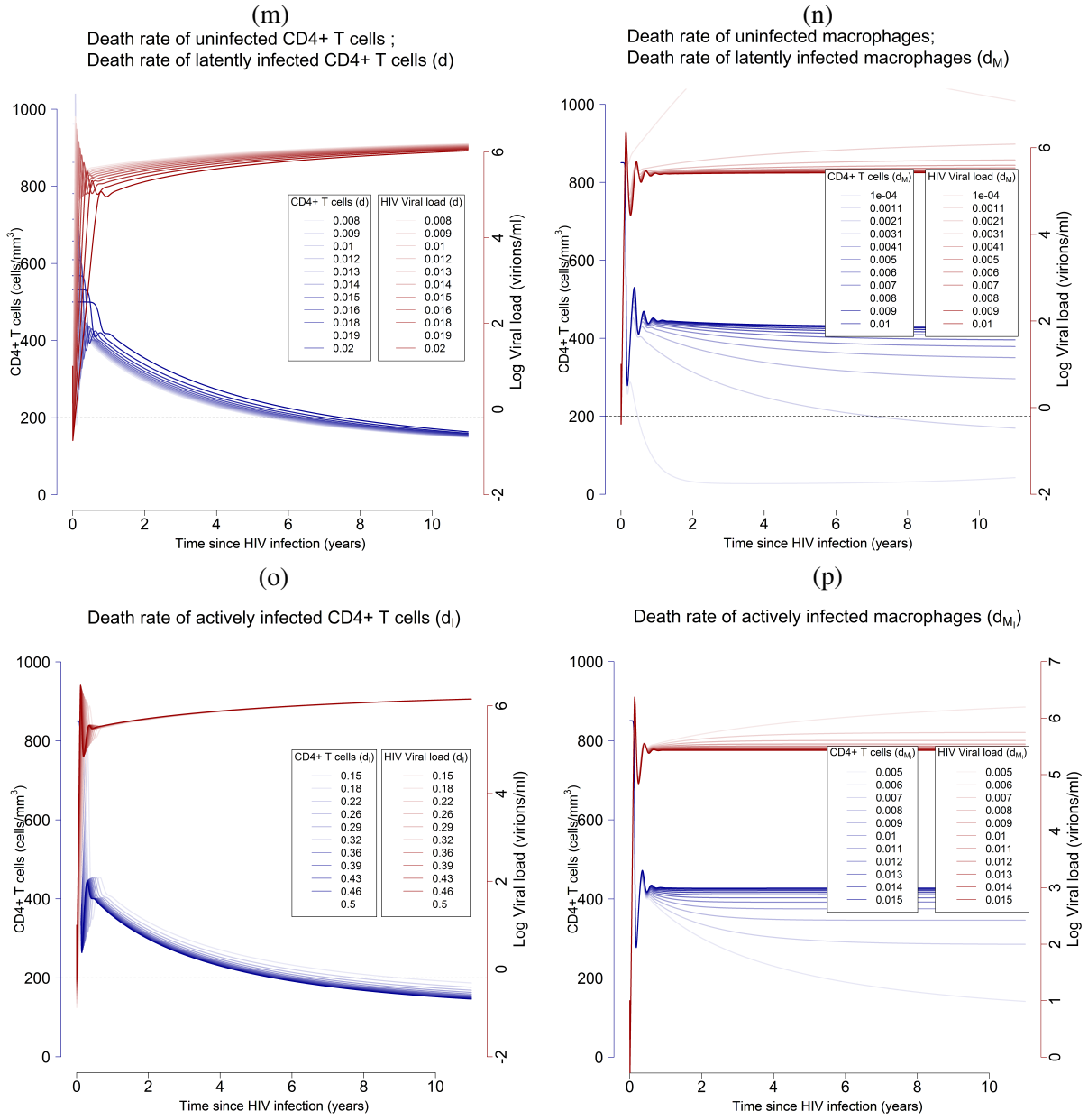

Figure 2.9: **(m)** Death rate of uninfected CD+ T cells (d), and death rate of latently infected CD4+ T cells (d). **(n)** Death rate of uninfected macrophages (d_M), and death rate of latently infected macrophages (d_M). **(o)** Death rate of actively infected CD4+ T cells (d_I). **(p)** Death rate of actively infected macrophages (d_{M_I}).

life course of the uninfected individual. Then, we analyzed the dynamics of HIV and CD4+ T cells in the presence of HIV infection, but macrophages were excluded. The HIV viral immune system dynamics model simulated the acute phase and a stable CD4+ T cell count and viral load during the clinically latent phase, but the late phase of HIV infection was not reached through the life course of the HIV-infected individual. Finally, we included the macrophages in the HIV viral immune system dynamics model. There was a steady decline of CD4+ T cell count during the clinically latent phase leading to the late phase of HIV infection in HIV-infected individuals. Thereby, we infer that macrophages are a significant driver of HIV progression from clinically latent phase to late phase in HIV-infected individuals.

We validated our HIV viral immune system dynamics model by analyzing and comparing HIV and CD4+ T cell dynamics from the simulations to the longitudinal clinical data of the patient cohort and prevalent knowledge of HIV viral-immune dynamics. The model, though parsimonious, simulated the dynamics of HIV viral load and CD4+ T cell during the acute, late and clinically latent phases of HIV infection, in concordance with the longitudinal clinical data of the patient cohort.

2.5 Discussion

2.5.1 Macrophage dynamics

Macrophages are one of the cell types targeted by HIV, but our understanding of macrophage dynamics and their role in determining the timing of progression to AIDS in HIV-infected individuals is limited. We addressed this knowledge gap by developing a conceptual model of viral immune dynamics of HIV, CD4+ T cells and macrophages, formulating the conceptual model with a mathematical model of viral immune system dynamics, and calibrating the viral immune system dynamics model to longitudinal clinical data of HIV viral load and CD4+ T cell counts in 39 HIV-infected individuals. The results of our developed model suggest that the initial peak in viral load during the acute phase of HIV infection is primarily due to virus production from CD4+ T cells, while virus production from macrophages steadily increases during the clinically latent and late phases to become the significant driver for HIV progression from the phase of clinical latency to the AIDS stage in treatment naive HIV-infected individuals.

2.5.2 HIV progression timeline to AIDS

We simulated the HIV viral immune system dynamics model for 39 treatment naive HIV-infected individuals to estimate the timing of progression to the AIDS stage. Based on model calibration to the patient cohort, we infer that the mean time from infection for progression to the AIDS stage is 5.75 years, which is shorter than the time of around 9 years reported for HIV-infected individuals in general (62; 63). This is likely because the patients in the cohort we were using data from were recruited following presentation with symptomatic HIV infection. As symptoms result from cytokine production associated with high-level viral replication during the acute phase of infection, and higher acute-phase viral replication is associated with establishment of higher persisting viral loads and more rapid disease progression, subjects presenting with

symptomatic primary infection would be expected to undergo faster than average disease progression. As seen in the simulation, there are 36 HIV-infected individuals who reached the AIDS stage, and based on model calibration to each individual, the time taken for progression to the AIDS stage among these patients is between one and a half year and about 15 years, with a median value of 4.81 years and mean value of 6.1 years. 3 patients did not reach the AIDS stage during the simulation timeline and their CD4+ T cell count reached a long term equilibrium above 200 cells/mm^3. Based on sensitivity analysis, we inferred that when all other parameters are fixed (including the infection rate of macrophages), there is a significant positive correlation between the death rate of actively infected macrophages and CD4+ T cell count, significant negative correlation with HIV viral load, and significant positive correlation with HIV progression timeline. Thereby, therapeutic regimens targeting actively infected macrophages have potential to significantly delay progression to the AIDS stage by extending the phase of clinical latency in HIV-infected individuals.

2.5.3 Clinical implications

The clinical implications of this study include estimation of HIV viral immune dynamics and HIV progression timeline to AIDS stage in treatment naive HIV-infected individuals. Clinicians can use the HIV viral immune system dynamics model and calibrate it to longitudinal clinical data of HIV viral load and CD4+ T cell count for each individual patient, to inform the patient on the expected long term impact of no treatment on their CD4+ T cell count. The HIV viral immune system dynamics model can assist in shared medical decision making between the clinicians and HIV-infected individuals to discuss treatment options compared to no treatment.

2.5.4 Limitations

We developed the HIV viral immune system dynamics model to analyze the dynamics of HIV, CD4+ T cells and macrophages in treatment naive HIV-infected individuals. While the model is calibrated with longitudinal clinical data of HIV viral load and CD4+ T cell counts, the macrophage dynamics are not calibrated with patient-level data. Interestingly, blood monocyte counts, which may provide insight into the number of monocyte-derived macrophages in tissues (but are not related to locally self-renewing tissue-resident macrophage populations), from the patients in this cohort remained fairly stable during the clinically-latent phase of infection when CD4+ T cell counts gradually declined, consistent with the model's prediction that total macrophage numbers remain stable at this time. Although the model is capable of showing the HIV progression from acute phase to clinical latency and finally AIDS stage, it did not show the faster decline in CD4+ T cell counts during the AIDS stage. The model is parsimonious and does not include the dynamics of other immune cells, such as dendritic cells and cytotoxic T lymphocytes, and their impact on HIV progression.

2.5.5 Future work

Future work will be directed towards validation and calibration of our HIV viral immune system dynamics model with macrophage data from clinical studies. A potential application area of this model is to analyze the impact of treatment interruptions on HIV progression timeline to AIDS in HIV-infected individuals.

Chapter 3

Epidemiological and Economic Impact of Pandemic Influenza in Chicago: Priorities for Vaccine Interventions

This study is based on the following paper:
Dorratoltaj N, Marathe A, Lewis B, Swarup S, Eubank S, Abbas K, Epidemiological and Economic Impact of Pandemic Influenza in Chicago: Priorities for Vaccine Interventions, *Emerging Infectious Diseases* (in review)

3.1 Abstract

The study objective is to estimate the direct and indirect epidemiological and economic impact of vaccine interventions during an influenza pandemic in Chicago, and assist in vaccine intervention priorities. Meltzer et al estimated the potential net value of different vaccination strategies, and identifies vaccination priorities for different age and risk groups during an influenza pandemic (64). A Monte Carlo based static model was used to estimate the costs and benefits due to the direct effect of vaccine interventions in the United States. We extend that study and conduct a cost-benefit analysis to infer influenza prevention priorities, by simulating the direct and indirect epidemiological and economic impact of vaccine interventions, during influenza pandemics in Chicago. We use agent-based modeling to simulate the transmission dynamics of influenza-like-illness using the susceptible-exposed-infectious-recovered epidemiological model on a collocation based synthetic social contact network. Population is distributed among high-risk and non-high risk among 0-19, 20-64 and 65+ years subpopulations. Different attack rate scenarios for catastrophic (58.11%), strong (38.62%), and moderate (28.96%) influenza pandemics are compared against vaccine intervention scenarios, at 40% coverage, 40% efficacy, and unit cost of $28.62. Vaccine prioritization criteria includes risk of death, total deaths, net benefits, and return on investment. Based on risk of death and return on investment, high-risk groups of the three age group subpopulations can be prioritized for vaccination, and vaccine intervention is cost-saving for all age and risk groups.

Keywords: Cost-benefit analysis, agent-based model, pandemic influenza, vaccine-based interventions

3.2 Introduction

The Advisory Committee on Immunization Practices (ACIP) recommends influenza vaccination for individuals aged 6 months and older to prevent and control seasonal and pandemic influenza (65). Evidence on the epidemiological and economic impact of vaccination for all age and risk groups from the societal standpoint assists in prioritization of vaccine interventions, especially when vaccine supplies are limited. Prior studies analyzed the direct epidemiological and economic impact of vaccine intervention strategies on controlling influenza pandemics (64; 66; 67; 68; 69; 70; 71; 72; 73; 74). This study complements prior studies by estimating the indirect effect in addition to the direct effect of epidemiological and economic impact of vaccine-based interventions. The objective of the vaccine interventions is to minimize deaths, hospitalizations, outpatient visits, and the number of ill people who do not seek medical care.

3.2.1 Direct epidemiological and economic effects

Direct effects account for the direct protection due to vaccine intervention. It does not take into account the secondary benefits of limiting the transmission chain to non-vaccinated subpopulation, that is, the benefit gained by free riders. Cost effectiveness of influenza vaccination for 65+ years (66), healthy working adults (67; 68), and children (75; 70) with a focus on direct effects have been studied. Prosser et al evaluate the economic impact of 2009 pandemic influenza vaccine intervention for all age and risk groups (69). They infer that vaccination of the subpopulation with a high risk of developing influenza related complications in each age group is cost saving, and vaccination of the healthy subpopulation in each age group is cost effective. Other studies have inferred that vaccine administration during previous and potential pandemics produces health benefits in terms of number of averted influenza cases and related health outcomes (71; 72; 73). These studies included the direct cost of hospitalizations, outpatient visits, and deaths, and included the related costs of vaccine production and administration, and lost productivity. Depending on the risk and age

group of the subpopulations, geographic region, and analytic methodology, the vaccine interventions may or may not be cost effective (76; 77).

3.2.2 Indirect epidemiological and economic effects

Indirect effects account for the indirect protection due to vaccine intervention. Effectively vaccinated individuals who develop protective immune response to the prevalent influenza strains, cut off transmission pathways to secondary and subsequent individuals. The indirect effect of vaccinating school children has been found to be significant, due to their social network dynamics and significance of their transmission pathways to their households and community (78; 79; 80; 81; 82). The epidemiological benefits and economic costs estimated by taking into account only the direct effect is relatively conservative, in comparison to taking into account both the direct and indirect effects. We improve the fidelity and robustness of the cost-benefit estimates to facilitate optimal prioritization of our vaccine interventions among different age and risk groups. Figure 3.1 illustrates the evaluation of the epidemiological and economic impact of influenza vaccine intervention using the static model (direct effects only) and dynamic model (direct + indirect effects).

3.2.3 Study objective

Meltzer et al estimated the potential net value of different vaccination strategies, and identified vaccination priorities for different age and risk groups during an influenza pandemic (64). A Monte Carlo based static model is used to estimate the costs and benefits due to the direct effect of vaccine interventions in the United States. We extend this study, and use an agent-based dynamic model to estimate the direct and indirect epidemiological and economic impact of vaccine interventions during an influenza pandemic in Chicago, and assist in vaccine intervention priorities.

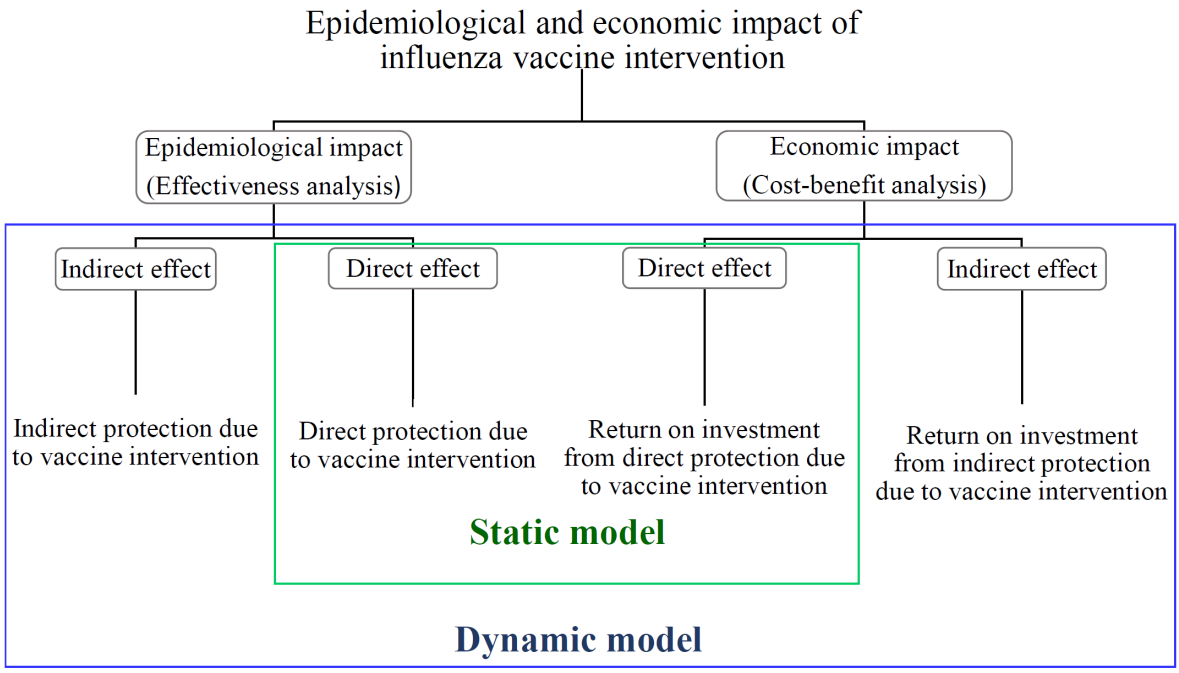

Figure 3.1: **Epidemiological and economic impact of influenza vaccine intervention.** The epidemiological and economic impact of influenza vaccine intervention include the direct and indirect effects. The static model simulates only the direct effects, while the dynamic model simulates both the direct and indirect effects. Direct effect is due to the direct protection of the influenza vaccine among vaccinated individuals who generate protective immune response to influenza infection. Indirect effect is due to indirect protection among non-vaccinated individuals who are protected from influenza acquisition from effectively vaccinated individuals, (i.e.) in the absence of vaccination, influenza transmission will have occurred between these individuals.

3.2.4 Public health significance

Population dynamics play an important role in influenza pandemic planning and response. Vaccination not only protects vaccinated individuals from contracting the disease, but also prevents the spread of infection in the network of people by breaking the transmission chain. To optimally allocate limited resources, it is important to inform decision makers and public health officials about both the direct and indirect effects of vaccine interventions.

3.3 Methods

3.3.1 Dynamic model - Agent based model

The Chicago metropolitan area is a major urban area in the United States, and had high influenza incidence during the 2009 pandemic (83). We analyze the impact of vaccine-based interventions on pandemic influenza in Chicago, using the population distribution of 9,047,574 people from the 2009 census data (84). The disease diffusion occurs on a collocation based synthetic social contact network for Chicago, based on dynamic agent-based modeling (85; 86; 87). The social contact network simulates the spatial and temporal dynamics of social behavior for each individual in Chicago. The transmission dynamics of an influenza-like-illness in the population is simulated using the susceptible-exposed-infectious-recovered (SEIR) epidemiological model on this synthetic social contact network. We estimate the direct and indirect effects of vaccine interventions on influenza pandemics of moderate, strong and catastrophic severities, in comparison to the base case scenario of no vaccine intervention.

3.3.2 Influenza related health outcomes, risk levels and age groups

Influenza related health outcomes for the infected individuals are *death, hospitalization, outpatient visits*, and *ill but not seeking medical care*. The risk levels are *high* and *non-high*, and the age groups are *0-19 years*, *20-64 years* and *65+ years*. Based on pre-existing medical conditions, influenza infected individuals may be in high or non-high risk of experiencing the different influenza related health outcomes. The distribution of the four influenza related health outcomes among the high and non-high risk cases in the three different age groups is based on the study by Meltzer et al. (64).

3.3.3 Base case scenario of no vaccine intervention

For the base-case scenario of no vaccine intervention, three different severities of an influenza pandemic are simulated using the dynamic model: moderate influenza with 28.96% attack rate, strong influenza with 38.62% attack rate, and catastrophic influenza with 58.11% attack rate. We use the dynamic model to simulate the epidemic curves for these 3 attack rates for the base-case scenario of no vaccine intervention, based on the average incidence from 25 replications (see Figure 3.2a and Table 3.1). The simulation timeline of the influenza pandemics are in accordance with prior experiences of influenza pandemics in the United States (88).

Table 3.1: **Pandemic cost per capita, attack rate, and reproduction number for different severities of pandemic influenza in the base case scenario of no vaccine intervention.** Pandemic cost per capita is the average cost of influenza related health outcomes among infected individuals for death, hospitalization, outpatient visit, and ill but not seeking medical care. The attack rate is the proportion of population infected by influenza during the influenza pandemic. Reproduction number is the number of secondary cases caused by the index case in a susceptible population.

Base-case scenario of no vaccine intervention	Catastrophic influenza	Strong influenza	Moderate influenza
Pandemic cost per capita	$1,434.58	$924.63	$683.43
Attack rate	58.11%	38.62%	28.96%
Reproduction number	1.50	1.26	1.18

3.3.4 Vaccine intervention

Effectiveness of influenza vaccines varies between 10% to 60% (89). We analyzed the impact of the vaccine intervention scenario of 40% efficacy and 40% compliance for all age and risk groups.

3.3.5 Direct epidemiological effect of vaccine intervention using static model

Using the simulation results of the base-case scenario of no vaccine intervention from the dynamic model, the influenza attack rates of moderate, strong and catastrophic pandemic scenarios are decreased by the

(a)

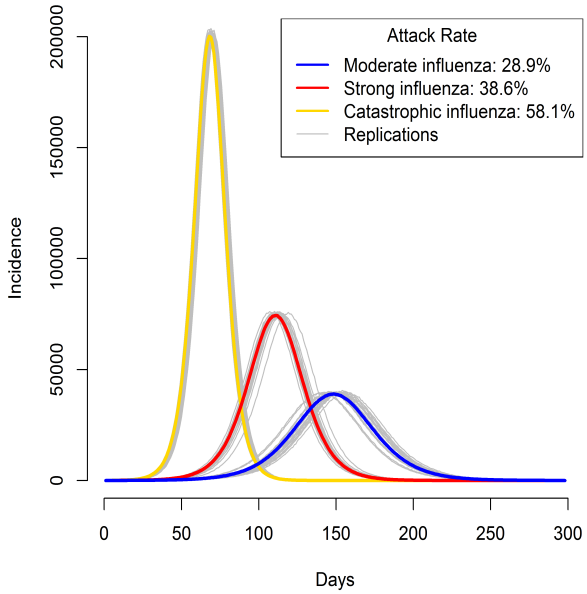

(b)

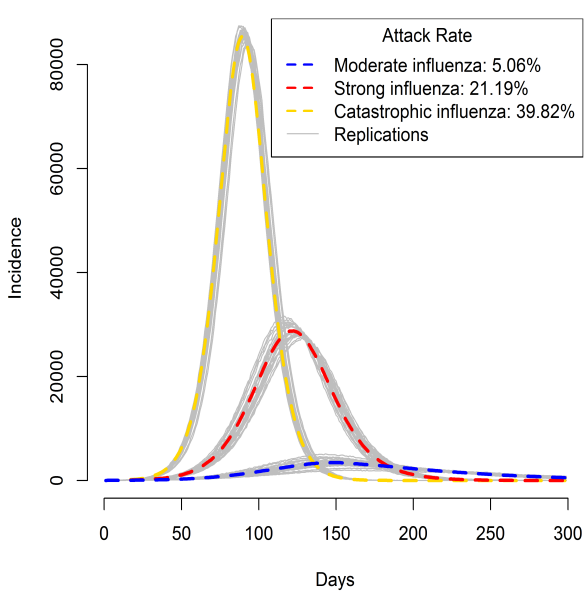

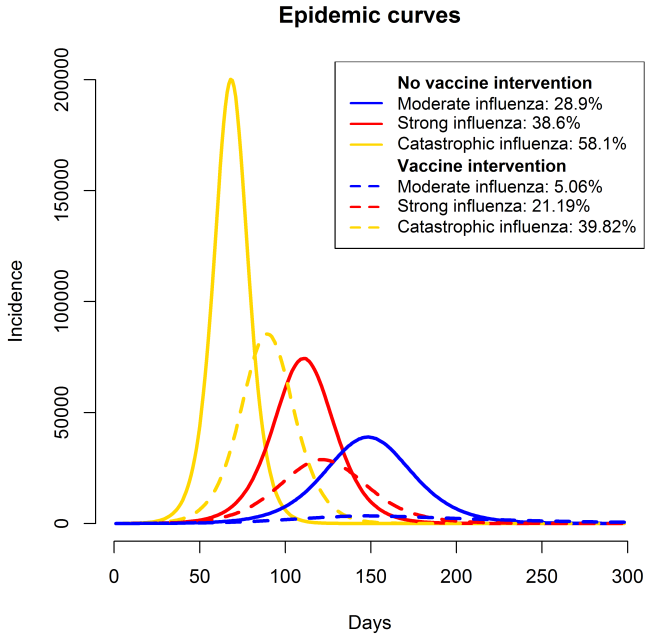

(c)

Figure 3.2: **Influenza incidence (average number of new cases per day) during the pandemic for no vaccine intervention and vaccine intervention scenarios.** The number of cases is the average of new cases over 25 simulations. **(a)** For the base case scenario of no vaccine intervention, the epidemic curves show the incidence during the catastrophic, strong and moderate influenza pandemic scenarios. Higher attack rates cause the earlier, more severe, and shorter pandemic duration, compared to the less severe but longer pandemics. **(b)** The epidemic curves show the epidemiological impact of vaccination. The vaccination intervention is applied 15 days after the start of pandemic and implemented for 60 days. The vaccine intervention scenarios are simulated at 40% efficacy and 40% compliance for all age and risk groups in the dynamic agent-based model. **(c)** The epidemic curves illustrate influenza incidence without and with vaccination intervention for the catastrophic, strong and moderate influenza pandemic scenarios. The severity and attack rates of the influenza pandemics are lowered due to vaccination.

proportional impact of the vaccine intervention at 40% coverage and 40% efficacy. Thereby, the influenza attack rates in the 3 age group sub-populations are decreased by 16% (40% efficacy × 40% compliance) in each of the three pandemic scenarios (see Table 3.2).

Table 3.2: **Pandemic cost per capita, attack rate, and reproduction number for catastrophic, strong and moderate pandemic influenza scenarios with and without vaccine intervention.** Pandemic cost per capita, attack rate and reproduction number with and without vaccine intervention are presented for catastrophic, strong and moderate influenza pandemic scenarios. The vaccine intervention is implemented at 40% compliance and 40% efficacy which decreases the pandemic cost per capita, attack rate and reproduction number. Pandemic cost per capita, attack rate and reproduction number are relatively lower in the dynamic model (direct + indirect effects) in comparison to the static model (direct effect only).

	No vaccine intervention	**Vaccine intervention**	
Catastrophic influenza	**Base case**	**Dynamic model**	**Static model**
Pandemic cost per capita	$1,434.58	$969.20	$1,216.50
Attack rate	58.11%	39.82%	48.82%
Reproduction number	1.50	1.28	1.37
Strong influenza	**Base case**	**Dynamic model**	**Static model**
Pandemic cost per capita	$924.63	$507.01	$788.13
Attack rate	38.62%	21.19%	32.44%
Reproduction number	1.26	1.12	1.21
Moderate influenza	**Base case**	**Dynamic model**	**Static model**
Pandemic cost per capita	$683.43	$127.23	$585.53
Attack rate	28.96%	5.06%	24.32%
Reproduction number	1.18	1.03	1.15

3.3.6 Direct and indirect epidemiological effects of vaccine intervention using dynamic model

We simulate the vaccine intervention scenarios at 40% efficacy and 40% compliance for all age and risk groups in the dynamic agent-based model. The vaccine intervention is initiated 15 days after the start of the pandemic and is carried out for 60 days. The dynamic model simulates the disease diffusion based on the social behavioral dynamics of the population in Chicago. It takes into account the indirect effect of limiting disease diffusion by effectively vaccinated individuals, who develop protective immune response and cut off transmission pathways to secondary and subsequent individuals. The influenza attack rates

for the 3 age group subpopulations in moderate, strong and catastrophic pandemic scenarios are estimated from the simulation results of the vaccine intervention scenarios (see Table 3.2). Figure 3.2b shows the epidemic curves (based on 25 replications for each scenario) for the three pandemic scenarios with the vaccine intervention (also, see Figure 3.2c).

3.3.7 Vaccine Cost

The cost of influenza vaccine is estimated to be $28.62, and includes the clinical personnel, non-clinical personnel, and all overhead costs (90). Direct medical costs and indirect productivity losses are estimated from a prior study, and are presented in Table 3.3 (91).

Table 3.3: **Cost of influenza related health outcomes for different age and risk groups.** The costs of influenza related health outcomes of death, hospitalization, outpatient, and ill but not seeking medical care are based on the study by Carias et al (91), and are updated to 2015 US dollars.

Influenza related health outcome/ Age group (years)	**Medical cost + Productivity losses ($)**	
Death	**Non high risk**	**High risk**
0-19	1,640,255	1,650,049
20-64	934,931	941,199
65+	276,971	290,052
Hospitalization	**Non high risk**	**High risk**
0-19	16,883	35,370
20-64	26,345	34,743
65+	14,980	22,478
Outpatient	**Non high risk**	**High risk**
0-19	508	1,051
20-64	634	904
65+	1,282	3,134
Ill, but not seeking medical care	**Non high risk**	**High risk**
0-19	129	129
20-64	88	88
65+	134	134

3.3.8 Pandemic Cost estimation - Monte Carlo simulation

Based on Meltzer's study (64), we develop a decision tree that includes the probability distribution of an influenza case experiencing the health outcomes of *death, hospitalization, outpatient visits*, and *ill but not seeking medical care*, and the cost associated with these health outcomes among the different age and risk groups (see Figure 3.3). All costs have been adjusted to 2015 US$ (see Table 3.3). We run a Monte Carlo simulation of 10,000 iterations using this decision tree to estimate the cost due to influenza related health outcomes among the different age and risk groups. This cost estimation process is conducted in all the three scenarios: base case scenario of no intervention using dynamic model, vaccine intervention scenario using static model, and vaccine intervention scenario using dynamic model. Within each of these scenarios, for each pandemic severity (moderate, strong and catastrophic), we compute the *pandemic cost, pandemic cost per capita, net benefits*, and *return on investment*, as illustrated in Table 3.4 (also, see Tables 3.1 and 3.2). The *pandemic cost* is the total cost associated with the health outcomes of influenza cases and the cost of vaccination, and *pandemic cost per capita* is the average pandemic cost per person. The *net benefits* are the difference in cost due to improved health outcomes from vaccination and the vaccination cost. *Return on investment* is the gain in net benefits relative to the vaccination cost.

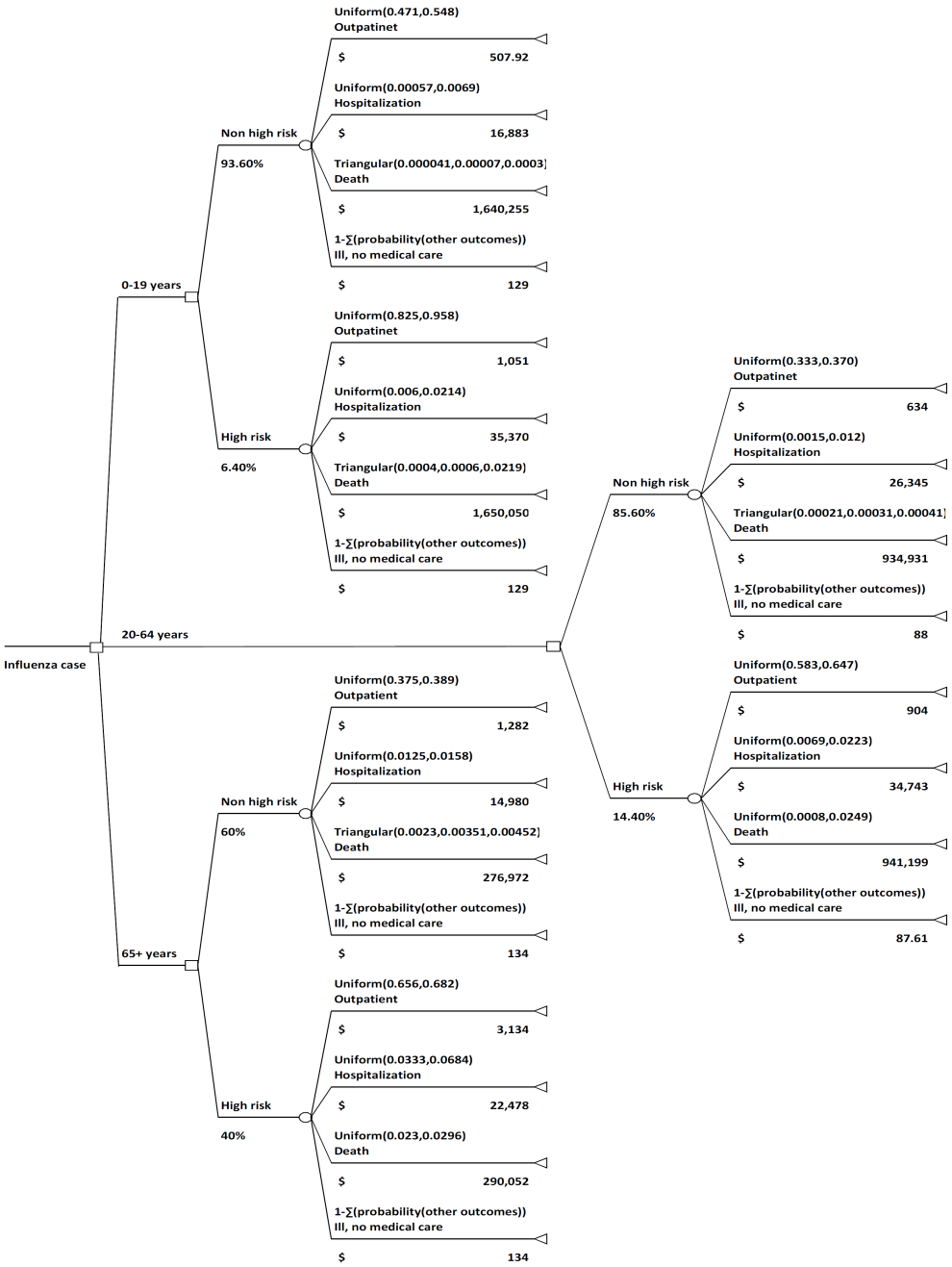

Figure 3.3: **Schematic of health outcomes for influenza cases.** For each influenza case, the probability of the different health outcomes depends on the age and risk group of the patient. Patients with pre-existing medical condition have a high risk of experiencing severe influenza related health outcomes. The probability of each health outcome is assigned an uniform or triangular distribution (64). For the uniform distribution, the lower and upper rate are presented; for triangular distribution, the lower, most probably, and higher rates are presented. Monte Carlo simulation is executed for 10,000 times.

Table 3.4: **Computation of pandemic cost, pandemic cost per capita, net benefits and return on investment.** The formulations to compute *pandemic cost, pandemic cost per capita, net benefits* and *return on investment* are presented below for the scenarios of without and with vaccine intervention. *Pandemic cost* is the total cost associated with the health outcomes of influenza cases and the cost of vaccination, and *pandemic cost per capita* is the average pandemic cost per person. The *net benefits* is the difference in cost due to improved health outcomes from vaccination and the vaccination cost. *Return on investment* is the gain in net benefits relative to the vaccination cost.

Metrics	No vaccine intervention	Vaccine intervention
Pandemic cost	Cost of influenza related health outcomes $\left(\sum_i \sum_j P_B^{ij} \boldsymbol{C^{ij}}\right)$	(Cost of influenza related health outcomes) + (Vaccination cost) $\left(\sum_i \sum_j P_I^{ij} \boldsymbol{C^{ij}}\right) + (C_v N_v)$
Pandemic cost per capita	Per capita (Cost of influenza related health outcomes) $\frac{\left(\sum_i \sum_j P_B^{ij} \boldsymbol{C^{ij}}\right)}{N}$	Per capita (Cost of influenza related health outcomes) + Per capita (Vaccination cost) $\frac{\left(\sum_i \sum_j P_I^{ij} \boldsymbol{C^{ij}}\right) + (C_v N_v)}{N}$
Net benefits	Not applicable	*Benefits - Costs* (Benefits from reduction in the cost of influenza related health outcomes due to reduction in influenza cases after vaccine intervention) – (Vaccination cost) $\left(\sum_i \sum_j (P_B^{ij} - P_I^{ij}) \boldsymbol{C^{ij}}\right) - (C_v N_v)$
Return on investment	Not applicable	Return on investment is the gain in net benefits relative to the vaccination cost, that is, dollars saved per \$1 investment in vaccine intervention $\frac{Net\ benefits}{Vaccination\ cost}$ $\frac{\left(\sum_i \sum_j (P_B^{ij} - P_I^{ij}) \boldsymbol{C^{ij}}\right) - (C_v N_v)}{C_v N_v}$

$\boldsymbol{P_B^{ij}}$	Number of infected people of age and risk group i with health outcome j in the base case scenario of no vaccine intervention
$\boldsymbol{P_I^{ij}}$	Number of infected people of age and risk group i with health outcome j after vaccine intervention
$\boldsymbol{i}$	Age and risk groups: 0-19 non-high risk, 0-19 high risk, 20-64 non-high risk, 20-64 high risk, 65+ non-high risk, 65+ high risk
$\boldsymbol{j}$	Influenza related health outcomes: death, hospitalization, outpatient visit, ill but not seeking medical care
$\boldsymbol{C^{ij}}$	Cost of influenza related health outcome j for age and risk group i
$\boldsymbol{C_v}$	Influenza vaccine cost
$\boldsymbol{N_v}$	Number of vaccinated people
$\boldsymbol{N}$	Total population

3.4 Results

3.4.1 Base case scenario of no vaccine intervention

The pandemic cost per capita is $1,434.58, $924.63 and $683.43 for catastrophic, strong, and moderate influenza scenarios respectively (see Table 3.1). The attack rate is 58.11%, 38.63% and 28.96% for catastrophic, strong, and moderate influenza scenarios respectively. The reproduction number is 1.50, 1.26 and 1.18 for catastrophic, strong, and moderate influenza scenarios respectively. The pandemic cost per capita is positively correlated with attack rate and reproduction number, with the highest in catastrophic influenza scenario followed by the strong and moderate influenza scenarios.

3.4.2 Vaccine interventions

The vaccine intervention is simulated at 40% compliance and 40% efficacy, using the static model and the dynamic model. The vaccine intervention decreases the pandemic cost per capita, attack rate and reproduction number in the catastrophic, strong and moderate influenza pandemic scenarios in both the static and dynamic models.

Figures 3.4a, 3.4b and 3.4c illustrate the comparison of pandemic cost per capita, attack rate and reproduction number in the catastrophic, strong and moderate influenza pandemic scenarios with and without vaccine intervention. In the catastrophic influenza pandemic scenario, the pandemic cost per capita, attack rate and reproduction number are $969.20, 39.82% and 1.28 respectively in the dynamic model, while they are $1,216.50, 48.82% and 1.37 respectively in the static model (see Table 3.2). In the strong influenza pandemic scenario, the pandemic cost per capita, attack rate and reproduction number are $507.01, 21.19% and 1.12 respectively in the dynamic model, while they are $788.13, 32.44% and 1.21 respectively in the static model. In the moderate influenza pandemic scenario, the pandemic cost per capita, attack rate and re-

Table 3.5: **Pandemic cost, net benefits and return on investment.** *Pandemic cost* is the total cost associated with the health outcomes of influenza cases and the cost of vaccination. *Net benefits* are the difference in cost due to improved health outcomes from vaccination and the vaccination cost. *Return on investment* is the gain in net benefits relative to the vaccination cost, that is, dollars saved per $1 investment in vaccine intervention.

Static model (Direct impacts)					
Pandemic Influenza	Pandemic cost with no vaccine intervention (Million $)	Pandemic cost with vaccine intervention (Million $)	Vaccination cost (Million $)	Net benefits (Million $)	Return on investment of vaccine intervention
Catastrophic	12,979.47	10,902.75	103.58	1,973.14	19.05
Strong	8,365.61	7,027.12	103.58	1,234.92	11.92
Moderate	6,183.40	5,194.06	103.58	885.77	8.55
Dynamic model (Direct + indirect impacts)					
Pandemic Influenza	Pandemic cost with no vaccine intervention (Million $)	Pandemic cost with vaccine intervention (Million $)	Vaccination cost (Million $)	Net benefits (Million $)	Return on investment of vaccine intervention
Catastrophic	12,979.47	8,665.34	103.58	4,210.55	40.65
Strong	8,365.61	4,483.61	103.58	3,778.42	36.48
Moderate	6,183.40	1047.56	103.58	5,032.27	48.59

production number are $127.23, 5.06% and 1.03 respectively in the dynamic model, while they are $585.53, 24.32% and 1.15 respectively in the static model.

3.4.3 Direct and indirect effects on return on investment

While the vaccine interventions are cost-saving in both the dynamic and static models, the return on investment is relatively higher in the dynamic model due to the combined impact of direct and indirect effects, in comparison to the static model which includes only the direct effect (see Figure 3.5 and Table 3.5).

3.4.4 Prioritization of vaccine intervention

Vaccine prioritization criteria includes *risk of death, total deaths, net benefits*, and *return on investment*. Based on these criteria, Table 3.6 shows the values for vaccine prioritizations of *high* and *non-high risk* groups among the *0-19, 20-64, 65+ years* subpopulations for the catastrophic, strong and moderate influenza pandemic scenarios; Table 3.7 shows the corresponding prioritization of the vaccine intervention.

(a)

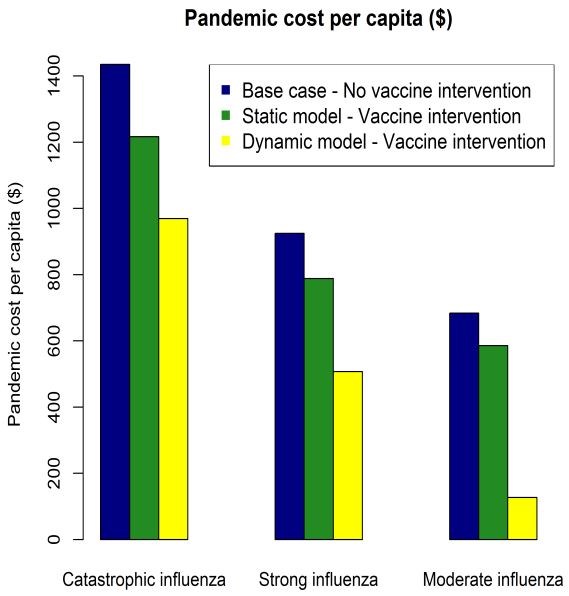

(b)

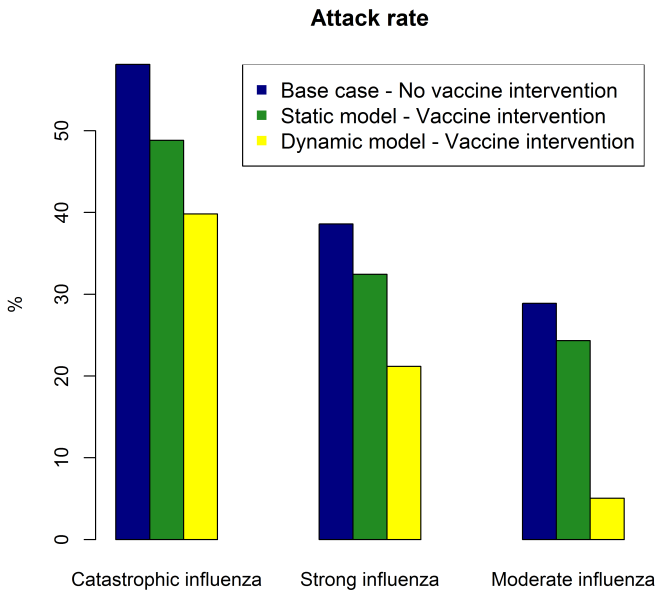

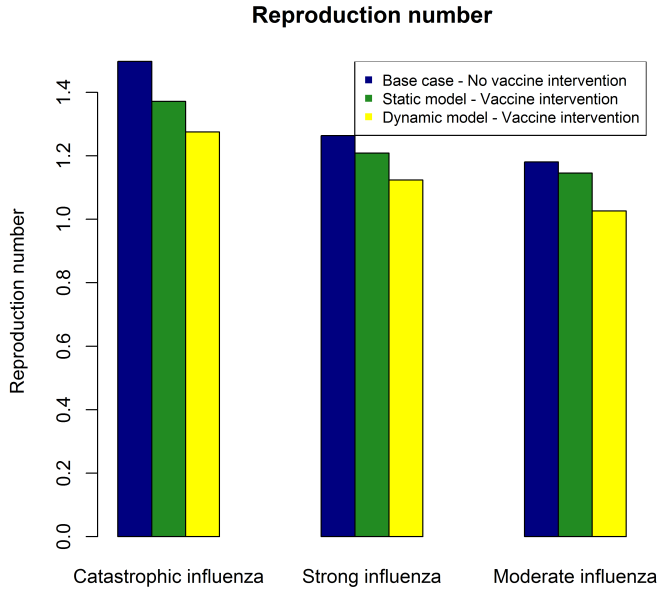

(c)

Figure 3.4: **Pandemic cost per capita, attack rate and reproduction number in the catastrophic, strong and moderate influenza pandemic scenarios with and without vaccine intervention.** Pandemic cost per capita, attack rate and reproduction number are relatively lower in the dynamic model due to the combined impact of direct and indirect effects, in comparison to the static model which includes only the direct effect. **(a)** Pandemic cost per capita in the catastrophic, strong and moderate influenza pandemic scenarios with and without vaccine intervention. **(b)** Attack rate in the catastrophic, strong and moderate influenza pandemic scenarios with and without vaccine intervention. **(c)** Reproduction number in the catastrophic, strong and moderate influenza pandemic scenarios with and without vaccine intervention.

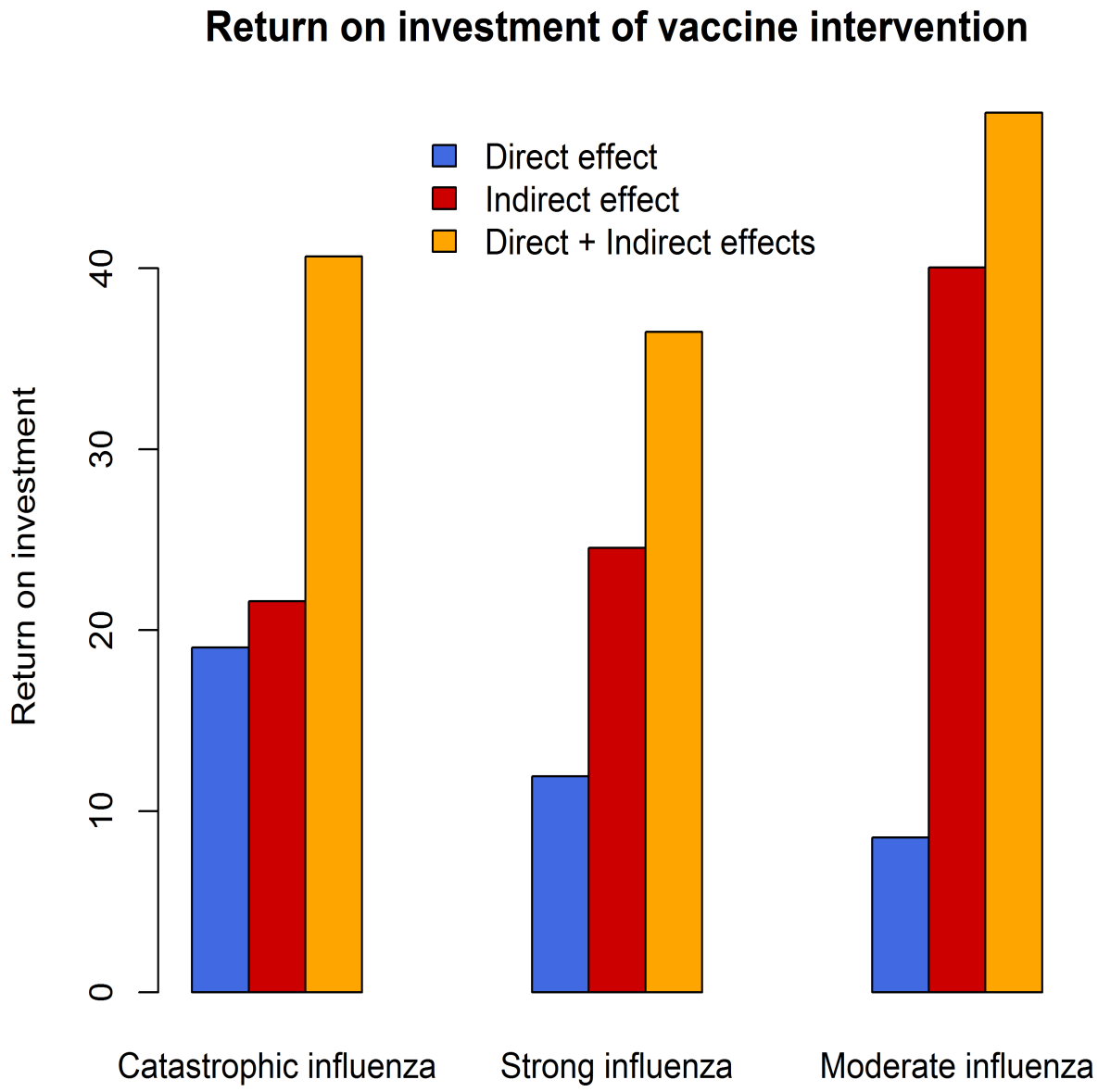

Figure 3.5: **Return on investment of vaccine intervention.** Return on investment is the gain in net benefits relative to the vaccination cost, that is, dollars saved per $1 investment in vaccine intervention. Economic impact of the vaccine intervention includes both the direct and indirect effects. The direct effect is evaluated from the static model, and the direct and indirect effects are evaluated from the dynamic model.

Risk of death:

Figure 3.6a illustrates the prioritization criteria for the vaccine intervention based on *risk of death*. In the catastrophic influenza pandemic scenario, the risk of death among the high risk 65+ years subpopulation is the highest at 950.58 deaths per 100,000 influenza cases, while it is the lowest among the non-high risk 0-19 years subpopulation at 8.66 deaths per 100,000 influenza cases. In the strong influenza pandemic scenario, the risk of death among the high risk 65+ years subpopulation is the highest at 532.63 deaths per 100,000 influenza cases, while it is the lowest among the non-high risk 0-19 years subpopulation at 6.45 deaths per 100,000 influenza cases. In the moderate influenza pandemic scenario, the risk of death among the high risk 65+ years subpopulation is the highest at 368.63 deaths per 100,000 influenza cases, while it is the lowest among the non-high risk 0-19 years subpopulation at 5.09 deaths per 100,000 influenza cases.

Total deaths:

Figure 3.6b illustrates the prioritization criteria for the vaccine intervention based on the proportion of *total deaths*. In the catastrophic influenza pandemic scenario, the proportion of total deaths among the high risk 20-64 years subpopulation is the highest at 0.49, while it is the lowest among the non-high risk 0-19 years subpopulation at 0.018. In the strong influenza pandemic scenario, the proportion of total deaths among the high risk 20-64 years subpopulation is the highest at 0.504 while it is the lowest among the non-high risk 0-19 years subpopulation at 0.021. In the moderate influenza pandemic scenario, the proportion of total deaths among the high risk 20-64 years subpopulation is the highest at 0.508, while it is the lowest among the non-high risk 0-19 years subpopulation at 0.023.

Net benefits:

Figure 3.6c illustrates the prioritization criteria for the vaccine intervention based on *net benefits*. In the catastrophic influenza pandemic scenario, the net benefits among the high risk 20-64 years subpopulation is the highest at $2,095.02 million, while it is the lowest among the non-high risk 65+ years subpopulation at $139.58 million. In the strong influenza pandemic scenario, the net benefits among the high risk 20-64 years subpopulation is the highest at $1,841.39 million, while it is the lowest among the non-high risk 65+ years subpopulation at $97.79 million. In the moderate influenza pandemic scenario, the net benefits among the high risk 20-64 years subpopulation is the highest at $2,377.38 million, while it is the lowest among the non-high risk 65+ years subpopulation at $112.36 million.

Return on investment:

Figure 3.6d illustrates the prioritization criteria for the vaccine intervention based on *return on investment*. In the catastrophic influenza pandemic scenario, the return on investment among the high risk 20-64 years subpopulation is the highest at 233.64 (i.e., $233.64 saved for every $1 invested in vaccine intervention), while it is the lowest among the non-high risk 0-19 years subpopulation at 7.2 (i.e., $7.2 saved for every $1 invested in vaccine intervention). In the strong influenza pandemic scenario, the return on investment among the high risk 0-19 years subpopulation is the highest at 232.24 (i.e., $232.24 saved for every $1 invested in vaccine intervention), while it is the lowest among the non-high risk 0-19 years subpopulation at 9.12 (i.e., $9.12 saved for every $1 invested in vaccine intervention). In the moderate influenza pandemic scenario, the return on investment among the high risk 0-19 years subpopulation is the highest at 366.09 (i.e., $366.09 saved for every $1 invested in vaccine intervention), while it is the lowest among the non-high risk 0-19 years subpopulation at 14.93 (i.e., $14.93 saved for every $1 invested in vaccine intervention).

Table 3.6: **Risk of death, total deaths, net benefits and return on investment for different age and risk groups in the catastrophic, strong, and moderate influenza pandemic scenarios.** *Risk of death* is estimated based on the number of influenza related deaths per 100,000 subpopulation for the specific age and risk groups. *Total deaths* is estimated based on the proportion of influenza related deaths for the specific age and risk groups among total influenza related deaths. *Net benefits* are the difference in cost due to improved health outcomes from vaccination and the vaccination cost. *Return on investment* is the gain in net benefits relative to the vaccination cost, that is, dollars saved per $1 investment in vaccine intervention.

Catastrophic influenza pandemic				
Age and risk group	**Risk of death (per 100,000 cases)**	**Proportion of total deaths**	**Net benefits (million $)**	**Return on investment**
Non-high risk 0-19 yrs	8.66	0.018	204.52	7.20
High risk 0-19 yrs	482.64	0.067	365.14	187.87
Non-high risk 20-64 yrs	18.46	0.070	798.88	14.99
High risk 20-64 yrs	766.20	0.490	2,095.02	233.64
Non-high risk 65+ yrs	124.48	0.058	139.58	21.27
High risk 65+ yrs	950.58	0.297	607.41	92.56
Strong Influenza pandemic				
Age and risk group	**Risk of death (per 100,000 cases)**	**Proportion of total deaths**	**Net benefits (million $)**	**Return on investment**
Non-high risk 0-19 yrs	6.45	0.021	259.24	9.12
High risk 0-19 yrs	359.41	0.081	451.37	232.24
Non-high risk 20-64 yrs	11.71	0.072	696.15	13.06
High risk 20-64 yrs	485.92	0.504	1,841.39	205.35
Non-high risk 65+ yrs	69.75	0.053	97.79	14.90
High risk 65+ yrs	532.63	0.269	432.47	65.90
Moderate influenza pandemic				
Age and risk group	**Risk of death (per 100,000 cases)**	**Proportion of total deaths**	**Net benefits (million $)**	**Return on investment**
Non-high risk 0-19 yrs	5.09	0.023	424.31	14.93
High risk 0-19 yrs	283.63	0.088	711.51	366.09
Non-high risk 20-64 yrs	8.56	0.073	913.25	17.13
High risk 20-64 yrs	355.40	0.508	2,377.38	265.12
Non-high risk 65+ yrs	48.27	0.051	112.36	17.12
High risk 65+ yrs	368.63	0.257	493.46	75.20

Table 3.7: **Prioritization of influenza vaccine intervention.** Prioritization of influenza vaccine intervention among different age and risk groups based on different criteria: risk of death, total deaths, net benefits, and return on investment. [a]*Risk of death* is estimated based on the number of influenza related deaths per 100,000 subpopulation for the specific age and risk groups. Risk of death is the highest among the high risk 65+ years subpopulation in the catastrophic, strong, and moderate influenza pandemic scenarios. [b]*Total deaths* is estimated based on the proportion of influenza related deaths for the specific age and risk groups among total influenza related deaths. The proportion of influenza related deaths is the highest among the high risk 20-64 years subpopulation in the catastrophic, strong, and moderate influenza pandemic scenarios. [c]*Net benefits* are the difference in cost due to improved health outcomes from vaccination and the vaccination cost. Net benefits are the highest among the high risk 20-64 years subpopulation in the catastrophic, strong, and moderate influenza pandemic scenarios. [d]*Return on investment* is the gain in net benefits relative to the vaccination cost, that is, dollars saved per $1 investment in vaccine intervention. Return on investment is highest among the high risk 20-64 years subpopulation in the catastrophic influenza pandemic, and it is highest among the high risk 0-19 years subpopulation in the strong and moderate influenza pandemic scenarios.

Prioritization criteria (Catastrophic influenza pandemic)				
Priority	**Risk of death[a]**	**Total deaths[b]**	**Net benefits[c]**	**Return on investment[d]**
1 (high)	High risk 65+ yrs	High risk 20-64 yrs	High risk 20-64 yrs	High risk 20-64 yrs
2	High risk 20-64 yrs	High risk 65+ yrs	Non-high risk 20-64 yrs	High risk 0-19 yrs
3	High risk 0-19 yrs	Non-high risk 20-64 yrs	High risk 65+ yrs	High risk 65+ yrs
4	Non-high risk 65+ yrs	High risk 0-19 yrs	High risk 0-19 yrs	Non-high risk 65+ yrs
5	Non-high risk 20-64 yrs	Non-high risk 65+ yrs	Non-high risk 0-19 yrs	Non-high risk 20-64 yrs
6 (low)	Non-high risk 0-19 yrs	Non-high risk 0-19 yrs	Non-high risk 65+ yrs	Non-high risk 0-19 yrs
Prioritization criteria (Strong influenza pandemic)				
Priority	**Risk of death**	**Total deaths**	**Net benefits**	**Return on investment**
1 (high)	High risk 65+ yrs	High risk 20-64 yrs	High risk 20-64 yrs	High risk 0-19 yrs
2	High risk 20-64 yrs	High risk 65+ yrs	Non-high risk 20-64 yrs	High risk 20-64 yrs
3	High risk 0-19 yrs	High risk 0-19 yrss	High risk 0-19 yrs	High risk 65+ yrs
4	Non-high risk 65+ yrs	Non-high risk 20-64 yr	High risk 65+ yrs	Non-high risk 65+ yrs
5	Non-high risk 20-64 yrs	Non-high risk 65+ yrs	Non-high risk 0-19 yrs	Non-high risk 20-64 yrs
6 (low)	Non-high risk 0-19 yrs	Non-high risk 0-19 yrs	Non-high risk 65+ yrs	Non-high risk 0-19 yrs
Prioritization criteria (Moderate influenza pandemic)				
Priority	**Risk of death**	**Total deaths**	**Net benefits**	**Return on investment**
1 (high)	High risk 65+ yrs	High risk 20-64 yrs	High risk 20-64 yrs	High risk 0-19 yrs
2	High risk 20-64 yrs	High risk 65+ yrs	Non-high risk 20-64 yrs	High risk 20-64 yrs
3	High risk 0-19 yrs	High risk 0-19 yrss	High risk 0-19 yrs	High risk 65+ yrs
4	Non-high risk 65+ yrs	Non-high risk 20-64 yr	High risk 65+ yrs	Non-high risk 20-64 yrs
5	Non-high risk 20-64 yrs	Non-high risk 65+ yrs	Non-high risk 0-19 yrs	Non-high risk 65+ yrs
6 (low)	Non-high risk 0-19 yrs	Non-high risk 0-19 yrs	Non-high risk 65+ yrs	Non-high risk 0-19 yrs

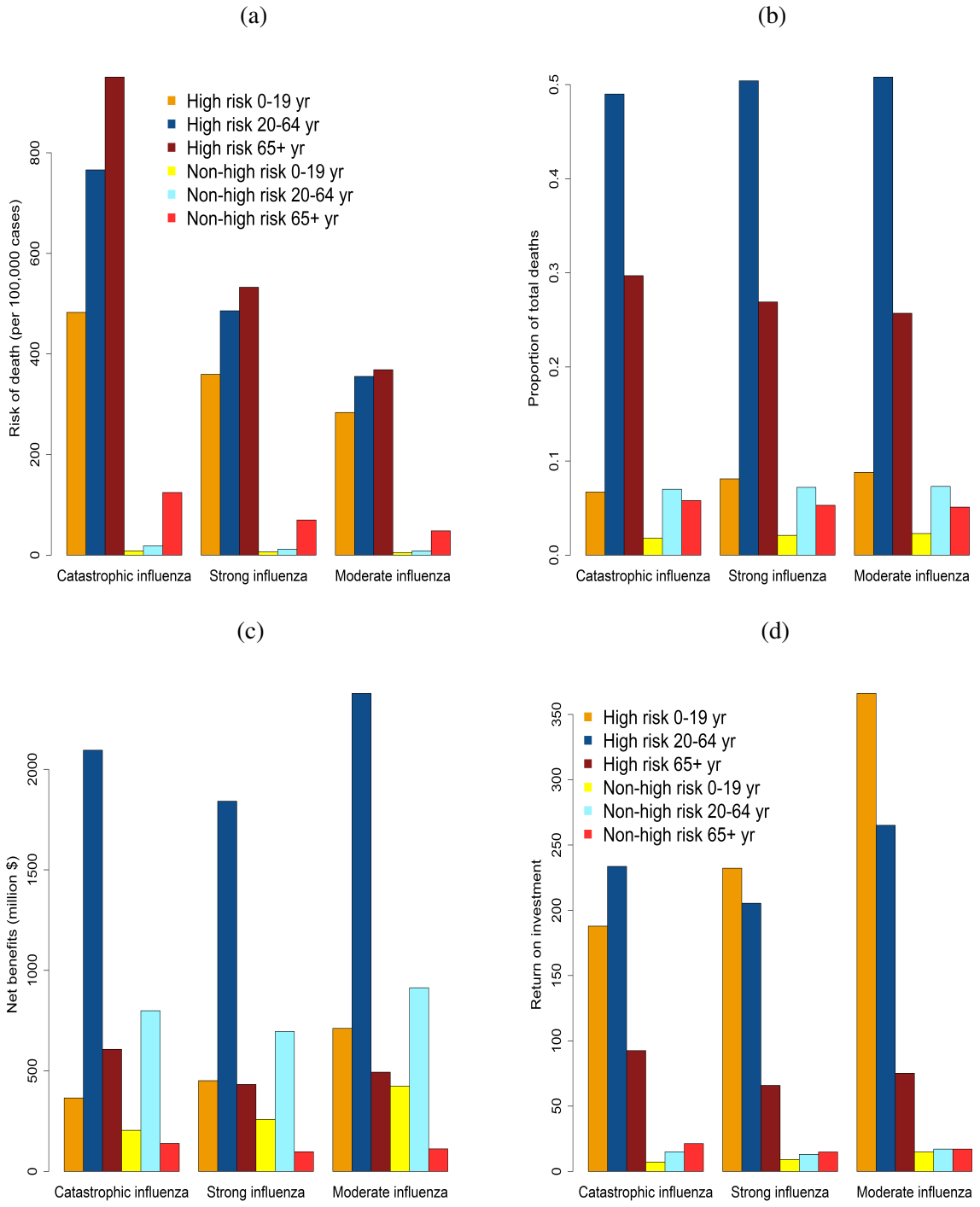

Figure 3.6: **Prioritization of influenza vaccine intervention.** Prioritization of influenza vaccine intervention among different age and risk groups based on different criteria: *risk of death, total deaths, net benefits*, and *return on investment*.**(a)** *Risk of death* is estimated based on the number of influenza related deaths per 100,000 subpopulation for the specific age and risk groups. Risk of death is the highest among the high risk 65+ years subpopulation in the catastrophic, strong, and moderate influenza pandemic scenarios. **(b)** *Total deaths* is estimated based on the proportion of influenza related deaths for the specific age and risk groups among total influenza related deaths. The proportion of influenza related deaths is the highest among the high risk 20-64 years subpopulation in the catastrophic, strong, and moderate influenza pandemic scenarios. **(c)** *Net benefits* are the difference in cost due to improved health outcomes from vaccination and the vaccination cost. Net benefits are the highest among the high risk 20-64 years subpopulation in the catastrophic, strong, and moderate influenza pandemic scenarios.**(d)** *Return on investment* is the gain in net benefits relative to the vaccination cost, that is, dollars saved per $1 investment in vaccine intervention. Return on investment is highest among the high risk 20-64 years subpopulation in the catastrophic influenza pandemic, and it is highest among the high risk 0-19 years subpopulation in the strong and moderate influenza pandemic scenarios.

3.5 Discussion

3.5.1 Direct and indirect epidemiological and economic effects of vaccine intervention

Direct effect is due to the immune protection gained by effectively vaccinated individuals, and indirect effect is due to blocking of the influenza transmission by effectively vaccinated individuals to susceptible individuals in their social network. The static model provides a conservative estimate of the epidemiological and economic benefits of influenza vaccine intervention by accounting for only the direct effect. The dynamic model provides a comprehensive estimate of the epidemiological and economic benefits of influenza vaccine intervention by accounting for both the direct and indirect effects.

The vaccine intervention has a higher probability of effectively vaccinating individuals who will have otherwise being infected in the absence of the vaccine intervention in more severe pandemic scenarios (such as catastrophic influenza). This is due to relatively higher attack rates and higher proportion of population at risk of influenza infection in comparison to less severe pandemic scenarios (such as moderate influenza). Thereby, the impact of the direct effect decreases from catastrophic, strong to moderate influenza pandemic scenarios (see Figure 3.5).

The vaccine intervention has a lower probability of breaking transmission pathways in more severe pandemic scenarios (such as catastrophic influenza), because the transmission network is densely connected in comparison to sparsely connected transmission networks in less severe pandemic scenarios (such as moderate influenza). Thereby, the impact of the indirect effect increases from catastrophic, strong to moderate influenza pandemic scenarios (see Figure 3.5).

Pandemic cost per capita, attack rate and reproduction number are relatively lower in the dynamic model due to the combined impact of the direct and indirect effects, in comparison to the static model which includes only the direct effect, in the catastrophic, strong and moderate influenza pandemic scenarios. While

the vaccine interventions are cost-saving in both the dynamic and static models, the return on investment is relatively higher in the dynamic model in comparison to the static model.

3.5.2 Prioritization of vaccine interventions

We analyzed vaccine prioritization criteria based on *risk of death, total deaths, net benefits* and *return on investment* for the high and non-high risk groups among 0-19, 20-64 and 65+ years subpopulations. The *risk of death* is the highest among the *high risk 65+ years* subpopulation in the catastrophic, strong and moderate influenza pandemic scenarios. The proportion of *total deaths* is the highest among the *high risk 20-64 years* subpopulation in the catastrophic, strong and moderate influenza pandemic scenarios. The *net benefits* are the highest among the *high risk 20-64 years* subpopulation in the catastrophic, strong and moderate influenza pandemic scenarios. The *return on investment* is the highest in the *high risk 20-64 years* subpopulation in the catastrophic influenza pandemic scenario, while it is highest in the *0-19 years* subpopulation in the strong and moderate influenza pandemic scenarios.

The proportion of total deaths and net benefits measure the epidemiological and economic impact respectively, and are dependent on the absolute size of the different risk and age group subpopulations. Risk of death and return on investment measure the epidemiological and economic impact respectively, and are independent of the absolute size of the different risk and age group subpopulations. Based on risk of death and return on investment, high-risk groups of the three age group subpopulations are recommended for prioritization of influenza vaccine intervention. Also, the vaccine intervention is cost-saving for all age and risk groups.

3.5.3 Public health implications

The Advisory Committee on Immunization Practices (ACIP) recommends the use of seasonal influenza vaccines, and they update information on the dosage for children, antigenic composition and influenza vaccine products, but do not address targeted vaccination strategies among subpopulations (92). The dynamic model provides improved estimates of the epidemiological and economic benefits of vaccine interventions in comparison to a static model, by accounting for both the direct and indirect effects. These estimates assist in prioritization of vaccine interventions among subpopulations of different risk and age groups, especially during influenza pandemics with limited availability of vaccines. Decision makers can use the dynamic model simulations to compare the epidemiological and economic impact of using different prioritization criteria of influenza vaccine interventions among different risk and age group subpopulations, thereby optimizing allocation of limited resources and improving evidence-based public health policy and practice.

3.5.4 Future work

We will conduct additional studies for a range of vaccine compliance and efficacy values at different attack rates of influenza pandemics in different rural and urban areas of the United States and at the country level, to infer objective prioritization criteria for influenza vaccine interventions among the different risk and age groups.

Chapter 4

Effectiveness and Partial Cost of Fungal Meningitis Outbreak Response in New River Valley: Local Health Department and Clinical perspectives

This study is based on the following paper:
Dorratoltaj N, O'Dell M, Bordwine P, Kerkering TM, Redican KJ, Abbas KM, Effectiveness and Partial Cost of Fungal Meningitis Outbreak Response in New River Valley: Local Health Department and Clinical perspectives, *Health Services Research* (in review)

4.1 Abstract

The study objective is to evaluate the effectiveness and cost of the fungal meningitis outbreak response in New River Valley of Virginia during 2012-2013, from the local public health department and clinical perspectives. The fungal meningitis outbreak affected 23 states with 751 cases and 64 deaths in 20 states in the United States; there were 56 cases and 5 deaths in Virginia. We conduct a partial economic evaluation of the fungal meningitis outbreak response in New River Valley. We collect the costs associated with the local health department and clinical facilities in the outbreak response, and estimate the epidemiological effectiveness using disability adjusted life years (DALYs) averted. We estimated the epidemiological effectiveness of this outbreak response to be 153 DALYs averted among the patients, and the costs incurred by the local health department and clinical facilities to be $30,413 and $39,580 respectively. We estimated the incremental cost-effectiveness ratio of $198 per DALY averted and $258 per DALY averted from the local health department and clinical perspectives respectively, thereby assisting in impact evaluation of the outbreak response by the local health department and clinical facilities.

Keywords: Cost-effectiveness analysis, fungal meningitis outbreak, local health department, clinical, New River Valley, Virginia

4.2 Introduction

4.2.1 Fungal meningitis

Fungal meningitis occurs in individuals infected by the predominant pathogen *Exserohilum rostratum*, which spreads in the spinal cord through the bloodstream, and leads to swelling of the protective membrane of the spinal cord or brain. It is not contagious and does not transmit directly between people. It can be found in soil, water, food, air, and vegetation. People exposed to this fungal pathogen generally experience no adverse effect. But, immunocompromised people are at higher risk for developing fungal infection and symptomatic effects. Symptoms include meningitis, encephalitis, and stroke. During the multistate fungal meningitis outbreak in the United States during 2012-2013, exposed patients with mild symptoms of fever, headache, back pain or other relevant symptoms were also tested (93).

4.2.2 Multistate fungal meningitis outbreak

In September 2012, Tennessee Department of Health confirmed cases of *Aspergillus fumigatus* meningitis following epidural steroid injection. After Tennessee, 19 other states reported cases caused by the predominant pathogen *Exserohilum rostratum* (94). The cause of the multi-state fungal meningitis outbreak was traced to fungal contaminated lots of preservative free methylprednisolone acetate that were used in the epidural steroid injections, and produced in a compounding pharmacy – New England Compounding Center in Framingham, Massachusetts (95). More than 13,000 patients had received the fungal contaminated epidural steroid injections in 23 states, and were at risk of developing fungal meningitis. The outbreak was the largest outbreak associated with steroid injections (96). There were 751 cases and 64 deaths in 20 states as of October 23rd 2013, and additional cases are not anticipated (97).

4.2.3 Fungal meningitis case definition

CDC defined a probable fungal meningitis case as a patient who had received the fungal contaminated epidural injections after May 21, 2012, with symptoms of meningitis, stroke, spinal infections, osteomyelitis or arthritis of peripheral joints. Probable cases with evidence of the fungal pathogen in culture, histopathology, or molecular assay were also defined as confirmed cases.

4.2.4 Fungal meningitis outbreak in Virginia

Virginia reported the 4th highest number of cases with 56 cases and 5 deaths. Two clinical facilities in Virginia had administered these fungal contaminated injections, with one facility located in New River Valley and the other facility located in neighboring Roanoke. New River Health District (NRHD) personnel conducted disease surveillance, case reporting, and referring probable cases to clinical facilities for diagnostics, treatment and/or hospitalization.

4.2.5 Clinical response

CDC released treatment guidelines, and voriconazole therapy was the recommended treatment (97). Confirmed cases in Virginia were prescribed similar treatment, and voriconazole therapy improved prognosis among the treated patients (98).

4.2.6 Multi-sectoral public health response

The multistate fungal meningitis outbreak was controlled through a multi-sectoral public health response. The outbreak response required effective coordination between the patients and immediate caregivers, treatment administered through hospitals, clinics and pharmacies, and a systematic effort between the public

health agencies at the local, state and federal levels. The outbreak was widely publicised after October 4, 2013, and the multi-sectoral public health response by CDC and its partners averted 3,150 methylprednisolone acetate injections, 153 cases of meningitis or stroke, and 124 deaths, in comparison to the 60-day case-fatality rates and clinical characteristics of fungal meningitis patients diagnosed before October 4, 2013 (99).

4.2.7 New River Health District

New River Health District is one of 35 local health districts of the Virginia Department of Health in Virginia, and includes the counties of Floyd, Giles, Montgomery, Pulaski, and the city of Radford (100). It is among 11 health districts in Virginia with residents who were injected with fungal contaminated epidural steroids. In this study, local health department refers to New River Health District.

4.2.8 Study objective

The objective of this study is to evaluate the effectiveness and cost of the fungal meningitis outbreak response in New River Valley of Virginia, from the local public health department and clinical perspectives.

4.2.9 Related studies

In a related study, we conducted an economic evaluation of the fungal meningitis outbreak response in New River Valley, from the local public health department perspective (101). In this paper, we extend the prior study to include the cost estimates from the clinical response to evaluate the effectiveness and cost of the fungal meningitis outbreak response in New River Valley, from both the clinical and local public health department perspectives. We also conducted a systematic review of the clinical response, outbreak investigation and epidemiology of the fungal meningitis outbreak in the United States (102). The multisectoral

public health response to the fungal meningitis epidemic from the hospitals, clinics, pharmacies, and the public health system at the local, state, and federal levels led to an efficient epidemiological investigation to trace the outbreak source and rapid implementation of multiple response plans. The systematic review reaffirmed the effective execution of a multisectoral public health response and efficient delivery of the core functions of public health assessment, policy development, and service assurances to improve population health.

4.2.10 Public health significance

The multistate fungal meningitis outbreak affected Virginia with 56 cases and 5 deaths. Impact evaluation of the outbreak response in New River Valley assists the local health department and clinical facilities in optimization and prioritization of limited resources.

4.3 Methods

4.3.1 Surveillance and outbreak investigation by New River Health District

The timeline of the fungal meningitis outbreak response by the New River Health District and clinical facilities in New River Valley was from October 2012 to March 2013. There were 91 patients who were exposed to the fungal contaminated epidural steroids and were followed up for further assistance. The local health department implemented the surveillance system for follow-up with the affected patients, based on guidelines from CDC. Figure 4.1 shows the surveillance and outbreak response process implemented by the New River Health District. When the multistate outbreak was confirmed by CDC, personnel from New River Health District visited the clinical facilities in New River Valley and Roanoke where the exposed patients received the fungal contaminated epidural steroid injections and collected their information. The local health department personnel were in continuous contact with the state health department and CDC to get the updated information regarding the probable symptoms and updated case definition. The health district epidemiologist and volunteers then contacted patients and screened them for specific clinical symptoms. Patients with symptoms specific to fungal meningitis were referred to their local clinical facility for further lab tests. The epidemiologist contacted the patients' physicians and/or local emergency department to provide information about probable patients who may get admitted with confirmed symptoms. The epidemiologist also provided up to date information and recommendations for managing symptomatic patients in the clinical facilities. If the results of the lab test met the case definition, the patient was referred to the local hospital for further medical care. If the patient did not have any further symptoms, the local health department personnel continued to follow up with the patient for 6 months after the last dose of the contaminated injection.

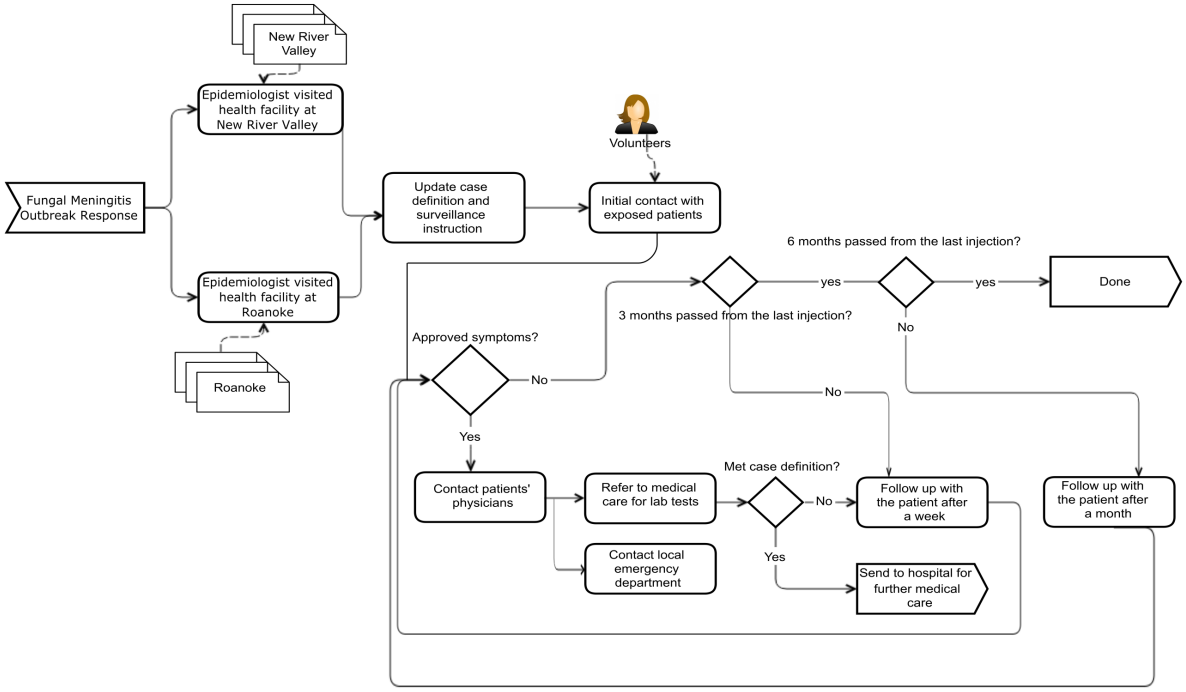

Figure 4.1: **Fungal meningitis outbreak response in New River Valley.** New River Valley patients who were administered with fungal contaminated epidural injections in the two clinical facilities of New River Valley and Roanoke were contacted by personnel of New River Health District. Exposed patients were followed up weekly for 3 months, and monthly for another 3 months. Symptomatic patients were referred to lab tests, and positively diagnosed patients were referred to hospitals for treatment.

4.3.2 Cost and effectiveness of the fungal meningitis outbreak response

Cost and effectiveness of the fungal meningitis outbreak response by the New River Health District and clinical facilities were compared to the do-nothing alternative (scenario of no intervention). Effectiveness measures the combined epidemiological impact of morbidity and mortality using the metric of disability adjusted life years (DALYs) averted (103).

4.3.3 Do-nothing alternative

Fungal meningitis is a rare disease, and the last recorded outbreak prior to the 2012-2013 outbreak was in 2002 with 5 cases (104). Health departments currently do not include fungal meningitis in their list of diseases or health conditions, as part of the reportable disease and/or sentinel surveillance process and case reporting activities. Thereby, we evaluate the fungal meningitis outbreak response in comparison to the do-nothing alternative in this economic evaluation.

4.3.4 Costs

Direct cost incurred by the New River Health District for the fungal meningitis outbreak response was estimated based on the total hours spent by the local health personnel involved in the outbreak response, and corresponding hourly wages. The outbreak response team in the local health department includes epidemiologist, health district director, planner, environmental health manager, clerical staff, administrative staff, nurse epidemiologist and volunteers, and data was provided by the New River Health District. Direct cost incurred by the clinical facilities was estimated based on the total cost of clinical care for the patients exposed to fungal contaminated epidural steroid injections.

4.3.5 Effectiveness

Effectiveness measures the epidemiological impact of the fungal meningitis outbreak response, using the metric of disability adjusted life years (DALYs) (103). DALYs measures the burden of (disease) fungal meningitis, as a combined metric of the epidemiological impacts of morbidity and mortality. Morbidity impact was measured by years of life lost due to disability (YLD), and mortality impact was measured by years of life lost due to premature mortality (YLL). Disability weight is used to quantify the disease severity on a scale of 0 (equivalent of perfect health) to 1 (equivalent of death) (105). The equations for YLD, YLL and DALY are below:

$$\text{YLD} = \text{Number of incident cases} \times \text{Disability weight} \times \text{Average duration of disease} \tag{4.1}$$

$$\text{YLL} = \text{Number of incident cases} \times \text{Case fatality rate} \times (\text{Life expectancy - Age of death}) \tag{4.2}$$

$$\text{DALY} = \text{YLD} + \text{YLL} \tag{4.3}$$

4.3.6 Cost-Effectiveness

Cost-effectiveness was measured using the incremental cost effectiveness ratio (ICER). ICER is computed as the ratio of the difference in costs and the difference in effectiveness (burden of disease) of the fungal meningitis outbreak response by the local health department and clinical facilities, compared to the do-nothing alternative. The equations for ICER is below:

$$\text{ICER}_1 = \frac{\text{Cost (outbreak response) - Cost (do-nothing alternative)}}{\text{Effectiveness (outbreak response) - Effectiveness (do-nothing alternative)}} \tag{4.4}$$

$$\text{ICER}_2 = \frac{\text{Cost (outbreak response) - Cost (do-nothing alternative)}}{\text{Burden of disease (do-nothing alternative) - Burden of disease (outbreak response)}} \tag{4.5}$$

4.4 Results

4.4.1 Time horizon

We conducted the economic evaluation of the fungal meningitis outbreak response in New River Valley, using the time horizon of October 2012 to March 2013.

4.4.2 Discount rate

No discount rate is used, since the time horizon of the study is less than a year.

4.4.3 Decision tree

Figure 4.2 illustrates the decision tree to compare the fungal meningitis outbreak response of the local health department and clinical/hospital facilities with the do-nothing alternative. In the outbreak response branch, positively diagnosed patients may receive treatment while negatively diagnosed patients do not receive treatment with corresponding costs and health benefits. Positively diagnosed patients may recover with treatment or die from fungal meningitis. The recovery rate of positively diagnosed patients with treatment was 90.32% (97). On the do-nothing branch, the positively diagnosed patients have a case fatality rate of 100%. There is no available or recorded estimates of case fatality rate among untreated fungal meningitis patients. The 100% case fatality rate among untreated fungal meningitis patients is based on the input of TMK (infectious disease physician who lead the clinical response to the fungal meningitis outbreak in New River Valley) that fungal meningitis, if left untreated, leads to a fatal outcome.

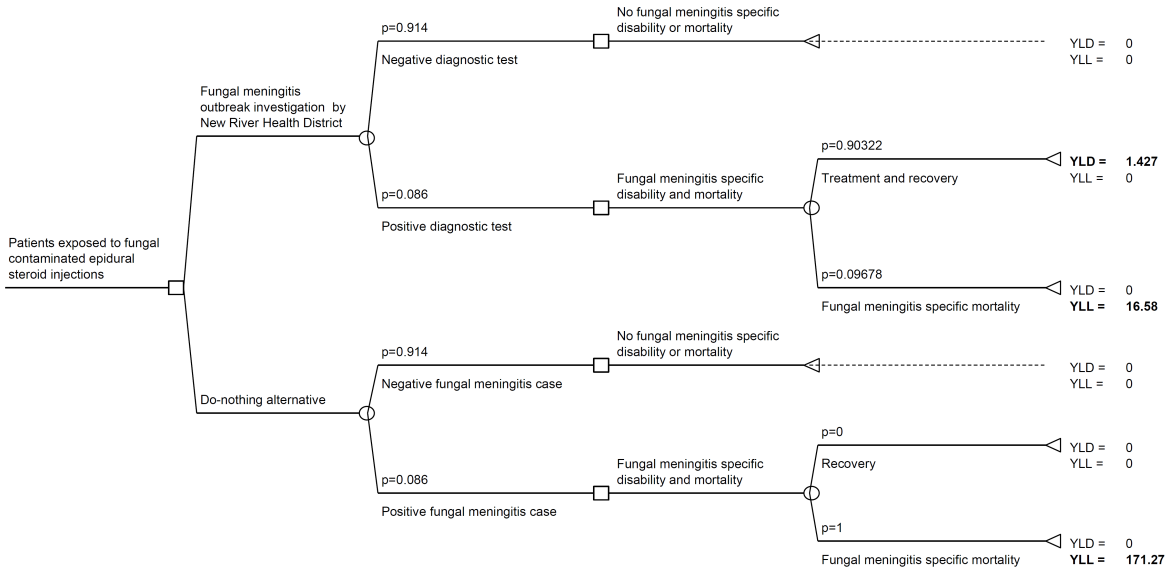

Figure 4.2: **The decision tree compares the fungal meningitis outbreak investigation in New River Health District with the do-nothing alternative.** Positively diagnosed patients from the outbreak investigation had a 90% survival rate with treatment compared to 100% mortality rate with the do-nothing alternative. The disability-adjusted life years or lost years of healthy life associated with the outbreak investigation is 18 DALYs compared to 171 DALYs associated with the do-nothing alternative. Thereby, 153 DALYs were averted due to the fungal meningitis outbreak response in New River Valley, compared to the do-nothing alternative.

Table 4.1: **Local health department costs.** Costs expended by the New River Health District to control the fungal meningitis outbreak in New River Valley.

New River Health District Personnel	Total hours	Hourly wage	Cost
Epidemiologists	386	$43.39	$16748.54
Health District Director	70.5	$95.70	$6746.85
Planner	32	$48.71	$1558.72
Environmental Health Manager	12	$42.58	$510.96
Clerical	12	$31.07	$372.84
Administration	8	$20.04	$160.32
Nurse Epidemiologist	16	$35.97	$575.52
Volunteers	143	$26.15	$3739.45
Total cost			**$30,413.20**

4.4.4 Cost - Local Health Department

Table 4.1 includes the distribution of costs among the different personnel of the New River Health District, who were involved in the fungal meningitis outbreak response. The hours spent by the personnel in the outbreak response and the corresponding hourly wages were provided by the New River Health District. We estimated that $30,413.20 was spent by the local health department in response to the fungal meningitis outbreak in New River Valley.

4.4.5 Cost - Clinical

Table 4.2 includes the distribution of costs of clinical care for patients to fungal contaminated epidural steroid injections in New River Valley. Among the 91 exposed patients, 12 lumbar punctures and 14 cerebrospinal fluid cultures were done, and 9 patients were admitted at the clinical facilities in Montgomery, Salem, Pulaski county, or Roanoke city. The average length of stay in these clinical facilities was 2.5 days with the range between 0 and 11 days for hospitalized patients. These data were obtained from the hospital records and patients' files. We estimated the cost associated with lumbar puncture of out-patients from (106), cost of cerebrospinal fluid cultures of out-patients from (107), and cost of hospitalization of in-patients from

Table 4.2: **Clinical costs.** The cost of clinical care in the local clinical facilities to control the fungal meningitis outbreak in New River Valley.

Type of cost	Number of patients	Average unit cost	Cost
Hospital admission	9	$3,908.11	$35,173.00
Lumbar Puncture	12	$285.57	$3,426.84
Cerebrospinal fluid (CSF) culture	14	$70.00	$980.00
Total cost			**$39,579.84**

the hospital records data. We estimated the that $39,579.84 was spent by the clinical facilities in response to the fungal meningitis outbreak in New River Valley.

4.4.6 Cost - Local health department and clinical

The local health department incurred a cost of $30,413.20 and the clinical facilities incurred a cost of $39,579.84 for a combined cost of $69,993.04 in the fungal meningitis outbreak response in New River Valley from October 2012 to March 2013.

4.4.7 Disability weight

Disability weight specific to fungal meningitis is not available, since it is a novel and rare disease. Bacterial meningitis and fungal meningitis have similar symptoms (108). Thereby, we used the disability weight of 0.615 for bacterial meningitis (109; 105) as the disability weight for fungal meningitis.

4.4.8 Years of life lost due to disability (YLD)

None of the 91 patients in New River Health District met the case definition of fungal meningitis, as defined by CDC. Using the average attack rate of 8.6% for fungal meningitis in Virginia among the patients who had received the contaminated epidural steroid injections, it was estimated that there would be 7.785 potential cases in New River Valley, as illustrated in Table 4.3. The average duration of treatment is 4 months

Table 4.3: **Potential cases of fungal meningitis in New River Valley.** Fungal meningitis attack rate for different injected lots. Potential attack rate of fungal meningitis in the New River Valley (NRV) was extracted from lot numbers and Virginia attack rate.

Lot #	**Injection Lots used for patients in New River Valley**	**Virginia Attack rate**	**Potential cases in New River Valley**
06292012 only	45	14.44%	6.498
06292012 with other lot	7	14.61%	1.023
05212012 only	24	1.1%	0.264
08102012 only	3	0%	0
05212012 + 08102012	0	17%	0
05212012 with other lot	12	0%	0
Total	**91**		**7.785**

for recovered patients, while the average duration of treatment among the fatal patients was near null. Using equation 4.1, 90.32% of patients who survived the fungal meningitis due to intervention, were getting treatment for 4 months in average. Patients who recovered from successful treatment lost 1.427 DALYs to account for the morbidity impact caused by fungal meningitis during the treatment duration. Thereby, we estimated the years of life lost due to disability (YLD) to be -1.427 DALYs averted due to the fungal meningitis outbreak response compared to the do-nothing alternative.

4.4.9 Years of life lost due to premature mortality (YLL)

The case fatality rate of fungal meningitis patients was 9.678% with treatment, while it is 100% without treatment. The average life expectancy in Virginia is 79 years (110), while the average age of patients in Virginia who were injected with fungal contaminated epidural steroids was 57 years. Using equation 4.2, we estimated the Years of life lost due to premature mortality (YLL) to be 154.69 DALYs averted due to the fungal meningitis outbreak response compared to the do-nothing alternative.

4.4.10 Effectiveness (DALY = YLD + YLL)

Using equation 4.3, we estimate the total disability adjusted life years to be 153.26 DALYs averted due to the fungal meningitis outbreak response compared to the do-nothing alternative. The computation of YLDs, YLLs and DALYs are illustrated in Table 4.4.

4.4.11 Cost-effectiveness

Using equation 4.4, incremental cost-effectiveness ratios (ICER) from the local health department perspective, clinical facilities perspective, and total (including both local health department and clinical facilities perspectives) were computed to be $198.43, $258.24, and $456.67 per DALY averted due to the fungal meningitis outbreak response compared to the do-nothing alternative.

4.4.12 Uncertainty and sensitivity analysis

We conducted sensitivity analysis for the duration of treatment, attack rate and disability weight.

Duration of treatment: We estimated that duration of treatment duration had an average of 4 months with a range of [1.5 months,18 months]. The corresponding impact on incremental cost-effectiveness ratio is [$197.29, $205.21] per DALY averted from the local health department perspective, [$256.76, $267.06] per DALY averted from the clinical perspective, and [$454.05, $472.26] per DALY averted from the local health department and clinical perspectives.

Attack rate: We estimated the attack rate to be 8.6% with a range of [1%, 17%] depending on the epidural injection lot. We tested the six potential scenarios of what if all the epidural injections administered to the patients in New River Valley had come from the six different lot numbers, as shown in Table 4.3. The corresponding impact on incremental cost-effectiveness ratio is [$1,697.58, $99.86] per DALY averted from the local health department perspective, [$2,209.23, $129.96] per DALY averted from the clinical perspective,

Table 4.4: **Epidemiological effectiveness of the fungal meningitis outbreak response.** Effectiveness of the fungal meningitis outbreak response in New River Valley is measured by Disability-Adjusted Life Years (DALYs) averted. DALYs is a combined measure of morbidity (YLDs - Years of Life lost due to Disability) and mortality (YLLs - Years of Life Lost due to premature mortality).

PARAMETER	**ESTIMATION**
Number of potential cases (proxy for incident cases)	7.785
Disability weight	0.615 [95% CI: 0.613, 0.616]
Average duration of treatment of recovered patients (proxy for average duration of disease)	0.33 years [mean: 4 months; range: 1.5-18 months]
Average duration of treatment of fatal patients	$\tilde{0}$ years [range: 1-8 days; 1 outlier case: 44 days]
YLD (outbreak response)	1.427 DALYs
YLD (no response)	0 DALYs
YLD (averted)	YLD (no response) - YLD (outbreak response) = 0 - 1.427 **= -1.427 DALYs averted (= 1.427 DALYs)**
Case fatality rate	
- outbreak response	9.68%
- no outbreak response	100%
Average life expectancy in Virginia	79 years
Average age of patients (proxy for average age of death)	57 years
YLL (outbreak response)	16.58 DALYs
YLL (no response)	171.27 DALYs
YLL (averted)	YLL (no response) - YLL (outbreak response) = 171.27 - 16.58 **= 154.69 DALYs averted**
DALYs (averted)	YLD (averted) + YLL (averted) 153.263 **= 153.26 DALYs averted**
YLD : Years Lost due to Disability YLD = Number of incident cases ×Disability weight × Average duration of disease	
YLL : Years of Life Lost due to premature death YLL = Number of incident cases × Case fatality rate × (Life expectancy - Age of death)	
DALY : Disability Adjusted Life Year; One DALY equals one lost year of healthy life. DALY = YLD + YLL	

and [$3,906.81, $229.81] per DALY averted from the local health department and clinical perspectives.

Disability weight: We estimated the disability weight for fungal meningitis to be 0.615 with a 95% confidence interval of [0.613,0.616]. The corresponding impact on incremental cost-effectiveness ratio is [$198.43, $198.44] per DALY averted from the local health department perspective, [$258.23, $258.24] per DALY averted from the clinical perspective, and [$456.66, $456.68] per DALY averted from the local health department and clinical perspectives.

4.5 Discussion

Local health departments conducted disease surveillance, case reporting, and referring probable cases to clinical facilities for diagnostics, treatment, and/or hospitalization during the 2012-2013 multistate fungal meningitis' outbreak in the United States. We estimated the total direct costs incurred by New River Health District and clinical facilities for the fungal meningitis outbreak response in New River Valley to be $69,993.04. We estimated morbidity impact of -1.427 DALYs for years of life lost due to disability averted and mortality impact of 154.69 DALYs for years of life lost due to premature mortality averted, for a combined morbidity and mortality impact (burden of fungal meningitis) of 153.26 DALYs averted for epidemiological effectiveness of the fungal meningitis outbreak response compared to the do-nothing alternative. We estimated the incremental cost effectiveness ratio of the fungal meningitis outbreak response in New River Valley to be $198.43, $258.24, and $456.67 per DALY averted from the local health department, clinical, and combined local health department and clinical perspectives respectively, compared to the do-nothing alternative.

4.5.1 Partial economic evaluation

While the fungal meningitis outbreak response required a coordinated effort by the CDC, FDA, state and local health departments, and includes the clinical response of diagnosis and treatment, the perspective of this analysis has focused only from the local health department and clinical perspectives. While the epidemiological effectiveness among the patients in New River Valley is a combined result of the coordinated effort of the health departments (local, state and federal) and the clinical facilities (labs and hospitals), the cost calculations had included only the costs incurred by the local health department and hospitals/clinics. Due to this asymmetry in the boundaries of calculation of effectiveness and costs, this study is a partial economic evaluation of the fungal meningitis outbreak response in New River Valley.

4.5.2 Cost-effectiveness threshold

New River Health District and Virginia Department of Health currently do not use a threshold to judge if an intervention or public health program is cost-effective.

4.5.3 Public health implications

Economic evaluation of the fungal meningitis outbreak response in New River Valley assists the local health department and clinical facilities to analyze the costs and epidemiological effectiveness of the outbreak response compared to the do-nothing alternative. We estimated the epidemiological effectiveness to be 153.26 DALYs averted, and the incremental cost-effectiveness ratio to be $456.67 per DALY averted from the local health department and clinical perspective. The disability adjusted life year (DALY) metric provides a uniform metric to estimate and compare the burden of different diseases, and the incremental cost-effectiveness ratio ($/DALY averted) provides a uniform metric to evaluate and compare the impact of different disease control and prevention programs, thereby assisting in the prioritization of public health programs.

4.5.4 Limitations

The cost calculations did not include indirect costs incurred by New River Health District and/or clinical facilities. There is lack of scientific studies and clinical knowledge of fungal meningitis, since it is a relatively rare disease. Thereby, the disability weight of fungal meningitis was estimated using the disability weight of bacterial meningitis, since both the diseases have common symptoms. There were variations in the cost calculations among different clinical facilities in New River Valley. While the fungal meningitis outbreak response required a coordinated effort by the CDC, FDA, state and local health departments (111; 112), the focus of this economic evaluation was only from the local health department and clinical perspectives.

Chapter 5

Conclusion

This dissertation has focused on the impact of infectious diseases from individual level and population level: first, analysing the HIV viral and immune system dynamics; second, focusing on the importance of population dynamics in influenza pandemic spread and control; and third, measuring the cost and effectiveness of interventions in response to the fungal meningitis outbreak from the local health department and clinical perspectives.

5.1 Viral and immune system dynamics of HIV-1, CD4+ T cells and macrophages during the acute, clinically latent and late phases of HIV infection

In chapter 2, the study objective was to analyze the dynamics of HIV-1, CD4+ T cells and macrophages during acute, clinically latent and late phases of HIV infection in order to predict their dynamics from acute infection to clinical latency and finally to AIDS in treatment naive HIV-infected individuals. This study incorporated the macrophage dynamics and their impact as HIV-1 reservoir and on virus production, to the viral-immune dynamics of HIV-1 and CD4+ T cells during the acute, clinically latent and late phases of

HIV infection. We developed a deterministic mathematical model of virus-host dynamics that incorporated the HIV-1, CD4+ T cell and macrophage populations. We calibrated the model against longitudinal clinical data of HIV viral load and CD4+ T cell counts from a cohort of 39 treatment naive HIV-infected individuals, collected at the Mortimer Market Centre in London, UK. Based on model calibration to the patient cohort, we inferred that the mean HIV progression timeline from time of infection to AIDS stage was 5.75 years. We predicted that the peak in viral load during the acute HIV infection was due to virus production by infected CD4+ T cells, while the virus production during the clinically latent and late phases of infection came from infected macrophages which dominated the overall virus production. This led to the conclusion that macrophages-induced viral production is the significant driver of HIV progression from asymptomatic phase to AIDS in HIV-infected individuals.

5.2 Epidemiological and economic impact of pandemic influenza in Chicago: Priorities for vaccine interventions

In chapter 3, the study objective was to estimate the direct and indirect epidemiological and economic impact of vaccine interventions during an influenza pandemic in Chicago, and assist in vaccine intervention priorities. Meltzer et al estimated the potential net value of different vaccination strategies, and identified vaccination priorities for different age and risk groups during an influenza pandemic (113). A Monte Carlo based static model was used to estimate the costs and benefits due to the direct effect of vaccine interventions in the United States. We extended that study and conducted a cost-benefit analysis to infer influenza prevention priorities, by simulating the direct and indirect epidemiological and economic impact of vaccine interventions, during influenza pandemics in Chicago. We used agent-based modeling to simulate the transmission dynamics of influenza-like-illness using the susceptible-exposed-infectious-recovered epidemiological model on a collocation based synthetic social contact network. Population was distributed

among high-risk and non-high risk among 0-19, 20-64 and 65+ years subpopulations. Different attack rate scenarios for catastrophic (58.11%), strong (38.62%), and moderate (28.96%) influenza pandemics were compared against vaccine intervention scenarios, at 40% coverage, 40% efficacy, and unit cost of $28.62. Vaccine prioritization criteria included risk of death, total deaths, net benefits, and return on investment. Based on risk of death and return on investment, high-risk groups of the three age group subpopulations could be prioritized for vaccination, and the vaccine interventions are cost-saving for all age and risk groups.

5.3 Effectiveness and partial cost of fungal meningitis outbreak response in New River Valley: Local health department and clinical perspectives

In chapter 4, the study objective was to evaluate the effectiveness and cost of the fungal meningitis outbreak response in New River Valley of Virginia during 2012-2013, from the local public health department and clinical perspectives. The fungal meningitis outbreak affected 23 states with 751 cases and 64 deaths in 20 states in the United States; there were 56 cases and 5 deaths in Virginia. We conducted a partial economic evaluation of the fungal meningitis outbreak response in New River Valley. We collected the costs associated with the local health department and clinical facilities in the outbreak response, and estimated the epidemiological effectiveness using disability adjusted life years (DALYs) averted. We estimated the epidemiological effectiveness of this outbreak response to be 153 DALYs averted among the patients, and the costs incurred by the local health department and clinical facilities to be $30,413 and $39,580 respectively. We estimated the incremental cost-effectiveness ratio of $198 per DALY averted and $258 per DALY averted from the local health department and clinical perspectives respectively, thereby assisting in economic evaluation of the outbreak response by the local health department and clinical facilities.

5.4 Moving forward: Multi-scale dynamics of infectious diseases

This dissertation add insights to mathematical modeling of infectious diseases at the immunological, epidemiological, and economic scales. The future work will focus on developing a multi-scale framework connecting the within-host dynamics at the individual level and between-host dynamics at the population level. The multi-scale framework enables us to address how evolutionary dynamic of a pathogen influences immunological and epidemiological impact of the infectious disease and identifies optimal control strategies from the economic perspective. Multi-scale models will gain significant role with the emerging availability of big data; however, making meaningful inferences and understanding the underlying dynamics will still be critical. Figure 5.1 illustrates multi-scale analysis of infectious disease dynamics connecting the different scales of evolution, immunology, epidemiology, and economics. Multi-scale modeling of infectious disease dynamics has good potential to derive meaningful inferences for decision making in clinical and public health practice, and improve health outcomes.

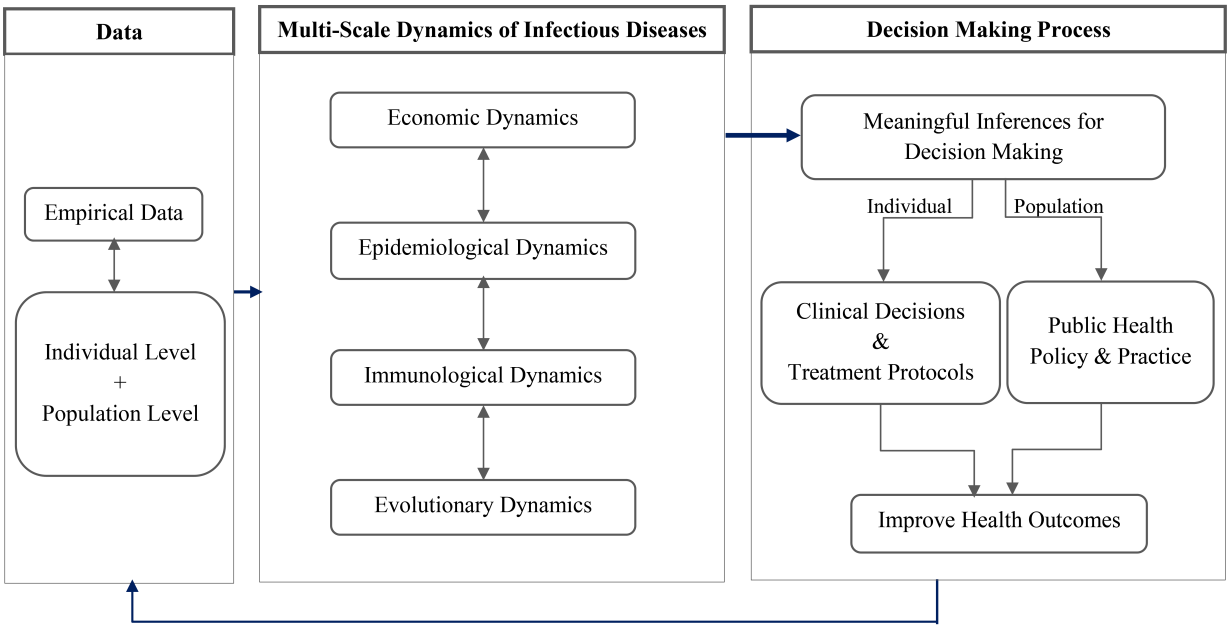

Figure 5.1: **Multi-scale dynamics of infectious diseases to improve individual and population health outcomes.** Multi-scale analysis of infectious disease dynamics connecting the different scales of evolution, immunology, epidemiology, and economics has good potential to derive meaningful inferences for decision making in clinical and public health practice, and improve health outcomes.

Bibliography

[1] Global Burden of Disease Study 2013 Collaborators. Global, regional, and national incidence, prevalence, and years lived with disability for 301 acute and chronic diseases and injuries in 188 countries, 1990-2013: a systematic analysis for the Global Burden of Disease Study 2013. Lancet (London, England). 2015 Aug;386(9995):743–800.

[2] Nowak MA. Evolutionary Dynamics: Exploring the Equations of Life. Harvard University Press;.

[3] Nelson MI, Wentworth DE, Das SR, Sreevatsan S, Killian ML, Nolting JM, et al. Evolutionary Dynamics of Influenza A Viruses in US Exhibition Swine. The Journal of Infectious Diseases. 2016 Jan;213(2):173–182.

[4] Nelson MI, Holmes EC. The evolution of epidemic influenza. Nature Reviews Genetics. 2007 Mar;8(3):196–205. Available from: http://www.nature.com/nrg/journal/v8/n3/full/nrg2053.html.

[5] Nelson MI, Wentworth DE, Culhane MR, Vincent AL, Viboud C, LaPointe MP, et al. Introductions and evolution of human-origin seasonal influenza a viruses in multinational swine populations. Journal of Virology. 2014 Sep;88(17):10110–10119.

[6] Rasmussen DA, Boni MF, Koelle K. Reconciling phylodynamics with epidemiology: the case of dengue virus in southern Vietnam. Molecular Biology and Evolution. 2014 Feb;31(2):258–271.

[7] Ben-Shachar R, Koelle K. Minimal within-host dengue models highlight the specific roles of the

immune response in primary and secondary dengue infections. Journal of the Royal Society, Interface / the Royal Society. 2015 Feb;12(103).

[8] Perelson AS. Modelling viral and immune system dynamics. Nature Reviews Immunology. 2002 Jan;2(1):28–36.

[9] Ciupe SM. Mathematical model of multivalent virus-antibody complex formation in humans following acute and chronic HIV infections. Journal of Mathematical Biology. 2015 Sep;71(3):513–532.

[10] Kronsteiner B, Bassaganya-Riera J, Philipson C, Viladomiu M, Carbo A, Abedi V, et al. Systems-wide analyses of mucosal immune responses to Helicobacter pylori at the interface between pathogenicity and symbiosis;7(1):3–21.

[11] Anderson RM, May RM. Infectious diseases of humans: Dynamics and control. OUP Oxford; 1992.

[12] Kermack WO, McKendrick AG. A Contribution to the Mathematical Theory of Epidemics. Proceedings of the Royal Society of London A: Mathematical, Physical and Engineering Sciences. 1927 Aug;115(772):700–721. Available from: http://rspa.royalsocietypublishing.org/content/115/772/700.

[13] Eubank S. Network based models of infectious disease spread. Japanese Journal of Infectious Diseases. 2005 Dec;58(6):S9–13.

[14] Eubank S, Guclu H, Kumar VSA, Marathe MV, Srinivasan A, Toroczkai Z, et al. Modelling disease outbreaks in realistic urban social networks. Nature. 2004 May;429(6988):180–184.

[15] Bloom DE, Canning D. The Health and Wealth of Nations. Science. 2000 Feb;287(5456):1207–1209. Available from: http://science.sciencemag.org/content/287/5456/1207.

[16] DCP3 - Disease Control Priorities - Economic evaluation for health - dcp-3.org;. Available from: http://dcp-3.org/.

[17] Nandi A, Colson AR, Verma A, Megiddo I, Ashok A, Laxminarayan R. Health and economic benefits of scaling up a home-based neonatal care package in rural India: a modelling analysis. Health Policy and Planning. 2015 Nov;p. czv113. Available from: http://heapol.oxfordjournals.org/content/early/2015/11/10/heapol.czv113.

[18] Megiddo I, Colson A, Chisholm D, Dua T, Nandi A, Laxminarayan R. Health and economic benefits of public financing of epilepsy treatment in India: An agent-based simulation model. Epilepsia. 2016 Mar;57(3):464–474. Available from: http://doi.wiley.com/10.1111/epi.13294.

[19] Maddon PJ, Dalgleish AG, McDougal JS, Clapham PR, Weiss RA, Axel R. The T4 gene encodes the AIDS virus receptor and is expressed in the immune system and the brain. Cell. 1986 Nov;47(3):333–348.

[20] Lifson JD, Feinberg MB, Reyes GR, Rabin L, Banapour B, Chakrabarti S, et al. Induction of CD4-dependent cell fusion by the HTLV-III/LAV envelope glycoprotein. Nature. 1986 Oct;323(6090):725–728.

[21] Abbas W, Herbein G. T-Cell Signaling in HIV-1 Infection. The Open Virology Journal. 2013 Jul;7:57–71. Available from: http://www.ncbi.nlm.nih.gov/pmc/articles/PMC3751038/.

[22] Koppensteiner H, Brack-Werner R, Schindler M. Macrophages and their relevance in Human Immunodeficiency Virus Type I infection. Retrovirology. 2012;9:82. Available from: http://dx.doi.org/10.1186/1742-4690-9-82.

[23] Iordanskiy S, Santos S, Bukrinsky M. Nature, nurture and HIV: The effect of producer cell on viral physiology. Virology. 2013 Sep;443(2):208–213.

[24] Arrildt KT, LaBranche CC, Joseph SB, Dukhovlinova EN, Graham WD, Ping LH, et al. Phenotypic

Correlates of HIV-1 Macrophage Tropism. Journal of Virology. 2015 Sep;p. JVI.00946–15. Available from: http://jvi.asm.org/content/early/2015/08/28/JVI.00946-15.

[25] Mefford ME, Kunstman K, Wolinsky SM, Gabuzda D. Bioinformatic analysis of neurotropic HIV envelope sequences identifies polymorphisms in the gp120 bridging sheet that increase macrophage-tropism through enhanced interactions with CCR5. Virology. 2015 Jul;481:210–222.

[26] Salimi H, Roche M, Webb N, Gray LR, Chikere K, Sterjovski J, et al. Macrophage-tropic HIV-1 variants from brain demonstrate alterations in the way gp120 engages both CD4 and CCR5. Journal of Leukocyte Biology. 2013 Jan;93(1):113–126.

[27] Sattentau QJ, Stevenson M. Macrophages and HIV-1: An Unhealthy Constellation. Cell Host & Microbe. 2016 Mar;19(3):304–310. Available from: http://www.cell.com/article/S1931312816300543/abstract.

[28] King DFL, Siddiqui AA, Buffa V, Fischetti L, Gao Y, Stieh D, et al. Mucosal Tissue Tropism and Dissemination of HIV-1 Subtype B Acute Envelope-Expressing Chimeric Virus;87(2):890–899. Available from: http://jvi.asm.org/content/87/2/890.

[29] Li Q, Estes JD, Schlievert PM, Duan L, Brosnahan AJ, Southern PJ, et al. Glycerol monolaurate prevents mucosal SIV transmission;458(7241):1034–1038. Available from: http://www.nature.com/nature/journal/v458/n7241/full/nature07831.html.

[30] Groot F, Welsch S, Sattentau QJ. Efficient HIV-1 transmission from macrophages to T cells across transient virological synapses. Blood. 2008 May;111(9):4660–4663.

[31] McMichael AJ, Borrow P, Tomaras GD, Goonetilleke N, Haynes BF. The immune response during acute HIV-1 infection: clues for vaccine development. Nature reviews Immunology. 2010 Jan;10(1):11–23. Available from: http://www.ncbi.nlm.nih.gov/pmc/articles/PMC3119211/.

[32] Brenchley JM, Douek DC. The mucosal barrier and immune activation in HIV pathogenesis. Current opinion in HIV and AIDS. 2008 May;3(3):356–361.

[33] Guillemin GJ, Brew BJ. Microglia, macrophages, perivascular macrophages, and pericytes: a review of function and identification. Journal of Leukocyte Biology. 2004 Mar;75(3):388–397.

[34] Moir S, Chun TW, Fauci AS. Pathogenic mechanisms of HIV disease. Annual Review of Pathology. 2011;6:223–248.

[35] Antia R, Halloran ME. Recent developments in theories of pathogenesis of AIDS. Trends in Microbiology. 1996 Jul;4(7):282–285. Available from: http://www.sciencedirect.com/science/article/pii/0966842X96100445.

[36] Forde J, Volpe JM, Ciupe SM. Latently infected cell activation: a way to reduce the size of the HIV reservoir? Bulletin of Mathematical Biology. 2012 Jul;74(7):1651–1672.

[37] Orenstein JM, Meltzer MS, Phipps T, Gendelman HE. Cytoplasmic assembly and accumulation of human immunodeficiency virus types 1 and 2 in recombinant human colony-stimulating factor-1-treated human monocytes: an ultrastructural study. Journal of Virology. 1988 Aug;62(8):2578–2586.

[38] Swingler S, Mann AM, Zhou J, Swingler C, Stevenson M. Apoptotic killing of HIV-1-infected macrophages is subverted by the viral envelope glycoprotein. PLoS pathogens. 2007 Sep;3(9):1281–1290.

[39] Reynoso R, Wieser M, Ojeda D, Bönisch M, Kühnel H, Bolcic F, et al. HIV-1 induces telomerase activity in monocyte-derived macrophages, possibly safeguarding one of its reservoirs. Journal of Virology. 2012 Oct;86(19):10327–10337.

[40] Department of Health & Human Services. Guidelines for the Use of Antiretro-

viral Agents in HIV-1-Infected Adults and Adolescents; 2016. Available from: http://www.aidsinfo.nih.gov/ContentFiles/AdultandAdolescentGL.pdf.

[41] Fauci AS. HIV and AIDS: 20 years of science. Nature Medicine. 2003 Jul;9(7):839–843. Available from: http://www.nature.com/nm/journal/v9/n7/full/nm0703-839.html.

[42] Burdo TH, Soulas C, Orzechowski K, Button J, Krishnan A, Sugimoto C, et al. Increased Monocyte Turnover from Bone Marrow Correlates with Severity of SIV Encephalitis and CD163 Levels in Plasma. PLOS Pathog. 2010 Apr;6(4):e1000842. Available from: http://journals.plos.org/plospathogens/article?id=10.1371/journal.ppat.1000842.

[43] Hasegawa A, Liu H, Ling B, Borda JT, Alvarez X, Sugimoto C, et al. The level of monocyte turnover predicts disease progression in the macaque model of AIDS. Blood. 2009 Oct;114(14):2917–2925.

[44] Kuroda MJ. Macrophages: do they impact AIDS progression more than CD4 T cells? Journal of Leukocyte Biology. 2010 Apr;87(4):569–573. Available from: http://www.jleukbio.org/content/87/4/569.

[45] Hernandez-Vargas EA, Middleton RH. Modeling the three stages in HIV infection. Journal of Theoretical Biology. 2013;320:33–40. Available from: http://www.sciencedirect.com/science/article/pii/S0022519312006170.

[46] Hadjiandreou M, Conejeros R, Vassiliadis VS. Towards a long-term model construction for the dynamic simulation of HIV infection. Mathematical biosciences and engineering: MBE. 2007 Jul;4(3):489–504.

[47] Zhang C, Zhou S, Groppelli E, Pellegrino P, Williams I, Borrow P, et al. Hybrid Spreading Mechanisms and T Cell Activation Shape the Dynamics of HIV-

1 Infection. PLOS Comput Biol. 2015 Apr;11(4):e1004179. Available from: http://journals.plos.org/ploscompbiol/article?id=10.1371/journal.pcbi.1004179.

[48] Chun TW, Stuyver L, Mizell SB, Ehler LA, Mican JA, Baseler M, et al. Presence of an inducible HIV-1 latent reservoir during highly active antiretroviral therapy. Proceedings of the National Academy of Sciences of the United States of America. 1997;94(24):13193–13197.

[49] Finzi D, Hermankova M, Pierson T, Carruth LM, Buck C, Chaisson RE, et al. Identification of a reservoir for HIV-1 in patients on highly active antiretroviral therapy. Science (New York, NY). 1997;278(5341):1295–1300.

[50] Kumar A, Abbas W, Herbein G. HIV-1 Latency in Monocytes/Macrophages. Viruses. 2014 Apr;6(4):1837–1860. Available from: http://www.ncbi.nlm.nih.gov/pmc/articles/PMC4014723/.

[51] Delemarre FG, Kors N, Kraal G, van Rooijen N. Repopulation of macrophages in popliteal lymph nodes of mice after liposome-mediated depletion. 1990;47(3):251–257.

[52] Sachsenberg N, Perelson AS, Yerly S, Schockmel GA, Leduc D, Hirschel B, et al. Turnover of CD4+ and CD8+ T lymphocytes in HIV-1 infection as measured by Ki-67 antigen. The Journal of Experimental Medicine. 1998 Apr;187(8):1295–1303.

[53] Kirschner D, Perelson A. A Model for the Immune System Response to HIV: AZT Treatment Studies. In: Mathematical Population Dynamics: Analysis of Hetergeneity and Theory of Epidemics. Wuerz Publishing, Winnipeg (1995);. p. 295–310.

[54] Chun TW, Carruth L, Finzi D, Shen X, DiGiuseppe JA, Taylor H, et al. Quantification of latent tissue reservoirs and total body viral load in HIV-1 infection;387(6629):183–188. Available from: http://www.nature.com/nature/journal/v387/n6629/abs/387183a0.html.

[55] Markowitz M, Louie M, Hurley A, Sun E, Di Mascio M, Perelson AS, et al. A novel antiviral intervention results in more accurate assessment of human immunodeficiency virus type 1 replication dynamics and T-cell decay in vivo. Journal of Virology. 2003 Apr;77(8):5037–5038.

[56] Huang Y, Liu D, Wu H. Hierarchical Bayesian Methods for Estimation of Parameters in a Longitudinal HIV Dynamic System. Biometrics. 2006 Jun;62(2):413–423. Available from: http://www.ncbi.nlm.nih.gov/pmc/articles/PMC2435289/.

[57] Kirschner D. Using mathematics to understand HIV immune dynamics. AMS Notices. 1996 Feb;p. 191–202.

[58] Haldar M, Murphy KM. Origin, development, and homeostasis of tissue-resident macrophages;262(1):25–35. Available from: http://onlinelibrary.wiley.com.ezproxy.lib.vt.edu/doi/10.1111/imr.12215/abstract.

[59] Novobilski A, Kamangar F. Absolute Percent Error Based Fitness Functions for Evolving Forecast Models. In: FLAIRS Conference; 2001. p. 591–595.

[60] Trucano TG, Swiler LP, Igusa T, Oberkampf WL, Pilch M. Calibration, validation, and sensitivity analysis: What's what. Reliability Engineering & System Safety. 2006 Oct;91(10–11):1331–1357. Available from: http://www.sciencedirect.com/science/article/pii/S0951832005002437.

[61] R: The R Project for Statistical Computing;. Available from: https://www.r-project.org/.

[62] Pantaleo G, Graziosi C, Fauci AS. The Immunopathogenesis of Human Immunodeficiency Virus Infection. New England Journal of Medicine. 1993 Feb;328(5):327–335. Available from: http://dx.doi.org/10.1056/NEJM199302043280508.

[63] Piatak M, Saag MS, Yang LC, Clark SJ, Kappes JC, Luk KC, et al. High levels of HIV-1 in plasma

during all stages of infection determined by competitive PCR. Science. 1993 Mar;259(5102):1749–1754. Available from: http://science.sciencemag.org/content/259/5102/1749.

[64] Meltzer MI, Cox NJ, Fukuda K. The economic impact of pandemic influenza in the United States: priorities for intervention. Emerg Infect Dis. 1999 Sep;5(5):659–671.

[65] CDC - ACIP - Advisory Committee on Immunization Practices (ACIP) Home Page - Vaccines;. Accessed: 2015-7-3. http://www.cdc.gov/vaccines/acip/.

[66] Mullooly JP, Bennett MD, Hornbrook MC, Barker WH, Williams WW, Patriarca PA, et al. Influenza Vaccination Programs for Elderly Persons: Cost-Effectiveness in a Health Maintenance Organization. Annals of Internal Medicine. 1994 Dec;121(12):947–952. Available from: http://dx.doi.org/10.7326/0003-4819-121-12-199412150-00008.

[67] Bridges Carolyn, Thompson William W, Meltzer Martin I, et al. Effectiveness and cost-benefit of influenza vaccination of healthy working adults: A randomized controlled trial. JAMA. 2000 Oct;284(13):1655–1663. Available from: http://dx.doi.org/10.1001/jama.284.13.1655.

[68] Lee PY, Matchar DB, Clements DA, Huber J, Hamilton JD, Peterson ED. Economic analysis of influenza vaccination and antiviral treatment for healthy working adults. Ann Intern Med. 2002 20 Aug;137(4):225–231.

[69] Prosser LA, Lavelle TA, Fiore AE, Bridges CB, Reed C, Jain S, et al. Cost-effectiveness of 2009 pandemic influenza A(H1N1) vaccination in the United States. PLoS One. 2011 29 Jul;6(7):e22308.

[70] Meltzer MI, Neuzil KM, Griffin MR, Fukuda K. An economic analysis of annual influenza vaccination of children. Vaccine. 2005 11 Jan;23(8):1004–1014.

[71] Borse RH, Shrestha SS, Fiore AE, Atkins CY, Singleton JA, Furlow C, et al. Effects of vaccine

program against pandemic influenza A(H1N1) virus, United States, 2009-2010. Emerg Infect Dis. 2013 Mar;19(3):439–448.

[72] Kostova D, Reed C, Finelli L, Cheng PY, Gargiullo PM, Shay DK, et al. Influenza Illness and Hospitalizations Averted by Influenza Vaccination in the United States, 2005-2011. PLoS One. 2013 19 Jun;8(6):e66312.

[73] Biggerstaff M, Reed C, Swerdlow DL, Gambhir M, Graitcer S, Finelli L, et al. Estimating the potential effects of a vaccine program against an emerging influenza pandemic–United States. Clin Infect Dis. 2015 1 May;60 Suppl 1:S20–9.

[74] Meltzer MI, Bridges CB. Economic analysis of influenza vaccination and treatment. Ann Intern Med. 2003 1 Apr;138(7):608; author reply 608–9.

[75] Prosser LA, Bridges CB, Uyeki TM, Hinrichsen VL, Meltzer MI, Molinari NAM, et al. Health benefits, risks, and cost-effectiveness of influenza vaccination of children. Emerg Infect Dis. 2006 Oct;12(10):1548–1558.

[76] Coleman MS, Fontanesi J, Meltzer MI, Shefer A, Fishbein DB, Bennett NM, et al. Estimating medical practice expenses from administering adult influenza vaccinations. Vaccine. 2005 4 Jan;23(7):915–923.

[77] Peasah SK, Azziz-Baumgartner E, Breese J, Meltzer MI, Widdowson MA. Influenza cost and cost-effectiveness studies globally–a review. Vaccine. 2013 4 Nov;31(46):5339–5348.

[78] Monto AS, Davenport FM, Napier JA, Francis T Jr. Effect of vaccination of a school-age population upon the course of an A2-Hong Kong influenza epidemic. Bull World Health Organ. 1969;41(3):537–542.

[79] Longini IM Jr, Koopman JS, Monto AS, Fox JP. Estimating household and community transmission parameters for influenza. Am J Epidemiol. 1982 May;115(5):736–751.

[80] Longini IM, Halloran ME, Nizam A, Wolff M, Mendelman PM, Fast PE, et al. Estimation of the efficacy of live, attenuated influenza vaccine from a two-year, multi-center vaccine trial: implications for influenza epidemic control. Vaccine. 2000 17 Mar;18(18):1902–1909.

[81] King JC Jr, Beckett D, Snyder J, Cummings GE, King BS, Magder LS. Direct and indirect impact of influenza vaccination of young children on school absenteeism. Vaccine. 2012 5 Jan;30(2):289–293.

[82] Glezen WP, Gaglani MJ, Kozinetz CA, Piedra PA. Direct and indirect effectiveness of influenza vaccination delivered to children at school preceding an epidemic caused by 3 new influenza virus variants. J Infect Dis. 2010 1 Dec;202(11):1626–1633.

[83] CDC-MMWR. 2009;.

[84] Bureau USC. Census.gov;.

[85] Beckman RJ, Baggerly KA, McKay MD. Creating synthetic baseline populations. Transp Res Part A: Policy Pract. 1996 Nov;30(6):415–429.

[86] Barrett CL, Bisset KR, Eubank SG, Feng X, Marathe MV. EpiSimdemics: An Efficient Algorithm for Simulating the Spread of Infectious Disease over Large Realistic Social Networks. In: Proceedings of the 2008 ACM/IEEE Conference on Supercomputing. SC '08. Piscataway, NJ, USA: IEEE Press; 2008. p. 37:1–37:12.

[87] Barrett C, Bisset K, Leidig J, Marathe A, Marathe M. Economic and social impact of influenza mitigation strategies by demographic class. Epidemics. 2011 Mar;3(1):19–31.

[88] Jhung MA, Swerdlow D, Olsen SJ, Jernigan D, Biggerstaff M, et al. Epidemiology of 2009 pandemic

influenza A (H1N1) in the United States. Clinical Infectious Diseases: An Official Publication of the Infectious Diseases Society of America. 2011 Jan;52 Suppl 1:S13–26.

[89] Seasonal Influenza Vaccine Effectiveness, 2005-2016 — Health Professionals — Seasonal Influenza (Flu);. Accessed: 2016-4-22. http://www.cdc.gov/flu/professionals/vaccination/effectiveness-studies.htm.

[90] Yoo BK, Szilagyi PG, Schaffer SJ, Humiston SG, Rand CM, Albertin CS, et al. Cost of universal influenza vaccination of children in pediatric practices. Pediatrics. 2009 Dec;124 Suppl 5:S499–506.

[91] Carias C, Reed C, Kim IK, Foppa IM, Biggerstaff M, Meltzer MI, et al. Net Costs Due to Seasonal Influenza Vaccination–United States, 2005-2009. PLoS One. 2015 31 Jul;10(7):e0132922.

[92] Grohskopf LA, Sokolow LZ, Olsen SJ, Bresee JS, Broder KR, Karron RA. Prevention and Control of Influenza with Vaccines: Recommendations of the Advisory Committee on Immunization Practices, United States, 2015-16 Influenza Season. MMWR Morb Mortal Wkly Rep. 2015 7 Aug;64(30):818–825.

[93] Smith RM, Schaefer MK, Kainer MA, Wise M, Finks J, et al. Fungal Infections Associated with Contaminated Methylprednisolone Injections. N Engl J Med. 2013 24 Oct;369(17):1598–1609.

[94] Kainer MA, Reagan DR, Nguyen DB, Wiese AD, Wise ME, et al. Fungal infections associated with contaminated methylprednisolone in Tennessee. N Engl J Med. 2012 6 Dec;367(23):2194–2203.

[95] CDC. Multistate Outbreak of Fungal Infection Associated with Injection of Methylprednisolone Acetate Solution from a Single Compounding Pharmacy. 2012;.

[96] Kauffman CA, Pappas PG, Patterson TF. Fungal Infections Associated with Contaminated Methylprednisolone Injections. N Engl J Med. 2013 27 Jun;368(26):2495–2500.

[97] CDC. Multistate Outbreak of Fungal Meningitis and Other Infections — CDC;. Accessed: 2015-6-29. http://www.cdc.gov/hai/outbreaks/meningitis.html.

[98] Kerkering TM, Grifasi ML, Baffoe-Bonnie AW, Bansal E, Garner DC, Smith JA, et al. Early clinical observations in prospectively followed patients with fungal meningitis related to contaminated epidural steroid injections. Ann Intern Med. 2013 5 Feb;158(3):154–161.

[99] Rachel M Smith, Gordana Derado, Matthew Wise, Julie R Harris, Tom Chiller, Martin I Meltzer, et al. Estimated Deaths and Illnesses Averted During Fungal Meningitis Outbreak Associated with Contaminated Steroid Injections, United States, 2012–2013. Emerging Infectious Disease journal. 2015;21(6):933.

[100] New River Health District, Virginia Department of Health;. Accessed: 2015-7-12. http://www.vdh.virginia.gov/LHD/index.htm.

[101] Abbas KM, Dorratoltaj N, O'Dell ML, Bordwine P, Kerkering TM, Redican KJ. Economic Evaluation of Fungal Meningitis Outbreak Response in New River Valley: Local Health Department Perspective. Frontiers in Public Health Services and Systems Research. 2015 9 Aug;4(4):21–28.

[102] Abbas KM, Dorratoltaj N, O'Dell ML, Bordwine P, Kerkering TM, Redican KJ. Clinical Response, Outbreak Investigation, and Epidemiology of the Fungal Meningitis Epidemic in the United States: Systematic Review. Disaster medicine and public health preparedness. 2016 Feb;10(1):145–151. Available from: http://www.ncbi.nlm.nih.gov/pmc/articles/PMC4795899/.

[103] Murray CJL, Vos T, Lozano R, Naghavi M, Flaxman AD, et al. Disability-adjusted life years (DALYs) for 291 diseases and injuries in 21 regions, 1990–2010: a systematic analysis for the Global Burden of Disease Study 2010. The Lancet. 2012 Dec;380(9859):2197–2223. Available from: http://linkinghub.elsevier.com/retrieve/pii/S0140673612616894.

[104] Center fo Disease Control. MMWR weekly: Exophiala Infection from Contaminated Injectable Steroids Prepared by a Compounding Pharmacy — United States, July–November 2002; 2002. http://www.cdc.gov/mmwr/preview/mmwrhtml/mm5149a1.htm.

[105] WHO. WHO — Metrics: Disability-Adjusted Life Year (DALY). World Health Organization; 2014. Accessed: 2015-6-29. http://www.who.int/healthinfo/global$_burden_disease/metrics_daly/en/$.

[106] Tung CE, So YT, Lansberg MG. Cost comparison between the atraumatic and cutting lumbar puncture needles. Neurology. 2012 Jan;78(2):109–113.

[107] Barenfanger J, Lawhorn J, Drake C. Nonvalue of culturing cerebrospinal fluid for fungi. J Clin Microbiol. 2004 Jan;42(1):236–238.

[108] Rosenstein NE, Perkins BA, Stephens DS, Popovic T, Hughes JM. Meningococcal Disease. New England Journal of Medicine. 2001 May;344(18):1378–1388. Available from: http://dx.doi.org/10.1056/NEJM200105033441807.

[109] WHO. THE GLOBAL BURDEN OF DISEASE. 2008;.

[110] U S Census Bureau. Life Expectancy - The 2012 Statistical Abstract - U.S. Census Bureau. 2011 15 Sep;.

[111] Bell BP, Khabbaz RF. Responding to the outbreak of invasive fungal infections: the value of public health to Americans. JAMA. 2013 6 Mar;309(9):883–884.

[112] Corvese K, Forlano L, Gibson L. A hybrid strategy for surveillance of individuals potentially exposed to contaminated methylprednisolone acetate–Virginia, 2012. J Public Health Manag Pract. 2013 Jul;19(4):289–293.

[113] Meltzer MI, Cox NJ, Fukuda K. The economic impact of pandemic influenza in the United States: priorities for intervention. Emerg Infect Dis. 1999 Sep;5(5):659–671.